ECMWF COPERNICUS REPORT

Copernicus Climate Change Service

Synthesis on the existing simulations at M16

C3S_34b_Lot2_SMHI – (PRINCIPLES)

Issued by: Erik Kjellström(SMHI)/ Jon Stark (SMHI) / Robert Vautard (CNRS)

Date: 02/10/2019

Ref: D34b_Lot2.4.3.2_Synthesis on the existing simulations at M16_v4

Official reference number service contract: 2017/C3S_34b_Lot2_SMHI/SC2

ECMWF COPERNICUS REPORT

Copernicus Climate Change Service

European Commission

Copernicus Europe's eyes on Earth

IMPLEMENTED BY ECMWF

Contributors

SMHI
Grigory Nikulin
Erik Kjellström
Lars Bärring

CNRS
Robert Vautard

DMI
Ole B. Christensen
Fredrik Boberg

ETHZ
Silje L. Sørland
Marie-Estelle Demory
Jan Rajczac
Christoph Schär

MÉTÉO-FRANCE
Samuel Somot
Lola Corre

ICTP
Erika Coppola
James Ciarlo

MOHC
Erasmo Buonomo

HZG GERICS
Katharina Bülow
Claas Teichmann

KNMI
Erik van Meijgaard
Emma Aalbers
Geert Lenderink

Table of contents

Chapter 1 to 4 contains an executive summary of the report while chapters 5 to 12 contain the comprehensive report.

1. Key findings

- As of 15 January 2019, 34 climate projection simulations were analyzed (vs. 20 in January 2018), using 9 Global Climate Models (GCMs) simulations downscaled by 9 Regional Climate Models (RCMs), for the historical period and a future period under the RCP8.5 forcing scenario. These climate projections allow a better understanding of the source of biases and drivers of trends of climate variables;

- No analyzed GCM-RCM simulation exhibit outlying temperature biases, despite some systematic biases across regions for a few models; GCMs and RCMs generally have a cold bias in North and Western Europe and a warm bias in South-Eastern Europe; This pattern is similar for means and hot temperatures; biases in frost days have varying patterns;

- RCMs do not reduce GCM temperature biases; Maximum and mean temperature bias patterns depend mostly on the GCM, while minimum temperature bias patterns are rather driven by RCMs;

- RCMs exhibit a systematic wet bias as compared to E-OBS observations; the biases appear to originate from both RCMs and GCMs; Models generally overestimate heavy precipitation relative to E-OBS, especially in winter;

- Wet RCM biases are also present in the water balance variables such as evaporation, runoff and soil moisture. Such variables largely show biases generally depending on the RCM;

- Models generally reproduce well observed dynamical patterns and surface winds, despite a few models with systematic sea level pressure departures from the observations; A general overestimation of ERA5 surface winds is found in simulations but could not be explained here;

- Sea level pressure patterns simulated by RCMs are generally well correlated with those of the driving GCMs, with pattern correlations of about 0.9 in winter. In summer correlations are lower as the driving large-scale flow is weaker and other drivers such as soil moisture relatively more important;

- Model biases in surface radiation range from -34.5W/m² over the Iberian Peninsula to more than +40 W/m² in the British Isles. Strong negative biases affect southern Europe, and more analyses are needed to understand these biases affected by clouds and aerosols uncertainties;

- Climate change trends in temperature are all positive; trends in precipitation show consistency across models, albeit with larger uncertainty over a few regions (Iberian Peninsula, France); Northern Europe is projected to become wetter and Southern Europe drier;

- The added value of RCM downscaling vs. GCM has been studied with new methods and show that the distributions are improved with downscaling, especially for precipitation;

- The spread of climate change responses across GCMs is modulated by downscaling depending on season; the spread is reduced in particular for temperature change in summer, while no such reduction is seen in winter;

2. Brief description of the methodology

Coordinated analysis

The strategy for coordinated rapid evaluation of simulations is to detect, as much as possible, errors or uncertainties in the ensemble of simulations. It consists of classical statistics. We first compare mean biases relative to observational data sets, and then we inter-compare changes between a reference and a future period for 13 indices.

Time periods considered for statistical analysis are:

- Reference past climate period: 1981-2010 (historical+RCP85)
- Mid-century future climate: 2036-2065 [RCP8.5 unless noted when also RCP2.6 has been assessed]

Climate change trends are calculated as differences in the climate between the two periods. Indices are for means and extremes of temperature, precipitation, sea level pressure, surface winds and radiation.

Specific analyses

We added to the coordinated analysis a few specific studies exploiting the full data set. This part adds innovative methodologies in order to assess the quality of simulations and their changes:

- The added value of RCMs relative to GCMs analysis quantifies how RCMs improve (or degrade) probability distribution functions (PDFs) relative to observations;
- The GCM and RCM spread of climate change signals analysis quantifies how changes in temperature and precipitation in RCMs relate to GCMs in a bivariate analysis for the two variables;
- The GCM-RCM correlation analysis compares sea level pressure patterns between GCMs and RCMs;
- The precipitation scaling analysis is a preliminary analysis of 3-hourly data investigating how extreme hourly precipitation scaling with dew point temperature compare between EUROCORDEX simulations and convection-permitting ones;
- The water balance analysis examines the ensemble of variables involved in the regional water cycle;

3. Available simulations as of 15/1/2019

As of 15/1/2019, the ensemble of available RCM-GCM simulations for both the historical period and the RCP8.5 scenario consists of 34 simulations using 9 GCMs and 9 RCMs (counting separately two versions of the WRF RCM). Several other scenario simulations are available but not analyzed here. Table 1 lists the simulations that were analyzed. For some of the simulations, some dynamical fields were not available (see footnotes). Compared to SC1 (service contract 1), a few simulations were withdrawn due to known issues.

Table 1: Simulations analyzed in this report (orange colour). The name of GCM simulations is given as "GCMrR" where "R" is the model ensemble realization.

GCM/RCM	CCLM	RACMO	RCA	HIRHAM	REMO	WRF361H	WRF381P	ALADIN	REGCM
ECEARTHr12									
ECEARTHr1									
ECEARTHr3									
MPIr1					(1)	(2,4,5)			
MPIr2					(1)				
HadGEMr1						(2,4,5)	(5)		
CNRMr1									
IPSLr1							(5,6)		
NORESMr1									
CANESMr1	(4)				(3,4)				
MIROCr1	(4)								

Footnotes: (1) This REMO version is REMO2009 while other versions are REMO2015
(2) Not available for sea level pressure
(3) Not available for sfcWind analysis
(4) Not available for sfcWindmax analysis
(5) Not available for the water balance analysis
(6) Problem detected in the course of the analysis for precipitation (a few years with negative values due to post-processing error), and for radiation. Should affect results for precipitation which were largely removed here, but the problem should not change results for radiation in a visible way.

4. Summary of biases and changes for temperature and precipitation

Temperature and precipitation are the most familiar variables to climate scientists and users of climate projections. As a summary of biases in Europe for temperature and precipitation, Figure 1 summarizes the main biases per eight sub-regions as frequently used in climate research for more than 10 years (Christensen and Christensen, 2007). The figure shows that, for each model, biases can be significant for one variable and not for another. No model or GCM-RCM combination has small biases for each subregion. However, some models exhibit moderate but large-scale biases affecting most subregions. Such is the case for EC-EARTH and CNRM-CM5 based downscaled simulations which are systematically too cold. An amplification of this bias is made by some RCMs such as RACMO, HIRHAM and RCA.

For precipitation, all GCM-RCM simulations have a too wet climate in all regions, which is not the case of GCMs. RCM downscaling systematically enhances the wet bias, a known behavior since the study of Kotlarski *et al*. (2016).

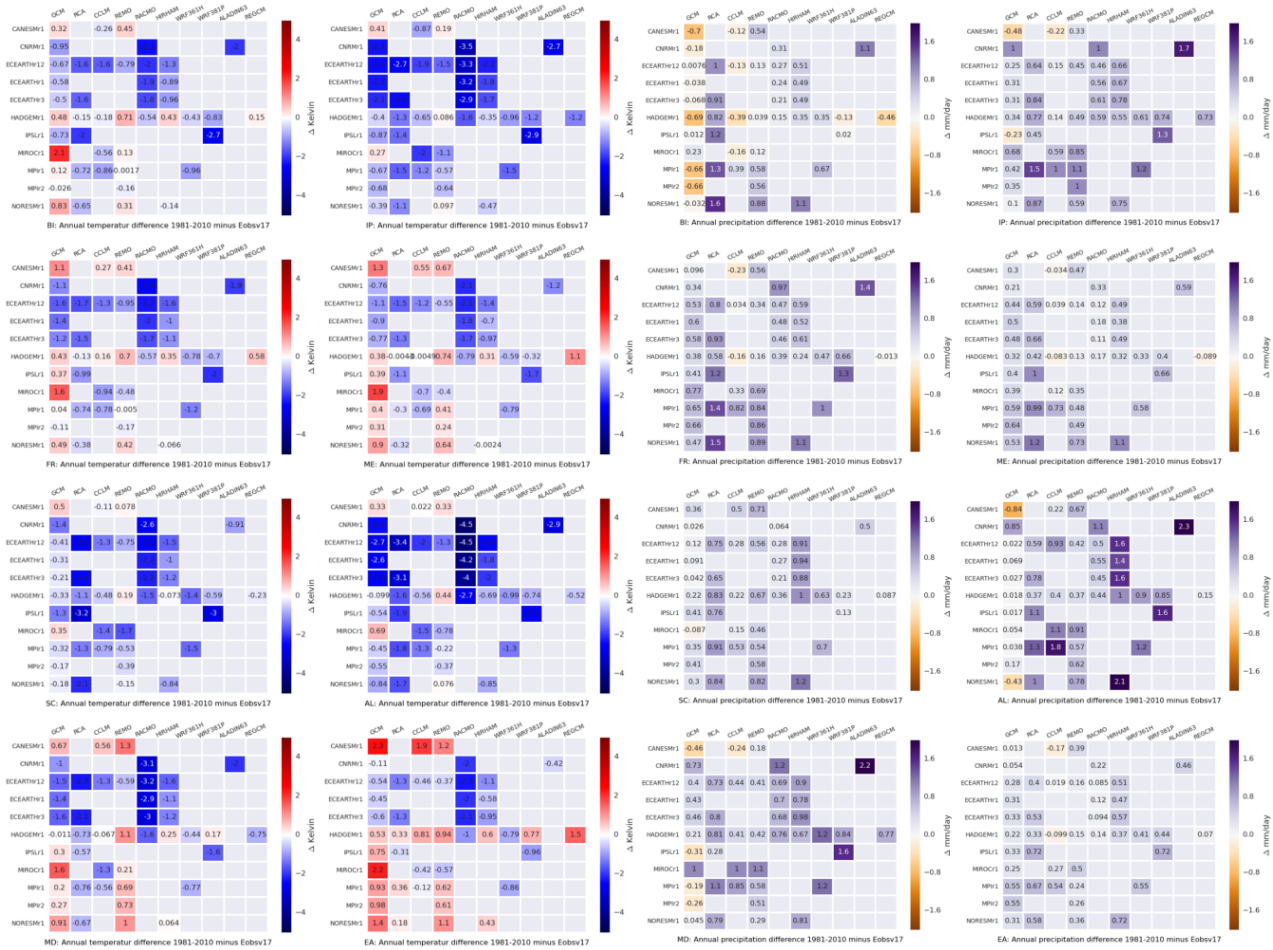

Figure 1: Annual mean temperature [K] (left 8 panels) and precipitation [mm/day] (right 8 panels) differences over 1981-2010 between each GCM and GCM/RCM and EOBSv17 averaged over eight subregions (BI=British Isles; IP=Iberian Peninsula; FR=France; ME=Mid Europe; SC=Scandinavia; AL=Alps; MD=Mediterranean; EA=Eastern Europe).

Figure 2 is similar to Figure 1 for changes instead of biases. It shows the homogeneity of the climate change signals for temperature and to a large extent also for precipitation. In some regions however, models disagree, such as for FR and BI for precipitation. Both trends appear to be a combination of GCM and RCM origin.

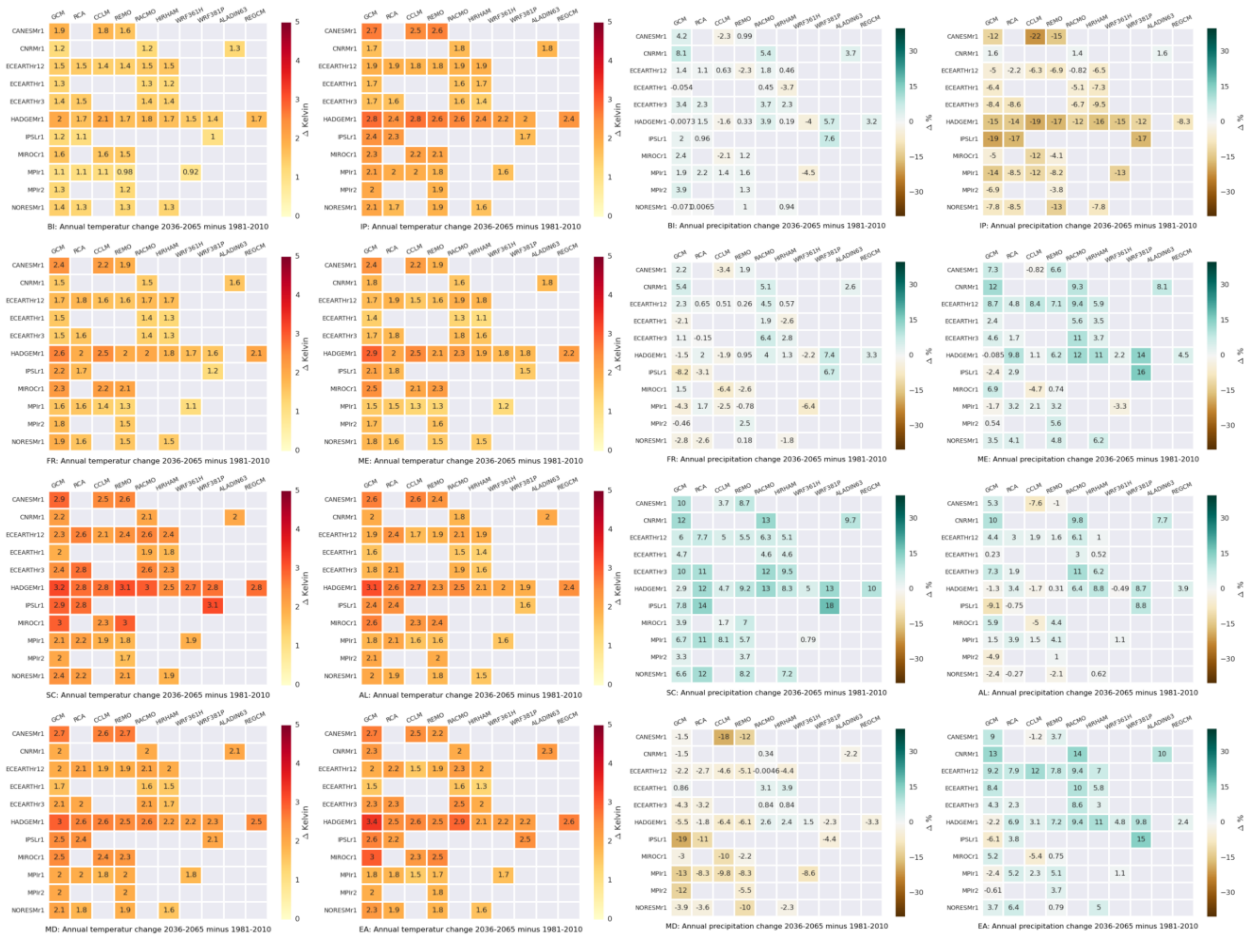

Figure 2: same as Figure 1 for changes (2050-ref) instead of biases.

5. Background and introduction

The goals of the work package four (WP4, C3S_34b_Lot240) are to (i) monitor the advancement by regular verifications of the progressive fulfilment of the spread requirements defined in C3S_34b_Lot240; (ii) perform, over a few key metrics the evaluation of existing and new simulations allowing a scientific “health check” of all simulations as they are produced, and (iii) provide regular syntheses and demonstrations.

In this report we review the state of the EURO-CORDEX ensemble after one year of the PRINCIPLES project. We first describe the current status of the matrix and we perform a rapid evaluation of the initial simulations. These simulations are included in (i) datasets that are already published on the Earth System Grid Federation, complete with a few other simulations that were not published at the time of this analysis (15 January 2019).

For the rapid evaluation, a set of diagnostics and analyses is proposed. The set consists in a coordinated analysis of biases over a number of indices in the form of maps and tables of numerical values for eight sub-regions originally defined in the European PRUDENCE project (Christensen and Christensen, 2007): BI=British Isles; IP=Iberian Peninsula; FR=France; ME=Mid Europe; SC=Scandinavia; AL=Alps; MD=Mediterranean; EA=Eastern Europe. A few specific analyses were also carried out by the project groups and are reported here.

Rapid coordinated evaluation was designed following a strategy that is described in Section 2; In Section 3 the model ensemble is described. In Section 4 the biases are calculated whenever observations make it possible. In Section 5 changes between the midcentury and the current period are described. Specific analyses are provided in Section 6.

6. Methodology

Coordinated analysis

The strategy for coordinated rapid evaluation of simulations is to detect, as much as possible, errors or uncertainties in the ensemble of simulations. It consists of classical statistics. We compare first mean biases relative to observational data sets, and then we inter-compare changes between a reference and a future period for 13 indices.

Time periods have been selected after discussion with the group and with ECMWF. They have been selected based on two main reasons: i) Their greater interest to users of the climate services products as communicated through other C3S projects and ii) their use in other context, e.g. as reference/evaluation for the seasonal forecast system. Note that the periods slightly differ from the first synthesis report, and we now use Scenario RCP8.5 as the main focus for the project. Unless otherwise noted the time periods analyzed are:

- Reference past climate period: 1981-2010 (historical+RCP85)
- Mid-century future climate: 2036-2065 (RCP8.5 unless noted in the text when also RCP2.6 has been assessed)

Trends are calculated as differences in the climate over the two periods. The various indices used here are described in Table 2, together with the observations used to compare with simulations.

Table 2: Diagnostics and indices used in this report.

Index / diagnostics	**ECV**	**Observation data**	**Presentation** Maps=obs, bias, change 2036-2065 minus ref, ind. models+ens+robust. Table : averages over PRUDENCE regions
Temperature			
Mean daily mean temperature	Tas	EOBS 0.22 interpolated to 0.11	Maps, Table
Mean daily maximum temperature	tasmax	EOBS 0.22 interpolated to 0.11	Maps, Table
Mean daily minimum temperature	tasmin	EOBS 0.22 interpolated to 0.11	Maps, Table
Mean #days with TX>35°C	tasmax	EOBS 0.22 interpolated to 0.11	Maps, Table
Mean #Frost days TN<=0C	tasmin	EOBS 0.22 interpolated to 0.11	Maps, Table
Precipitation			
Mean annual precipitation	Pr	EOBS 0.22 brought to 0.11	Maps for yearly. Table for seasonal DJF, JJA
Mean annual RX1day	Pr	EOBS 0.22 brought to 0.11	Maps for yearly. Table for seasonal DJF, JJA
Frequency of Wet days (>1mm)	Pr	EOBS 0.22 brought to 0.11	Table for seasonal DJF, JJA
p99 of wet days	Pr	EOBS 0.22 brought to 0.11	Table for seasonal DJF, JJA
Dynamics			
Sea Level Pressure	Psl	ERA5	Maps
Mean Wind Speed	sfcWind	ERA5	Maps, Table
Mean annual Max wind speed	sfcWindmax	ERA5	Maps, Table
Radiation			
Radiation	Rsds	Heliosat	Maps, Table

Observations used

The observations used here for precipitation and temperature are taken from E-OBS 0.22° (Haylock *et al*. 2008) and are either interpolated (for temperature) or brought to 0.11°C resolution by copying values on each of the 4 subgrid cells, which is equivalent to a nearest-neighbor interpolation. For the dynamical variables the new ERA5 reanalysis is used over the reference period. For radiation, we used data from the Heliosat (SARAH) (Müller *et al*., 2015) remote-sensed surface radiation dataset. The latter is interpolated to the common EURO-CORDEX horizontal grid for the period 1983 – 2012 (not available before).

Specific analyses

We added to the coordinated analysis a few specific studies exploiting the full data set. This part adds innovative methodologies in order to assess the quality of simulations and their changes:

- The added value of RCMs relative to GCMs analysis quantifies how RCMs improve (or degrade) PDFs relative to observations;
- The GCM and RCM spread of climate change signals analysis quantifies how changes in temperature and precipitation in RCMs relate to GCMs in a bivariate analysis for the two variables;
- The GCM-RCM correlation analysis compares sea level pressure patterns between GCMs and RCMs;

Two further specific analyses on precipitations were added

- The precipitation scaling analysis is a preliminary analysis of 3-hourly data investigating how extreme hourly precipitation scaling with dew point temperature compare between EUROCORDEX simulations and convection-permitting ones;
- The water balance analysis examines the ensemble of variables involved in the regional water cycle;

7. Available simulations as of 15/1/2019

The ensemble of (on ESGF) simulations available on 15/1/2019 are considered, including different members of an ensemble using the same models (GCM, RCM), and different versions of the same model (for REMO). Two WRF versions were used but were considered as two different models due to a number of differences in parameterizations and implementation. On total 9 RCMs and 9 GCMs were used with 3 additional GCM members, and 34 GCM-RCM simulations are currently available. Table 1 lists the simulations that were analyzed. For some of the simulations, some dynamical fields were not available (see footnotes). Compared to SC1, a few simulations were withdrawn due to known issues:

- Simulations using model-level data from the CNRM-CM5 GCM, for which data were not corresponding to the actual simulation
- Simulations from WRF331F with a known problem of SST interpolation along some coastal areas. Simulations were replaced by those from the WRF381P WRF model version (documentation in progress).

Note that for the downscaling of IPSL with WRF381P, an error was detected at the last minute in the post-processing chain, and results for precipitation should not be interpreted. This does not affect other variables (very slightly radiation, but not at all temperature and neither dynamics).

8. Model biases

8.1 Temperature biases

We first analyze the biases of each model for the most classical variables, temperature and precipitation. The analysis is made by comparing model seasonal means and variances of daily temperatures and precipitation amount over the reference period with observations from E-OBS 0.22° interpolated to the EUROCORDEX grid.

Figure 3 and Table 3 show the annual mean temperature biases for each simulation. In general, temperature biases remain within a few degrees but can be quite large in some cases, up to about 5 degrees in absolute value. There are well defined large-scale bias patterns, which have also been described in previous studies (see eg. Kotlarski *et al.*, 2016). None of the new simulations seem to exhibit a behavior that is not consistent with previous analyses and other models. The ensemble mean biases are negative, within 2 degrees, and are more marked in the Iberian Peninsula and in the Alpine regions. Some models have systematic substantial negative biases all over Europe such as all ECEARTH-RACMO simulations, CNRMr1-driven and IPSLr1-driven simulations.

The bias patterns clearly exhibit a signature of the driving GCM in most cases, indicating a dynamical origin of biases. However this tendency s modulated by the RCM. The biases do not seem sensitive to the GCM member of the ensemble, thus little influence of interdecadal variability is expected.

Essentially the same conclusions hold for the mean maximum daily temperature (Figure 4 and Table 4). In this case the ensemble mean bias is stronger with substantial underestimations in BI, IP, SC and AL. All ECEARTH based simulations are biased all over Europe.

Regarding minimum daily temperatures (Figure 5 and Table 5), the RCM signal is stronger, pointing to local land-atmosphere combined with surface and boundary layer processes driving much of the bias structure. For instance RACMO exhibits systematic negative biases and REMO almost systematic positive biases, and biases patterns are often well characterized for each RCM. Ensemble mean biases are less pronounced as biases are more diverse among models.

Extreme positive temperatures (Max daily temperatures) are not frequent enough (Figure 6 and Table 6) in Western Europe but too frequent in Eastern Europe and Mediterranean areas, pointing again to land-atmosphere processes in drier and more continental-climate areas. Most models underestimate the frequency of hot days in the IP region, and overestimate it in Eastern Mediterranean regions.

For freezing days, as for daily minimum temperature, the bias patterns are really specific for each RCM (Figure 7 and Table 7). Large and generalized frequency underestimations (eg. For REMO) or overestimations (e.g. For RACMO and WRF [over Northern Europe]) are found.

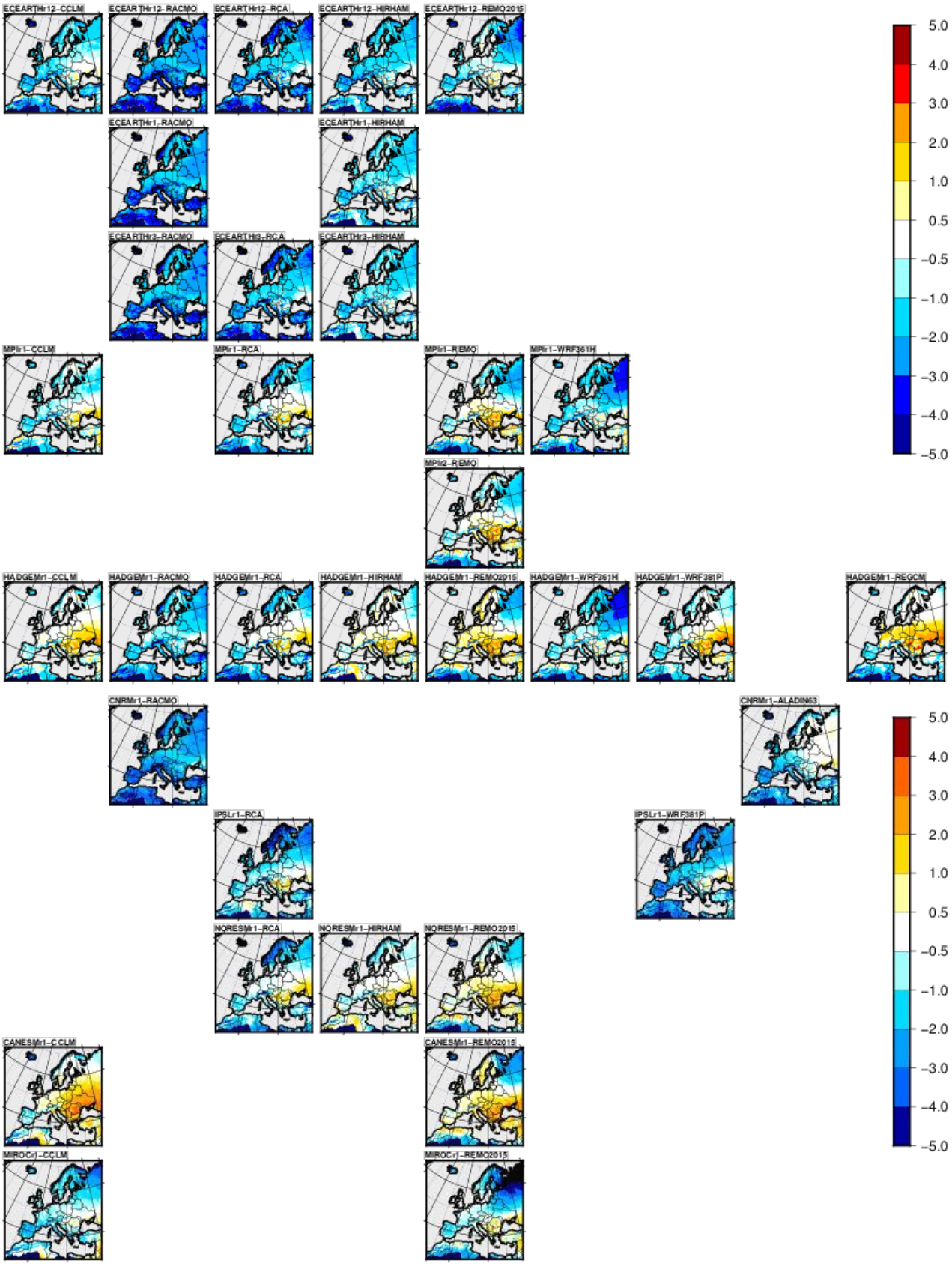

Figure 3: Biases of the mean temperature for each model, in °C.

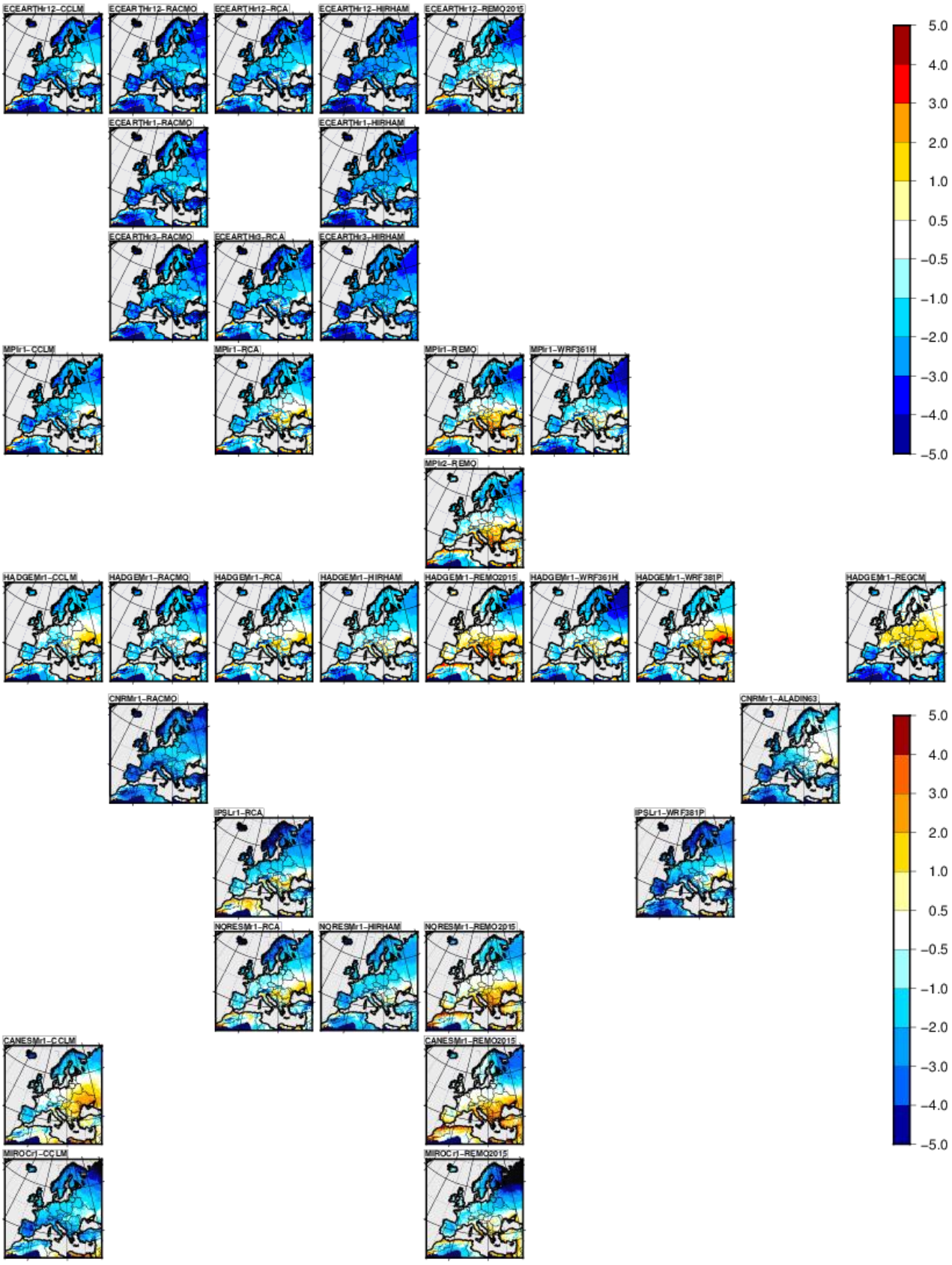

Figure 4: Same as Figure 3 for the maximum daily temperature

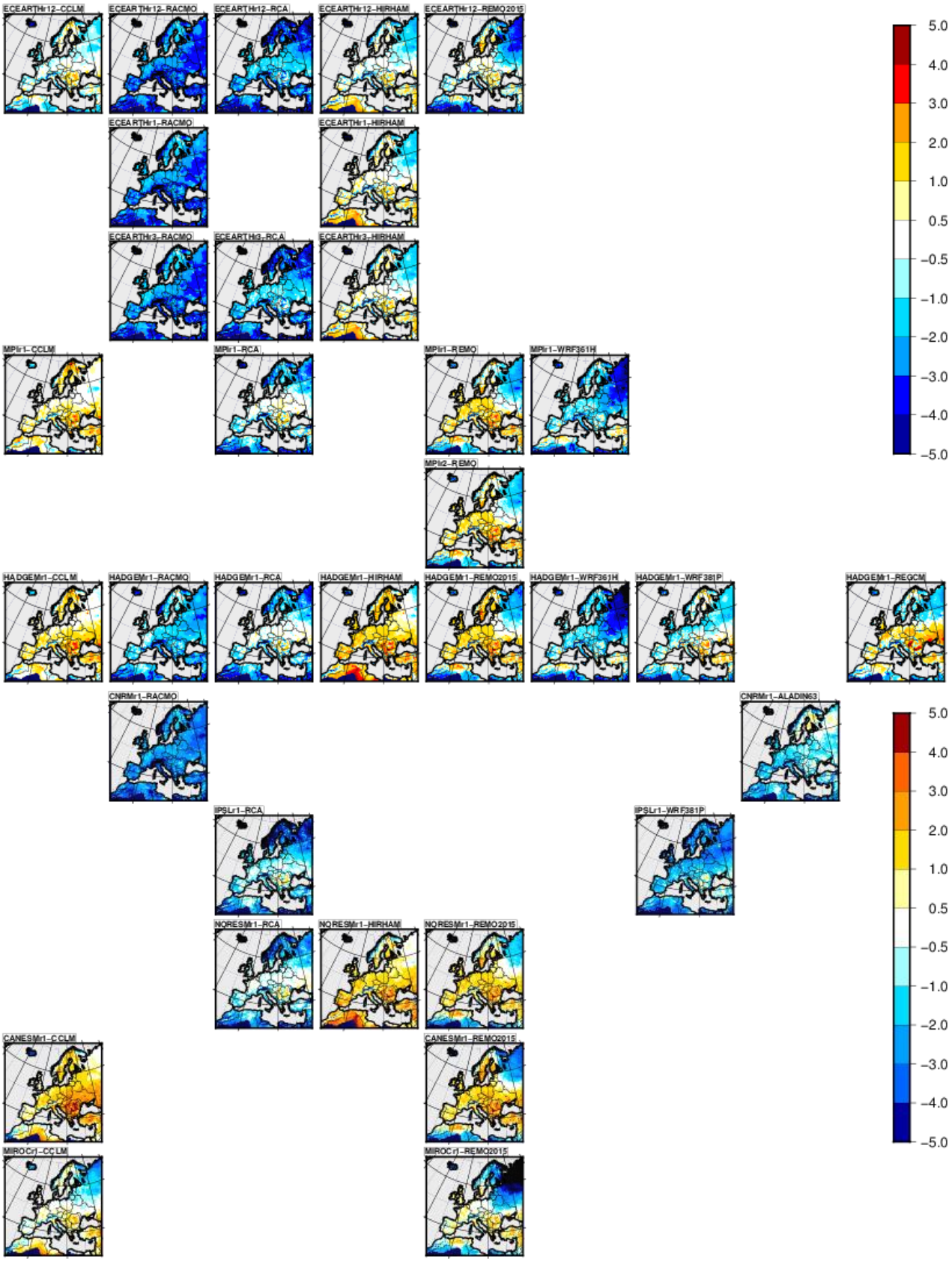

Figure 5: Same as in Figure 3 for the daily minimum temperature

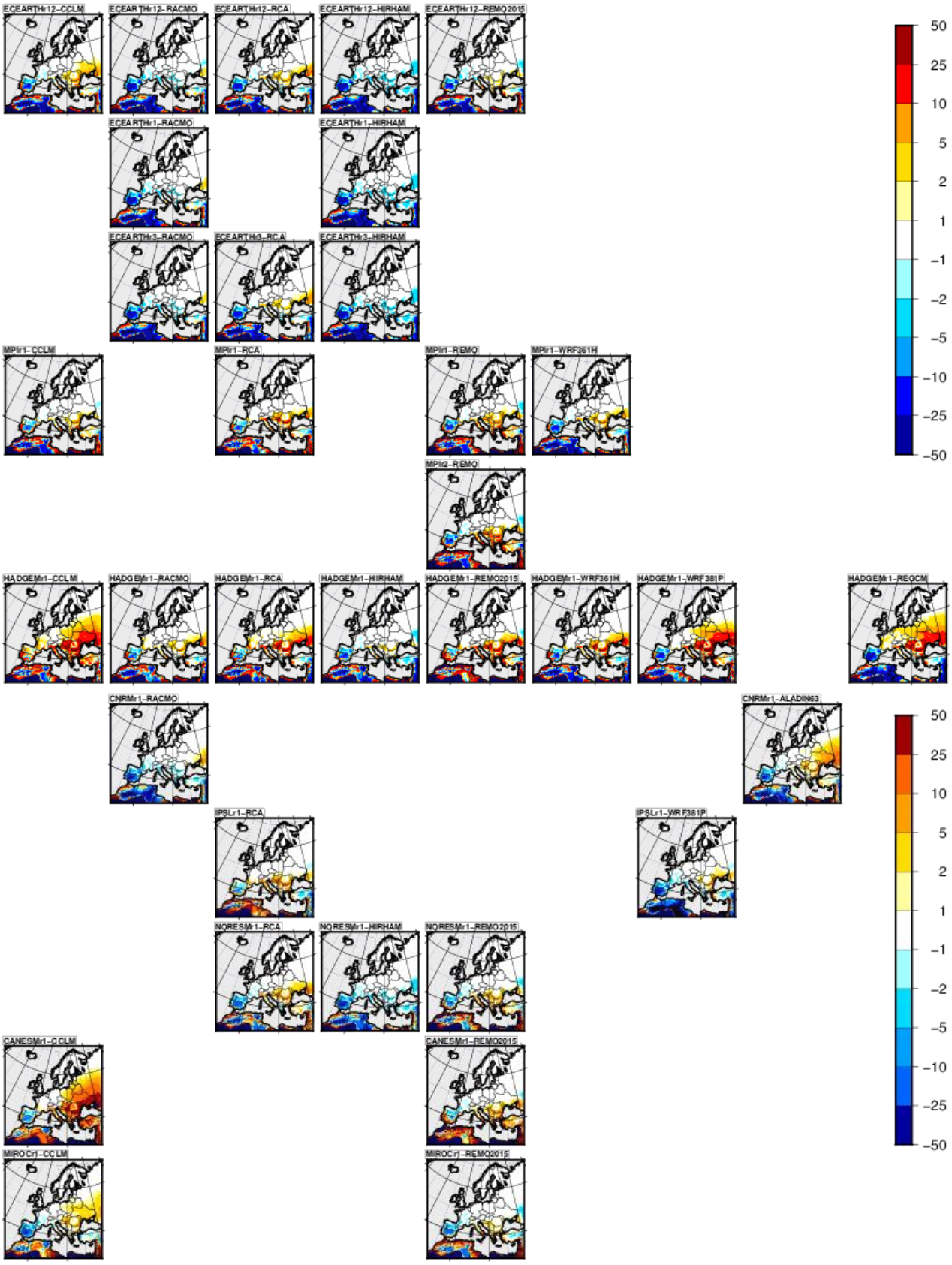

Figure 6: same as Fig. 3 for the bias of the number of days with TX>35°C

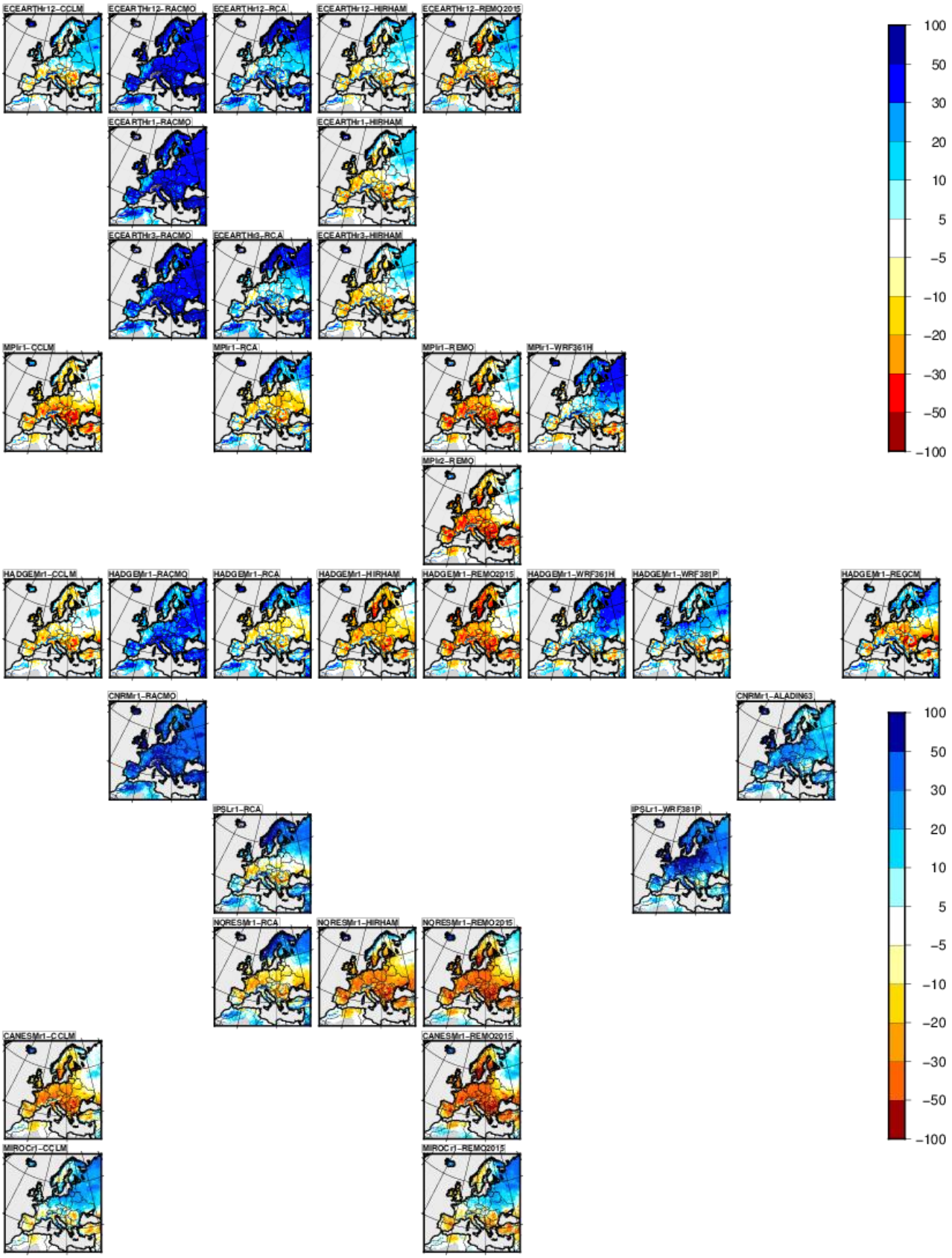

Figure 7: Same as Fig. 3 for the bias of the number of days with TN<0°C.

Table 3: Annual mean temperature for the eight PRUDENCE regions based on E-OBS. Biases w.r.t. E-OBS for the 34 GCM-RCM combinations and the ensemble mean. Colored numbers indicate biases larger than 2°C in absolute value.

	BI	IP	FR	ME	SC	AL	MD	EA
E-OBS (°C)	9.10	13.67	11.25	9.16	2.89	8.19	12.66	8.55
Ensemble Mean bias (°C)	-0.85	-1.46	-0.76	-0.55	-1.20	-1.63	-0.81	-0.15
CANESMr1-CCLM	-0.27	-0.80	0.31	0.59	0.03	0.05	0.62	2.05
CANESMr1-REMO2015	0.41	0.26	0.45	0.71	0.22	0.39	1.39	1.35
CNRMr1-ALADIN63	-2.06	-2.68	-1.92	-1.14	-0.81	-2.89	-2.03	-0.32
CNRMr1-RACMO	-2.42	-3.49	-2.43	-2.07	-2.54	-4.45	-3.14	-1.89
ECEARTHr12-CCLM	-1.59	-1.79	-1.27	-1.14	-1.25	-1.94	-1.30	-0.36
ECEARTHr12-HIRHAM	-1.30	-2.15	-1.55	-1.34	-1.47	-2.37	-1.54	-1.01
ECEARTHr12-RACMO	-2.05	-3.27	-2.26	-2.14	-2.42	-4.43	-3.22	-2.17
ECEARTHr12-REMO2015	-0.82	-1.46	-0.92	-0.53	-0.65	-1.27	-0.57	-0.25
ECEARTHr1-HIRHAM	-1.01	-1.68	-1.05	-0.95	-1.16	-1.93	-1.25	-0.84
ECEARTHr1-RACMO	-1.91	-3.12	-2.02	-1.81	-2.14	-4.12	-2.97	-1.92
ECEARTHr3-HIRHAM	-1.01	-1.68	-1.05	-0.95	-1.16	-1.93	-1.25	-0.84
ECEARTHr3-RACMO	-1.83	-2.84	-1.73	-1.66	-2.12	-3.97	-3.03	-2.03
ECEARTHr3-RCA	-1.57	-2.33	-1.44	-1.24	-2.40	-3.07	-2.17	-1.15
ECEARTHr12-RCA	-1.64	-2.59	-1.71	-1.49	-2.45	-3.38	-2.25	-1.18
HADGEMr1-CCLM	-0.20	-0.57	0.19	0.03	-0.40	-0.52	-0.05	0.92
HADGEMr1-HIRHAM	0.39	-0.28	0.38	0.34	0.00	-0.64	0.24	0.71
HADGEMr1-RACMO	-0.59	-1.57	-0.55	-0.77	-1.42	-2.63	-1.64	-0.91
HADGEMr1-RCA	-0.16	-1.21	-0.08	0.03	-1.04	-1.56	-0.71	0.44
HADGEMr1-REGCM	0.21	-1.11	0.63	1.15	-0.07	-0.39	-0.60	1.66
HADGEMr1-REMO2015	0.67	0.16	0.74	0.77	0.29	0.49	1.08	1.06
HADGEMr1-WRF361H	-0.49	-0.87	-0.76	-0.56	-1.41	-0.95	-0.47	-0.67
HADGEMr1-WRF381P	-0.90	-1.13	-0.68	-0.31	-0.51	-0.67	0.22	0.87
IPSLr1-RCA	-1.95	-1.32	-0.93	-1.02	-3.20	-1.86	-0.49	-0.20
IPSLr1-WRF381P	-2.80	-2.83	-2.03	-1.73	-2.90	-2.43	-1.59	-0.86
MIROCr1-CCLM	-0.59	-1.90	-0.93	-0.67	-1.30	-1.47	-1.26	-0.31
MIROCr1-REMO2015	0.05	-1.01	-0.47	-0.38	-1.62	-0.74	0.18	-0.45
MPIr1-CCLM	-0.89	-1.10	-0.76	-0.67	-0.71	-1.27	-0.53	-0.01
MPIr1-RCA	-0.72	-1.46	-0.70	-0.27	-1.22	-1.70	-0.69	0.46
MPIr1-REMO	-0.05	-0.48	0.02	0.44	-0.46	-0.11	0.75	0.75
MPIr1-WRF361H	-1.00	-1.45	-1.20	-0.76	-1.44	-1.25	-0.75	-0.74
MPIr2-REMO	-0.21	-0.56	-0.15	0.27	-0.31	-0.27	0.80	0.75
NORESMr1-HIRHAM	-0.18	-0.41	-0.05	0.02	-0.76	-0.79	0.11	0.55
NORESMr1-RCA	-0.65	-1.06	-0.35	-0.28	-2.07	-1.64	-0.59	0.29
NORESMr1-REMO2015	0.27	0.18	0.45	0.67	-0.10	0.15	1.08	1.20

Table 4: Same as Table 3 for daily maximum temperature bias.

	BI	IP	FR	ME	SC	AL	MD	EA
E-OBS (°C)	12.81	19.36	15.71	13.43	6.82	12.60	17.70	13.29
Ensemble Mean bias (°C)	-1.52	-1.85	-1.14	-1.05	-1.96	-1.64	-0.67	-0.63
CANESMr1-CCLM	-0.92	-1.46	-0.28	-0.25	-1.27	-0.82	0.34	1.16
CANESMr1-REMO2015	-0.16	0.75	0.21	0.12	-0.71	0.89	2.80	0.90
CNRMr1-ALADIN63	-2.49	-3.24	-2.19	-1.39	-1.28	-2.78	-2.05	-0.51
CNRMr1-RACMO	-2.95	-3.47	-2.58	-2.04	-2.81	-3.98	-2.77	-1.75
ECEARTHr12-CCLM	-2.28	-2.56	-1.94	-1.98	-2.45	-2.92	-1.85	-1.31
ECEARTHr12-HIRHAM	-2.54	-3.69	-2.80	-2.64	-2.71	-3.14	-2.42	-2.38
ECEARTHr12-RACMO	-2.60	-3.02	-2.24	-2.03	-2.72	-3.73	-2.65	-1.97
ECEARTHr12-REMO2015	-1.36	-1.15	-1.08	-0.95	-1.41	-0.80	0.59	-0.58
ECEARTHr1-HIRHAM	-2.22	-3.25	-2.26	-2.22	-2.41	-2.68	-2.15	-2.25
ECEARTHr1-RACMO	-2.42	-2.91	-1.98	-1.71	-2.43	-3.42	-2.39	-1.75
ECEARTHr3-HIRHAM	-2.22	-3.25	-2.26	-2.22	-2.41	-2.68	-2.15	-2.25
ECEARTHr3-RACMO	-2.28	-2.63	-1.60	-1.46	-2.39	-3.22	-2.44	-1.81
ECEARTHr3-RCA	-2.29	-2.42	-1.72	-1.73	-2.77	-2.97	-2.03	-1.64
ECEARTHr12-RCA	-2.40	-2.61	-2.00	-1.96	-2.82	-3.24	-2.08	-1.57
HADGEMr1-CCLM	-0.80	-1.27	-0.32	-0.70	-1.60	-1.29	-0.54	0.06
HADGEMr1-HIRHAM	-0.72	-1.46	-0.53	-0.74	-1.34	-0.67	-0.27	-0.51
HADGEMr1-RACMO	-1.07	-1.30	-0.40	-0.61	-1.80	-1.84	-1.07	-0.74
HADGEMr1-RCA	-0.82	-1.14	-0.03	-0.18	-1.51	-1.23	-0.49	0.16
HADGEMr1-REGCM	-0.22	-2.03	0.77	1.06	-0.12	0.05	-0.89	1.38
HADGEMr1-REMO2015	0.26	0.55	0.87	0.52	-0.61	1.21	2.35	0.86
HADGEMr1-WRF361H	-0.87	-0.99	-0.41	-0.51	-2.06	-0.55	-0.27	-0.59
HADGEMr1-WRF381P	-0.83	-1.49	-0.34	-0.12	-1.08	-0.99	0.23	1.01
IPSLr1-RCA	-2.86	-1.10	-1.33	-1.70	-3.70	-1.82	-0.08	-0.74
IPSLr1-WRF381P	-2.82	-3.60	-2.07	-1.74	-3.38	-3.00	-1.97	-0.92
MIROCr1-CCLM	-1.34	-3.07	-1.82	-1.53	-2.41	-2.60	-2.16	-1.37
MIROCr1-REMO2015	-0.49	-1.13	-0.88	-0.85	-2.17	-0.41	0.98	-0.84
MPIr1-CCLM	-1.85	-2.21	-1.79	-1.88	-2.20	-2.39	-1.21	-1.30
MPIr1-RCA	-1.59	-1.77	-1.21	-0.91	-1.82	-1.72	-0.62	-0.04
MPIr1-REMO	-0.89	-0.68	-0.48	-0.22	-1.37	0.25	1.75	0.38
MPIr1-WRF361H	-1.36	-1.75	-1.08	-0.81	-2.11	-0.90	-0.48	-0.68
MPIr2-REMO	-1.05	-0.75	-0.71	-0.40	-1.25	0.07	1.82	0.34
NORESMr1-HIRHAM	-1.48	-2.07	-1.44	-1.40	-2.15	-1.71	-0.81	-0.92
NORESMr1-RCA	-1.38	-1.05	-0.72	-0.77	-2.50	-1.47	-0.28	-0.01
NORESMr1-REMO2015	-0.40	0.45	0.03	0.07	-1.01	0.59	2.41	0.83

Table 5: Same as Table 3 for daily minimum temperature bias.

	BI	IP	FR	ME	SC	AL	MD	EA
E-OBS (°C)	5.53	8.04	6.80	5.08	-1.00	4.00	7.83	4.22
Ensemble Mean bias (°C)	-0.35	-0.51	-0.16	-0.20	-0.98	-1.62	-0.59	-0.09
CANESMr1-CCLM	0.39	0.51	1.18	1.36	1.09	1.06	1.50	2.60
CANESMr1-REMO2015	1.18	0.99	1.35	1.57	0.87	0.46	1.27	1.89
CNRMr1-ALADIN63	-2.18	-2.03	-1.75	-1.32	-0.99	-3.26	-2.14	-0.87
CNRMr1-RACMO	-2.37	-3.00	-2.22	-2.41	-2.85	-4.98	-3.34	-2.55
ECEARTHr12-CCLM	-0.89	-0.39	-0.29	-0.33	-0.28	-0.86	-0.25	0.28
ECEARTHr12-HIRHAM	-0.10	-0.17	-0.04	-0.11	-0.63	-1.66	-0.38	0.02
ECEARTHr12-RACMO	-2.04	-3.04	-2.25	-2.53	-2.76	-5.14	-3.67	-2.90
ECEARTHr12-REMO2015	-0.05	-0.55	-0.03	0.19	-0.29	-1.22	-0.49	0.13
ECEARTHr1-HIRHAM	0.15	0.33	0.42	0.25	-0.29	-1.24	-0.07	0.23
ECEARTHr1-RACMO	-1.93	-2.83	-2.00	-2.21	-2.50	-4.83	-3.41	-2.64
ECEARTHr3-HIRHAM	0.15	0.33	0.42	0.25	-0.29	-1.24	-0.07	0.23
ECEARTHr3-RACMO	-1.84	-2.50	-1.74	-2.10	-2.46	-4.68	-3.41	-2.73
ECEARTHr3-RCA	-1.34	-1.95	-1.21	-1.15	-2.95	-3.54	-2.45	-1.31
ECEARTHr12-RCA	-1.37	-2.29	-1.48	-1.40	-3.00	-3.87	-2.56	-1.43
HADGEMr1-CCLM	0.44	0.79	1.00	0.69	0.59	0.36	0.93	1.41
HADGEMr1-HIRHAM	1.45	1.44	1.60	1.35	0.99	-0.57	1.09	1.57
HADGEMr1-RACMO	-0.60	-1.30	-0.63	-1.24	-1.65	-3.42	-2.11	-1.71
HADGEMr1-RCA	0.03	-0.95	-0.11	-0.13	-1.51	-2.15	-1.05	0.06
HADGEMr1-REGCM	0.45	0.29	0.72	1.07	-0.74	-0.87	-0.12	1.40
HADGEMr1-REMO2015	1.34	1.03	1.37	1.34	0.90	0.40	1.06	1.30
HADGEMr1-WRF361H	-0.54	-0.68	-1.17	-1.07	-1.56	-1.75	-0.80	-1.62
HADGEMr1-WRF381P	-1.10	-0.44	-0.95	-0.89	-0.57	-0.47	0.41	-0.10
IPSLr1-RCA	-1.57	-1.26	-0.68	-0.83	-3.67	-2.33	-1.06	-0.38
IPSLr1-WRF381P	-3.01	-1.80	-2.02	-2.21	-3.16	-2.12	-1.14	-1.68
MIROCr1-CCLM	0.21	-0.14	0.30	0.15	-0.42	-0.25	0.08	0.40
MIROCr1-REMO2015	0.87	0.27	0.63	0.33	-1.56	-0.61	0.47	-0.16
MPIr1-CCLM	0.06	0.56	0.54	0.49	0.59	-0.11	0.57	0.97
MPIr1-RCA	-0.31	-0.93	-0.27	-0.02	-1.55	-2.08	-0.93	0.32
MPIr1-REMO	0.99	0.78	1.15	1.35	0.14	-0.01	0.85	1.14
MPIr1-WRF361H	-0.79	-0.84	-1.18	-0.97	-1.41	-1.89	-0.96	-1.42
MPIr2-REMO	0.84	0.69	1.05	1.21	0.34	-0.15	0.89	1.19
NORESMr1-HIRHAM	1.05	1.67	1.56	1.35	0.24	0.04	1.28	1.64
NORESMr1-RCA	-0.47	-0.88	-0.14	-0.24	-2.58	-2.21	-1.07	-0.06
NORESMr1-REMO2015	1.10	1.10	1.46	1.50	0.48	0.24	1.00	1.63

Table 6: Same as Table 3 for the bias of the number of days with daily maximum temperature above 35 degrees. Numbers are colored when the bias exceeds 2 days.

	BI	IP	FR	ME	SC	AL	MD	EA
E-OBS (°C)	0.00	11.27	1.04	0.39	0.00	0.73	4.27	0.56
Ensemble Mean bias (°C)	0.00	-2.91	-0.27	-0.13	0.04	0.57	3.81	2.18
CANESMr1-CCLM	0.02	-1.57	0.65	0.16	0.37	3.20	12.14	13.61
CANESMr1-REMO2015	-0.00	6.39	-0.68	-0.37	-0.00	0.24	15.52	1.20
CNRMr1-ALADIN63	-0.00	-5.65	-0.64	-0.12	0.07	0.09	0.83	2.32
CNRMr1-RACMO	-0.00	-8.73	-0.98	-0.35	-0.00	-0.69	-2.32	-0.32
ECEARTHr12-CCLM	0.00	-0.76	-0.49	-0.29	0.01	-0.04	2.43	1.44
ECEARTHr12-HIRHAM	-0.00	-9.32	-1.04	-0.39	-0.00	-0.72	-3.02	-0.52
ECEARTHr12-RACMO	0.00	-7.91	-0.94	-0.37	-0.00	-0.68	-1.76	-0.32
ECEARTHr12-REMO2015	-0.00	-2.87	-0.94	-0.38	-0.00	-0.46	4.77	0.23
ECEARTHr1-HIRHAM	-0.00	-9.12	-1.04	-0.39	-0.00	-0.70	-3.03	-0.53
ECEARTHr1-RACMO	-0.00	-8.26	-0.94	-0.37	-0.00	-0.64	-1.38	-0.33
ECEARTHr3-HIRHAM	-0.00	-9.12	-1.04	-0.39	-0.00	-0.70	-3.03	-0.53
ECEARTHr3-RACMO	-0.00	-8.28	-0.97	-0.38	-0.00	-0.65	-2.12	-0.34
ECEARTHr3-RCA	-0.00	-5.44	-0.32	-0.23	0.01	0.58	-0.61	0.72
ECEARTHr12-RCA	-0.00	-5.42	-0.55	-0.34	-0.00	0.48	-0.11	0.97
HADGEMr1-CCLM	0.01	6.23	2.31	0.67	0.20	3.79	10.75	9.72
HADGEMr1-HIRHAM	-0.00	-1.99	-0.60	-0.36	-0.00	0.24	0.99	0.31
HADGEMr1-RACMO	0.01	0.39	0.98	0.32	0.01	0.35	1.99	1.11
HADGEMr1-RCA	0.03	2.01	2.15	0.57	0.02	3.30	4.42	4.71
HADGEMr1-REGCM	0.03	-7.70	1.59	1.70	0.24	1.71	0.15	8.46
HADGEMr1-REMO2015	0.00	8.56	0.66	-0.19	-0.00	1.48	17.25	3.09
HADGEMr1-WRF361H	0.01	0.84	0.04	-0.08	-0.00	1.23	1.79	2.96
HADGEMr1-WRF381P	0.00	-3.04	0.05	0.46	0.19	1.72	8.28	9.98
IPSLr1-RCA	-0.00	0.48	0.54	-0.14	-0.00	2.40	7.02	2.23
IPSLr1-WRF381P	0.00	-10.03	-0.96	-0.01	0.01	-0.47	-2.53	1.02
MIROCr1-CCLM	-0.00	-6.51	-0.85	-0.04	0.12	-0.14	1.08	2.45
MIROCr1-REMO2015	-0.00	-2.67	-0.81	-0.35	0.00	-0.00	10.38	0.36
MPIr1-CCLM	0.00	2.50	-0.22	-0.32	-0.00	0.20	5.01	0.74
MPIr1-RCA	0.00	0.36	0.09	-0.25	-0.00	1.49	3.72	2.17
MPIr1-REMO	0.01	0.79	-0.35	-0.28	-0.00	0.65	12.68	1.68
MPIr1-WRF361H	-0.00	-2.88	-0.51	-0.29	-0.00	0.55	0.42	1.08
MPIr2-REMO	-0.00	0.41	-0.77	-0.33	-0.00	0.62	14.93	1.93
NORESMr1-HIRHAM	-0.00	-7.98	-1.03	-0.39	-0.00	-0.65	-2.01	-0.46
NORESMr1-RCA	-0.00	-4.69	-0.70	-0.34	0.00	1.29	1.50	1.96
NORESMr1-REMO2015	-0.00	1.85	-0.80	-0.38	-0.00	0.43	13.41	1.05

Table 7: Same as Table 6 for the bias of the number of freezing days (minimum daily temperature below 0°C). Numbers higher than 20 days are colored.

	BI	IP	FR	ME	SC	AL	MD	EA
E-OBS (°C)	51.16	40.97	52.23	84.66	181.97	115.96	55.60	114.47
Ensemble Mean bias (°C)	3.72	0.80	-5.37	-0.66	12.00	16.06	2.15	0.26
CANESMr1-CCLM	-12.21	-15.08	-28.19	-27.53	-11.28	-18.61	-18.27	-27.59
CANESMr1-REMO2015	-31.36	-24.63	-36.76	-42.16	-28.42	-31.29	-29.73	-38.08
CNRMr1-ALADIN63	55.80	24.64	24.90	30.88	20.11	46.29	22.56	21.08
CNRMr1-RACMO	62.27	43.47	34.10	48.66	42.92	77.90	45.43	45.37
ECEARTHr12-CCLM	10.14	-2.08	-5.85	2.35	10.66	6.07	-0.17	0.46
ECEARTHr12-HIRHAM	-1.62	-3.88	-10.24	-3.63	6.93	16.58	-1.47	-0.85
ECEARTHr12-RACMO	40.24	43.33	27.85	41.11	45.44	79.46	46.70	43.75
ECEARTHr12-REMO2015	-13.72	-10.45	-15.89	-11.59	-6.36	-4.82	-11.79	-7.00
ECEARTHr1-HIRHAM	-5.13	-9.27	-15.64	-10.19	3.94	9.88	-5.95	-6.09
ECEARTHr1-RACMO	38.27	38.14	24.32	36.25	43.22	75.07	42.83	41.40
ECEARTHr3-HIRHAM	-5.13	-9.27	-15.64	-10.19	3.94	9.88	-5.95	-6.09
ECEARTHr3-RACMO	38.27	32.31	20.48	32.83	43.33	71.60	42.98	41.74
ECEARTHr3-RCA	12.74	11.26	-1.83	3.68	39.78	42.61	18.57	10.22
ECEARTHr12-RCA	10.77	17.14	2.24	8.04	38.29	47.34	20.19	13.63
HADGEMr1-CCLM	-7.66	-8.06	-13.67	-9.37	-3.64	-3.76	-5.21	-9.19
HADGEMr1-HIRHAM	-21.16	-9.28	-18.43	-19.56	-16.69	5.09	-7.26	-19.33
HADGEMr1-RACMO	17.99	27.20	14.19	25.46	26.57	53.99	33.73	30.23
HADGEMr1-RCA	-10.66	5.58	-7.19	-9.15	13.99	25.07	6.97	-7.95
HADGEMr1-REGCM	-10.70	-3.03	-8.92	-18.21	10.90	10.28	3.42	-18.84
HADGEMr1-REMO2015	-29.29	-18.92	-24.44	-24.62	-25.57	-23.52	-19.50	-20.61
HADGEMr1-WRF361H	-7.73	1.94	2.71	5.77	20.02	11.67	0.10	16.04
HADGEMr1-WRF381P	23.50	1.38	13.26	23.29	14.23	8.59	-2.35	10.76
IPSLr1-RCA	19.13	7.06	-10.64	-4.49	43.35	27.48	4.99	-5.13
IPSLr1-WRF381P	78.66	19.77	33.41	56.49	44.65	37.59	13.61	35.69
MIROCr1-CCLM	3.71	-5.37	0.26	11.27	13.51	2.57	2.80	10.07
MIROCr1-REMO2015	-12.22	-13.72	-4.96	5.68	3.87	-5.15	-12.02	5.55
MPIr1-CCLM	-11.73	-12.75	-20.11	-19.85	-4.74	-7.39	-12.70	-21.83
MPIr1-RCA	-4.95	-0.77	-10.94	-11.41	16.12	20.18	-1.14	-16.22
MPIr1-REMO	-24.93	-20.76	-25.39	-25.06	-13.87	-19.25	-21.46	-20.76
MPIr1-WRF361H	-2.49	-3.12	-0.87	3.09	23.66	11.23	-5.37	10.81
MPIr2-REMO	-23.47	-21.50	-27.73	-27.15	-15.68	-19.74	-22.40	-22.68
NORESMr1-HIRHAM	-18.25	-22.35	-28.01	-30.12	-5.59	-10.58	-20.11	-31.40
NORESMr1-RCA	-3.29	-6.52	-17.94	-15.65	30.80	20.79	-2.25	-11.65
NORESMr1-REMO2015	-27.43	-25.36	-31.15	-37.41	-20.30	-26.97	-26.80	-36.53

8.2 Precipitation biases

Mean precipitation biases are shown in Figure 8 (yearly) and in Tables 8 and 9 (winter and summer separately). Bias patterns exhibit a mixture of GCM and RCM signals. However, in general precipitations are overestimated, sometimes by a large factor reaching more than 50% (e.g. for some RCA and HIRHAM simulations in Northern and Central Europe). Biases are consistent with previous analyses (eg. From Kotlarski *et al*., 2016).

In general, precipitation bias is strong in winter with relative overall bias in the range of 20-55%, and weaker in summer for Central to Northern Europe while it is strong in Mediterranean regions (Tables 8 and 9). However due to weak mean precipitation there, we expect percentage of change to be very sensitive.

Heavy precipitation is characterized in Figure 9 (yearly) and in Tables 10 and 11 (for seasonal analysis). In this case models mostly overestimate the E-OBS values. A few models do, however, have reduced biases (and sometimes positive biases), such as CCLM, WRF381P and REGCM. Careful interpretations must be drawn from this, as we need to keep in mind that E-OBS observational dataset may itself have biases in the extremes due to averaging in relatively large cells (0.22°C).

Seasonal analysis (Tables 10 and 11) shows that in this case positive biases are higher in summer than in winter. This may be due to convective situations with very local extreme precipitation for which E-OBS may not be well suited.

The number of wet days (with amount larger than 1mm/day, see Tables 12 and 13) is positively biased as for the mean precipitation, with a larger winter bias than the summer bias. Among those wet days, extremes as characterized by the 99th percentile daily amount behave as the extremes in all days measured by RX1d, with positive biases again in winter and summer (Tables 14 and 15). Note that some models keep a pretty homogeneously weak bias in winter and summer such as RACMO downscaling EC-EARTH or HADGEM, and WRF381P downscaling IPSL and REGCM downscaling HADGEM.

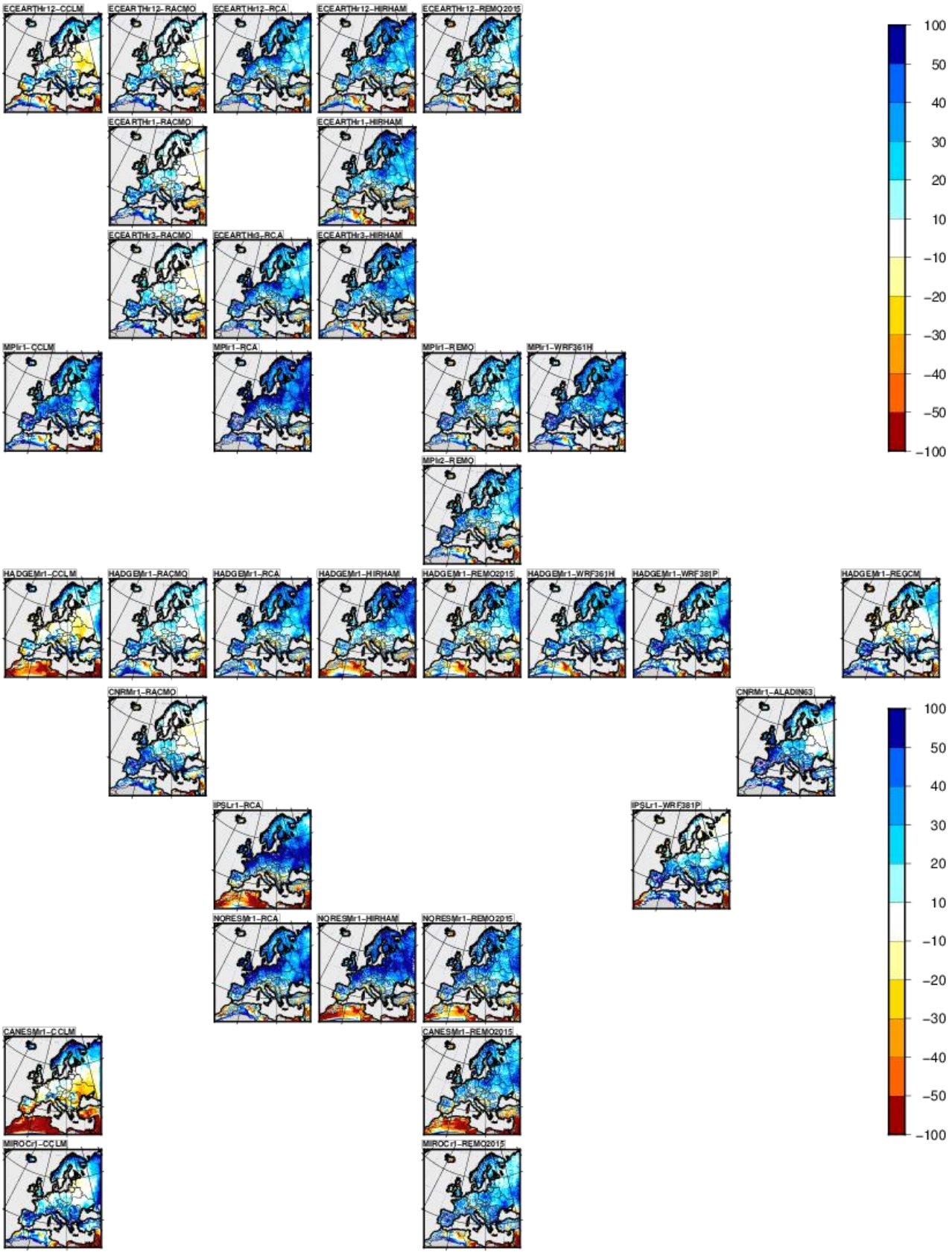

Figure 8: Bias of the mean precipitation for each model in % of EOBS climatology.

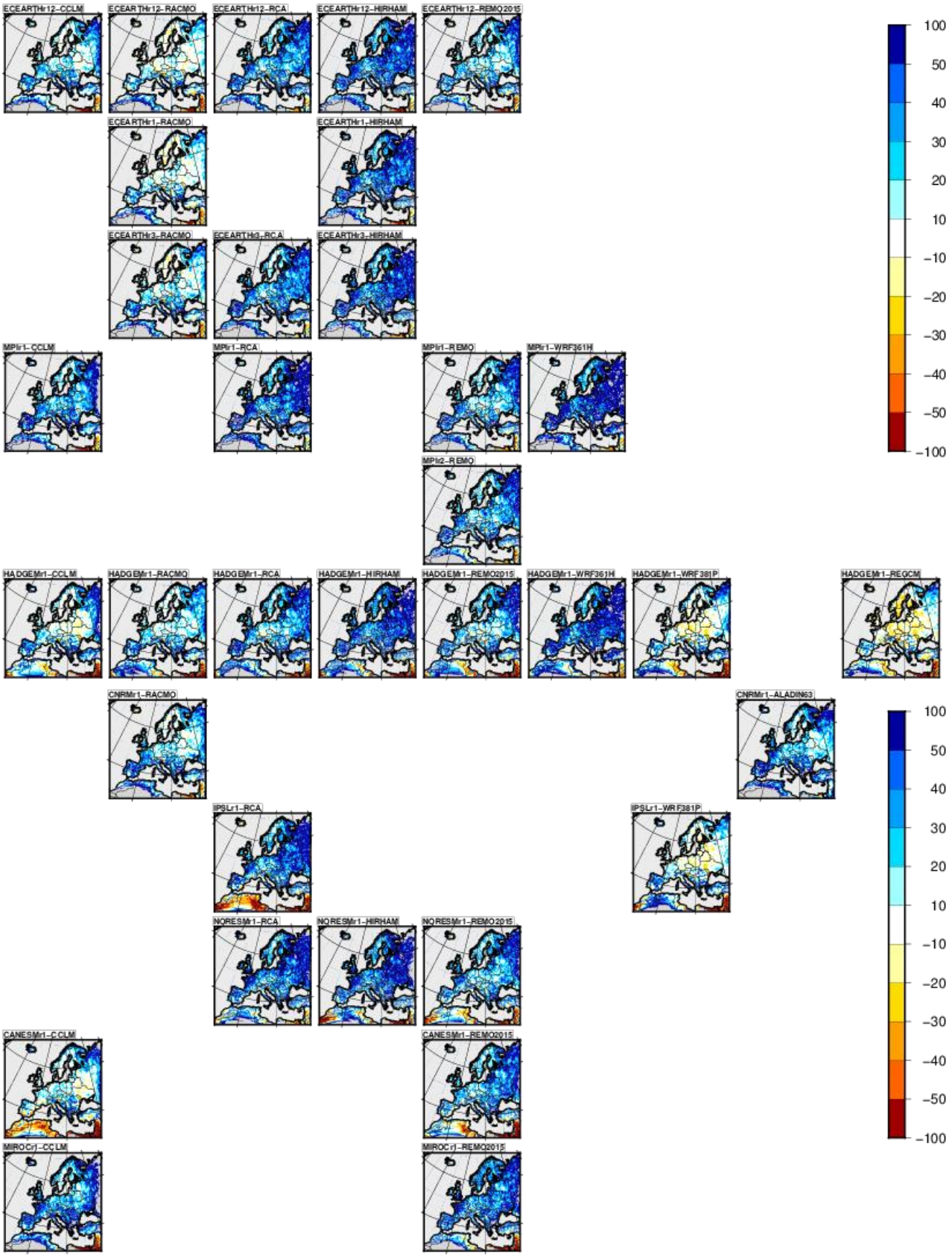

Figure 9: Same as Figure 8 for the RX1D bias (annual maximum of daily amount).

Tables on precipitation indices

The tables hereafter list results for a number of precipitation indices inferred from all available EUR-11 simulations for the eight Prudence Regions.

Each table utilizes the same layout as for Tables 3 to 7. At the top-left the parameter followed by the season (DJF or JJA) is indicated. The top row lists the acronyms of the eight PRUDENCE subregions. The 2nd row lists the absolute values (either in mm/day or %) derived from the observational dataset E-OBS version 17.0 compiled on the 0.22° (~25 km) rotated-pole grid. The 3rd row lists the bias (%) of the ensemble mean relative to the E-OBS. The next 34 rows list the bias of each of the individual GCM-RCM combinations.

The following precipitation indices are tabulated:

- Rmean [mm/d]: the daily-mean precipitation
- RX1d [mm/d]: 30-year mean maximum 1-day precipitation
- wdf [%]: wet-day frequency
- R99w [mm/d]: 99th percentile of daily precipitation for wet days

Wet days are defined as days on which the amount of precipitation is equal to or above 1 mm. All indices are calculated either per year, or for each of the four seasons. Regarding RX5d, the central day of the 5-day period determines the year and the season it belongs to.

The ensemble mean for each of the precipitation indices is obtained by averaging the precipitation indices from all 33 model members with equal weight for both the reference period and the future period (IPSLr1-WRF381P is removed).

In order to obtain the relative biases/changes in each of the indices per PRUDENCE sub-region, the relative biases/changes are first determined at the grid box level, and then averaged across the region. For ease of computation of the bias, the E-OBS data set is projected onto the EUR 0.11° domain without interpolation, making use of the feature that each grid cell in EUR-22 exactly encompasses four grid cells in EUR-11.

Table 8: Winter (DJF) mean precipitation (Rmean DJF) for the eight PRUDENCE regions based on E-OBS. Biases w.r.t. E-OBS for the 34 GCM-RCM combinations and the ensemble mean.

	BI	IP	FR	ME	SC	AL	MD	EA
E-OBS (mm/day)	3.41	2.04	2.26	1.96	1.87	2.60	2.10	1.20
Ensemble mean bias (%)	20	51	45	33	37	54	43	47
CANESMr1-CCLM	24	25	36	43	63	56	8	58
CANESMr1-REMO2015	22	33	57	42	53	53	**-3**	42
CNRMr1-ALADIN63	34	101	56	28	28	84	109	52
CNRMr1-RACMO	12	54	46	23	10	56	49	34
ECEARTHr12-CCLM	6	23	11	11	34	34	24	32
ECEARTHr12-HIRHAM	29	52	41	34	50	57	66	50
ECEARTHr3-HIRHAM	32	59	46	37	49	68	67	56
ECEARTHr1-HIRHAM	31	52	43	38	62	80	52	57
ECEARTHr12-RACMO	14	31	28	10	24	29	38	16
ECEARTHr1-RACMO	14	34	34	20	31	48	31	26
ECEARTHr3-RACMO	15	36	37	18	24	40	39	26
ECEARTHr12-RCA	37	47	46	22	42	37	41	20
ECEARTHr3-RCA	40	49	55	32	40	50	43	33
ECEARTHr12-REMO2015	4	17	18	9	31	21	3	16
HADGEMr1-CCLM	7	30	26	34	35	47	34	62
HADGEMr1-HIRHAM	29	46	46	49	59	67	51	67
HADGEMr1-RACMO	15	37	44	29	28	43	47	43
HADGEMr1-RCA	40	47	51	37	51	45	41	42
HADGEMr1-REMO2015	2	15	25	23	34	28	0	29
HADGEMr1-REGCM	**-28**	10	**-7**	**-5**	2	7	14	25
HADGEMr1-WRF361H	17	39	41	29	36	38	61	48
HADGEMr1-WRF381P	**-4**	36	34	28	20	49	42	67
IPSLr1-RCA	45	53	94	65	41	88	28	63
IPSLr1-WRF381P	N/A	N/A	N/A	N/A	N/A	N/A	N/A	N/A
MIROCr1-CCLM	**-7**	56	11	28	32	46	60	74
MIROCr1-REMO2015	**-16**	37	12	19	12	31	43	57
MPIr1-CCLM	12	103	52	37	31	78	62	71
MPIr1-RCA	37	116	77	37	36	81	77	50
MPIr1-REMO	14	86	62	35	25	61	39	46
MPIr2-REMO	14	83	56	34	31	62	30	43
MPIr1-WRF361H	17	95	54	24	31	56	71	50
NORESMr1-HIRHAM	49	78	93	83	68	112	78	86
NORESMr1-REMO2015	27	35	68	58	45	58	5	47
NORESMr1-RCA	49	72	94	60	42	73	62	50

Table 9: As Table 8 for Rmean JJA.

	BI	IP	FR	ME	SC	AL	MD	EA
E-OBS (mm/day)	2.45	0.69	1.81	2.33	2.48	3.26	0.87	2.28
Ensemble mean bias (%)	25	110	27	15	20	29	113	1
CANESMr1-CCLM	**-37**	**-55**	**-55**	**-38**	**-7**	**-17**	**-44**	**-61**
CANESMr1-REMO2015	7	91	23	21	19	42	98	21
CNRMr1-ALADIN63	71	213	104	26	16	88	331	**-5**
CNRMr1-RACMO	39	231	78	19	**-7**	57	290	4
ECEARTHr12-CCLM	0	10	**-8**	**-5**	2	38	58	**-26**
ECEARTHr12-HIRHAM	16	31	24	22	32	48	61	21
ECEARTHr3-HIRHAM	9	68	27	18	26	45	86	16
ECEARTHr1-HIRHAM	13	39	21	13	32	38	46	9
ECEARTHr12-RACMO	18	85	23	7	4	25	93	**-4**
ECEARTHr1-RACMO	16	99	26	11	4	22	86	**-5**
ECEARTHr3-RACMO	9	125	14	2	**-4**	18	131	**-2**
ECEARTHr12-RCA	50	73	27	34	34	4	84	13
ECEARTHr3-RCA	42	123	35	32	27	10	126	19
ECEARTHr12-REMO2015	22	119	34	20	17	37	108	12
HADGEMr1-CCLM	**-27**	**-16**	**-47**	**-43**	**-8**	**-16**	15	**-61**
HADGEMr1-HIRHAM	**-4**	17	**-11**	**-4**	28	8	27	**-6**
HADGEMr1-RACMO	6	87	**-5**	**-8**	6	7	69	**-20**
HADGEMr1-RCA	33	117	2	3	32	**-14**	143	**-12**
HADGEMr1-REMO2015	10	170	10	9	29	33	153	1
HADGEMr1-REGCM	5	400	8	**-9**	14	23	215	**-21**
HADGEMr1-WRF361H	22	93	23	18	30	49	191	17
HADGEMr1-WRF381P	21	243	49	22	15	40	168	**-1**
IPSLr1-RCA	50	58	25	30	31	7	93	22
IPSLr1-WRF381P	N/A	N/A	N/A	N/A	N/A	N/A	N/A	N/A
MIROCr1-CCLM	11	59	36	**-6**	**-14**	53	166	**-30**
MIROCr1-REMO2015	39	248	77	32	27	73	244	24
MPIr1-CCLM	35	42	38	40	30	57	60	6
MPIr1-RCA	80	130	59	58	54	14	106	21
MPIr1-REMO	31	126	32	19	17	13	76	**-3**
MPIr2-REMO	33	118	45	24	17	15	69	2
MPIr1-WRF361H	46	110	54	41	44	48	153	30
NORESMr1-HIRHAM	29	51	32	25	36	38	37	16
NORESMr1-REMO2015	40	199	36	26	25	35	117	11
NORESMr1-RCA	82	132	51	48	37	7	84	8

Table 10: As Table 8 for RX1d DJF.

	BI	IP	FR	ME	SC	AL	MD	EA
E-OBS (mm/day)	23.8	23.6	21.5	18.4	15.5	32.7	23.9	12.8
Ensemble mean bias (%)	17	50	22	9	19	36	62	36
CANESMr1-CCLM	11	21	8	8	24	14	26	35
CANESMr1-REMO2015	27	48	29	22	35	55	48	47
CNRMr1-ALADIN63	15	67	16	0	14	29	84	42
CNRMr1-RACMO	2	42	10	**-3**	**-1**	33	55	23
ECEARTHr12-CCLM	4	28	3	**-3**	7	9	43	22
ECEARTHr12-HIRHAM	24	51	20	12	25	44	91	44
ECEARTHr3-HIRHAM	27	58	26	11	25	56	92	46
ECEARTHr1-HIRHAM	26	60	26	9	31	64	85	48
ECEARTHr12-RACMO	4	25	7	**-2**	5	24	52	14
ECEARTHr1-RACMO	2	32	13	**-4**	11	38	51	22
ECEARTHr3-RACMO	5	30	11	**-2**	9	31	52	22
ECEARTHr12-RCA	20	48	23	3	7	25	55	18
ECEARTHr3-RCA	26	50	25	3	10	32	53	22
ECEARTHr12-REMO2015	15	40	13	8	21	36	60	28
HADGEMr1-CCLM	10	35	15	5	16	11	43	35
HADGEMr1-HIRHAM	32	64	33	23	39	59	89	55
HADGEMr1-RACMO	9	39	21	6	17	33	56	33
HADGEMr1-RCA	31	61	32	12	26	32	60	36
HADGEMr1-REMO2015	16	48	25	15	31	43	59	37
HADGEMr1-REGCM	**-15**	12	**-11**	**-10**	**-5**	4	17	14
HADGEMr1-WRF361H	18	49	20	6	28	21	79	43
HADGEMr1-WRF381P	8	37	11	8	19	18	49	49
IPSLr1-RCA	17	50	35	13	8	40	34	36
IPSLr1-WRF381P	N/A	N/A	N/A	N/A	N/A	N/A	N/A	N/A
MIROCr1-CCLM	13	46	8	9	18	13	56	46
MIROCr1-REMO2015	14	59	18	13	15	43	78	51
MPIr1-CCLM	7	65	18	3	14	22	58	38
MPIr1-RCA	21	87	36	4	14	42	74	37
MPIr1-REMO	21	79	34	15	24	57	80	44
MPIr2-REMO	21	81	36	19	26	66	76	42
MPIr1-WRF361H	15	71	25	3	25	29	78	43
NORESMr1-HIRHAM	41	57	46	33	38	71	90	56
NORESMr1-REMO2015	32	45	41	33	32	55	55	41
NORESMr1-RCA	31	50	42	19	13	41	63	31

Table 11: As Table 8 for RX1d JJA.

	BI	IP	FR	ME	SC	AL	MD	EA
E-OBS (mm/day)	23.1	14.5	22.8	25.0	25.4	35.8	15.7	26.1
Ensemble mean bias (%)	25	50	34	22	19	24	67	18
CANESMr1-CCLM	**-12**	**-34**	**-14**	7	6	9	**-13**	**-14**
CANESMr1-REMO2015	15	41	30	18	24	27	52	28
CNRMr1-ALADIN63	47	109	67	34	18	50	170	18
CNRMr1-RACMO	28	97	49	21	2	35	128	12
ECEARTHr12-CCLM	12	25	24	17	5	37	68	10
ECEARTHr12-HIRHAM	29	44	57	36	36	51	80	47
ECEARTHr3-HIRHAM	35	73	64	39	33	51	99	43
ECEARTHr1-HIRHAM	36	46	59	36	37	44	72	41
ECEARTHr12-RACMO	3	30	10	**-1**	**-1**	15	50	0
ECEARTHr1-RACMO	3	33	11	4	**-1**	8	40	0
ECEARTHr3-RACMO	9	60	15	7	0	14	66	10
ECEARTHr12-RCA	25	32	30	27	25	14	48	19
ECEARTHr3-RCA	29	56	29	25	23	17	72	24
ECEARTHr12-REMO2015	23	47	29	20	13	21	50	10
HADGEMr1-CCLM	3	4	**-5**	**-5**	1	7	39	**-22**
HADGEMr1-HIRHAM	35	23	43	32	42	32	35	40
HADGEMr1-RACMO	7	25	10	4	6	10	33	0
HADGEMr1-RCA	27	23	8	8	24	**-11**	44	**-3**
HADGEMr1-REMO2015	22	54	14	10	22	10	49	5
HADGEMr1-REGCM	**-8**	84	**-4**	**-15**	**-14**	**-15**	35	**-18**
HADGEMr1-WRF361H	44	71	52	48	36	47	162	55
HADGEMr1-WRF381P	3	57	4	**-12**	**-3**	**-8**	53	**-20**
IPSLr1-RCA	37	4	27	29	31	6	34	30
IPSLr1-WRF381P	N/A	N/A	N/A	N/A	N/A	N/A	N/A	N/A
MIROCr1-CCLM	33	63	68	39	14	59	156	23
MIROCr1-REMO2015	55	106	78	41	37	42	110	35
MPIr1-CCLM	24	49	38	30	20	47	70	25
MPIr1-RCA	41	61	49	39	36	22	56	26
MPIr1-REMO	21	68	37	17	17	22	43	8
MPIr2-REMO	21	59	40	21	17	19	42	17
MPIr1-WRF361H	38	94	65	58	42	52	136	62
NORESMr1-HIRHAM	41	41	61	35	39	40	55	46
NORESMr1-REMO2015	36	64	31	19	20	12	46	14
NORESMr1-RCA	51	39	39	35	33	6	34	21

Table 12: As Table 8 for winter (DJF) wet day frequency (wdf). Units %.

	BI	IP	FR	ME	SC	AL	MD	EA
E-OBS (%)	50.8	27.5	39.4	38.5	37.9	30.3	30.8	29.8
Ensemble mean bias (%)	9	20	25	23	20	24	3	18
CANESMr1-CCLM	18	13	26	34	40	43	**-10**	30
CANESMr1-REMO2015	0	2	28	23	25	6	**-34**	8
CNRMr1-ALADIN63	16	44	35	24	12	51	30	19
CNRMr1-RACMO	14	33	37	27	9	41	20	16
ECEARTHr12-CCLM	6	9	6	11	26	29	0	15
ECEARTHr12-HIRHAM	15	16	21	24	26	15	**-1**	17
ECEARTHr3-HIRHAM	15	19	23	23	26	17	**-2**	20
ECEARTHr1-HIRHAM	15	12	19	28	33	18	**-10**	20
ECEARTHr12-RACMO	15	19	20	12	18	18	12	3
ECEARTHr1-RACMO	15	20	22	21	22	22	6	10
ECEARTHr3-RACMO	15	23	27	20	17	24	13	10
ECEARTHr12-RCA	27	22	28	22	31	18	7	6
ECEARTHr3-RCA	29	23	36	31	29	26	10	15
ECEARTHr12-REMO2015	**-5**	**-7**	4	2	12	**-9**	**-29**	**-6**
HADGEMr1-CCLM	3	10	14	24	21	39	8	34
HADGEMr1-HIRHAM	8	4	16	26	27	8	**-12**	24
HADGEMr1-RACMO	11	18	26	23	15	23	16	18
HADGEMr1-RCA	24	16	25	27	30	17	5	16
HADGEMr1-REMO2015	**-10**	**-13**	4	7	10	**-8**	**-33**	1
HADGEMr1-REGCM	**-13**	20	6	6	7	26	17	19
HADGEMr1-WRF361H	3	10	21	20	12	15	8	18
HADGEMr1-WRF381P	**-7**	18	23	20	6	31	12	30
IPSLr1-RCA	36	23	59	55	30	46	**-1**	33
IPSLr1-WRF381P	N/A	N/A	N/A	N/A	N/A	N/A	N/A	N/A
MIROCr1-CCLM	**-12**	31	5	19	17	40	25	36
MIROCr1-REMO2015	**-23**	3	**-2**	7	0	0	**-7**	18
MPIr1-CCLM	6	55	33	29	18	59	23	39
MPIr1-RCA	24	57	44	32	23	42	26	23
MPIr1-REMO	**-1**	29	28	19	5	13	**-10**	12
MPIr2-REMO	**-2**	26	25	16	10	12	**-16**	10
MPIr1-WRF361H	3	41	27	18	10	27	16	19
NORESMr1-HIRHAM	21	33	49	50	36	35	5	37
NORESMr1-REMO2015	4	5	33	30	19	11	**-27**	14
NORESMr1-RCA	31	44	59	45	31	40	19	25

Table 13: As Table 12 for wdf JJA.

	BI	IP	FR	ME	SC	AL	MD	EA
E-OBS (%)	42.4	10.9	29.5	37.8	39.7	35.9	13.5	34.2
Ensemble mean bias (%)	12	106	14	7	8	21	85	**-4**
CANESMr1-CCLM	**-32**	**-53**	**-54**	**-42**	**-9**	**-18**	**-46**	**-62**
CANESMr1-REMO2015	**-1**	82	14	15	9	31	78	15
CNRMr1-ALADIN63	31	154	56	4	**-5**	44	191	**-16**
CNRMr1-RACMO	27	231	58	15	**-8**	58	251	7
ECEARTHr12-CCLM	**-4**	**-1**	**-17**	**-9**	**-1**	21	27	**-29**
ECEARTHr12-HIRHAM	4	13	6	11	11	14	16	7
ECEARTHr3-HIRHAM	**-5**	41	6	5	5	14	33	5
ECEARTHr1-HIRHAM	0	20	3	4	9	10	8	**-3**
ECEARTHr12-RACMO	20	107	23	13	5	33	94	2
ECEARTHr1-RACMO	20	117	26	16	5	34	90	2
ECEARTHr3-RACMO	9	135	14	4	**-4**	30	122	2
ECEARTHr12-RCA	38	89	17	21	18	**-1**	64	4
ECEARTHr3-RCA	29	126	22	18	13	4	87	8
ECEARTHr12-REMO2015	5	118	22	11	7	29	95	11
HADGEMr1-CCLM	**-29**	**-24**	**-49**	**-43**	**-9**	**-16**	**-4**	**-59**
HADGEMr1-HIRHAM	**-16**	14	**-19**	**-9**	5	**-2**	8	**-12**
HADGEMr1-RACMO	7	125	**-3**	**-5**	4	23	86	**-14**
HADGEMr1-RCA	20	134	**-3**	**-3**	16	**-8**	108	**-10**
HADGEMr1-REMO2015	**-4**	182	6	4	15	34	157	5
HADGEMr1-REGCM	15	426	20	4	32	61	265	**-6**
HADGEMr1-WRF361H	**-6**	74	**-4**	**-6**	7	20	97	**-6**
HADGEMr1-WRF381P	18	256	51	27	19	55	153	15
IPSLr1-RCA	34	79	15	16	12	6	79	8
IPSLr1-WRF381P	N/A	N/A	N/A	N/A	N/A	N/A	N/A	N/A
MIROCr1-CCLM	**-6**	34	7	**-21**	**-23**	29	84	**-41**
MIROCr1-REMO2015	7	200	41	12	6	50	184	12
MPIr1-CCLM	24	19	18	28	24	26	26	2
MPIr1-RCA	53	123	34	34	30	2	75	9
MPIr1-REMO	21	116	26	18	10	13	73	5
MPIr2-REMO	23	111	35	23	11	16	66	6
MPIr1-WRF361H	16	71	16	8	15	12	74	2
NORESMr1-HIRHAM	8	40	14	17	12	17	7	6
NORESMr1-REMO2015	14	187	25	18	14	30	110	10
NORESMr1-RCA	50	135	32	28	19	4	64	1

Table 14: R99w DJF

	BI	IP	FR	ME	SC	AL	MD	EA
E-OBS (mm/day)	25.0	30.0	24.0	20.6	17.4	40.5	29.5	15.5
Ensemble mean bias (%)	14	48	16	4	14	31	65	31
CANESMr1-CCLM	5	20	3	0	14	3	34	25
CANESMr1-REMO2015	23	48	21	17	26	54	74	48
CNRMr1-ALADIN63	11	55	7	**-5**	11	14	71	35
CNRMr1-RACMO	**-1**	31	2	**-7**	**-4**	21	48	18
ECEARTHr12-CCLM	1	30	2	**-6**	1	1	44	17
ECEARTHr12-HIRHAM	19	52	15	6	19	40	94	40
ECEARTHr3-HIRHAM	22	57	20	6	18	50	97	40
ECEARTHr1-HIRHAM	21	59	21	3	22	59	94	43
ECEARTHr12-RACMO	0	23	2	**-6**	1	20	50	13
ECEARTHr1-RACMO	**-3**	27	9	**-7**	5	35	51	19
ECEARTHr3-RACMO	1	27	5	**-6**	4	25	47	17
ECEARTHr12-RCA	14	46	16	**-3**	2	19	57	19
ECEARTHr3-RCA	17	48	18	**-3**	4	26	51	20
ECEARTHr12-REMO2015	16	51	12	7	16	44	84	30
HADGEMr1-CCLM	8	42	13	3	10	3	43	25
HADGEMr1-HIRHAM	30	78	30	18	32	61	100	50
HADGEMr1-RACMO	6	39	16	4	13	29	52	28
HADGEMr1-RCA	23	66	28	8	18	30	63	33
HADGEMr1-REMO2015	19	69	26	16	29	53	90	38
HADGEMr1-REGCM	**-13**	11	**-11**	**-10**	**-8**	1	13	9
HADGEMr1-WRF361H	18	56	17	2	25	19	77	38
HADGEMr1-WRF381P	8	38	8	4	19	16	45	38
IPSLr1-RCA	10	51	22	3	3	31	38	29
IPSLr1-WRF381P	N/A	N/A	N/A	N/A	N/A	N/A	N/A	N/A
MIROCr1-CCLM	16	35	7	6	13	3	46	33
MIROCr1-REMO2015	20	59	20	11	16	47	84	44
MPIr1-CCLM	6	50	11	**-3**	9	9	48	28
MPIr1-RCA	15	68	27	**-1**	10	33	65	31
MPIr1-REMO	23	72	28	12	23	57	89	41
MPIr2-REMO	21	74	28	15	24	64	89	39
MPIr1-WRF361H	16	60	19	**-1**	22	22	72	37
NORESMr1-HIRHAM	33	47	32	21	28	61	91	45
NORESMr1-REMO2015	28	46	32	25	26	54	75	37
NORESMr1-RCA	21	36	27	10	6	31	60	25

Table 15: R99w JJA

	BI	IP	FR	ME	SC	AL	MD	EA
E-OBS (mm/day)	25.8	26.6	27.6	28.1	28.3	41.5	25.9	31.0
Ensemble mean bias (%)	18	28	31	20	17	20	58	20
CANESMr1-CCLM	**-2**	9	23	31	10	21	43	30
CANESMr1-REMO2015	10	14	23	11	20	18	36	19
CNRMr1-ALADIN63	36	55	50	34	20	37	100	26
CNRMr1-RACMO	16	33	31	18	5	19	61	10
ECEARTHr12-CCLM	10	34	32	20	6	30	75	24
ECEARTHr12-HIRHAM	25	59	56	32	32	48	101	43
ECEARTHr3-HIRHAM	34	75	66	39	31	47	113	40
ECEARTHr1-HIRHAM	33	66	61	33	33	43	101	43
ECEARTHr12-RACMO	**-3**	5	4	**-4**	**-3**	6	29	**-1**
ECEARTHr1-RACMO	**-6**	10	4	**-1**	**-2**	1	24	**-3**
ECEARTHr3-RACMO	2	27	13	5	1	7	37	10
ECEARTHr12-RCA	10	13	26	20	20	17	45	17
ECEARTHr3-RCA	17	23	23	19	18	18	60	22
ECEARTHr12-REMO2015	16	13	22	15	11	13	32	4
HADGEMr1-CCLM	15	41	26	17	6	17	69	13
HADGEMr1-HIRHAM	39	44	64	38	41	39	64	51
HADGEMr1-RACMO	4	2	14	6	5	7	25	8
HADGEMr1-RCA	19	**-5**	10	10	19	**-5**	27	0
HADGEMr1-REMO2015	21	10	12	7	18	5	20	0
HADGEMr1-REGCM	**-13**	3	**-7**	**-16**	**-20**	**-24**	**-6**	**-15**
HADGEMr1-WRF361H	44	54	56	53	33	43	137	60
HADGEMr1-WRF381P	**-4**	**-2**	**-8**	**-18**	**-8**	**-18**	14	**-25**
IPSLr1-RCA	23	**-12**	23	24	27	10	30	28
IPSLr1-WRF381P	N/A	N/A	N/A	N/A	N/A	N/A	N/A	N/A
MIROCr1-CCLM	33	55	65	51	26	46	137	51
MIROCr1-REMO2015	45	41	57	33	34	26	60	26
MPIr1-CCLM	12	47	32	20	12	40	75	25
MPIr1-RCA	22	28	41	28	25	25	51	22
MPIr1-REMO	11	30	28	8	13	22	33	4
MPIr2-REMO	10	27	27	10	12	16	37	12
MPIr1-WRF361H	29	69	58	53	35	51	125	60
NORESMr1-HIRHAM	32	45	55	26	34	33	90	43
NORESMr1-REMO2015	24	16	19	10	13	4	30	7
NORESMr1-RCA	30	8	28	23	26	7	35	19

8.3 Dynamics

Dynamics is characterized by atmospheric circulations and winds. The mean atmospheric circulation is measured by sea level pressure. Regarding biases, most models have only light biases with values lower than 2 hPa in absolute value (see Figure 10). Sea level pressure biases are interestingly not always dependent on GCM, such as for ECEARTH downscaled simulations. A few simulations have more pronounced biases (reaching up to 8 hPa in some areas) such as for WRF381P RCM simulations, CANESMr1-CCLM and IPSLr1-RCA. In the WRF381P case, the simulation boundaries were taken relatively far from the boundary of the EURO-CORDEX domain (about 500 km) which could explain a larger departure from the GCM and reanalysis dynamics. As far as flow is concerned, gradients of bias of sea level pressure are important. For a few models a North-South gradient is important such as for NORESMr1 or MIROCr1 downscaled simulations. In the first case the bias is likely to induce a westerly flow bias and in the second case an easterly flow bias.

For wind speeds and storm wind speeds there is a general positive bias (see Figures 11 and 12) which is difficult to explain. Surface wind speed is a highly parameterized diagnostic from models and reanalyses. In many cases, high winds from models are underestimating observations from stations, due to the fine structure of wind patterns in storms. Note also that models tend to have similar bias patterns with different amplitudes. Overestimation is stronger in Southern Europe than in Northern Europe, especially over mountainous areas. Thus the overall overestimation and the patterns here are difficult to interpret.

However, a few interesting points can be noted from Figures 10 and 11 and Tables 16 and 17. The wind biases essentially depend on the RCM and not on the GCM. This confirms that surface wind speeds mostly depend on RCM parameterizations and surface data. A few RCMs (WRF381P, REGCM and RCA to a lesser extent) have larger overestimations than other models.

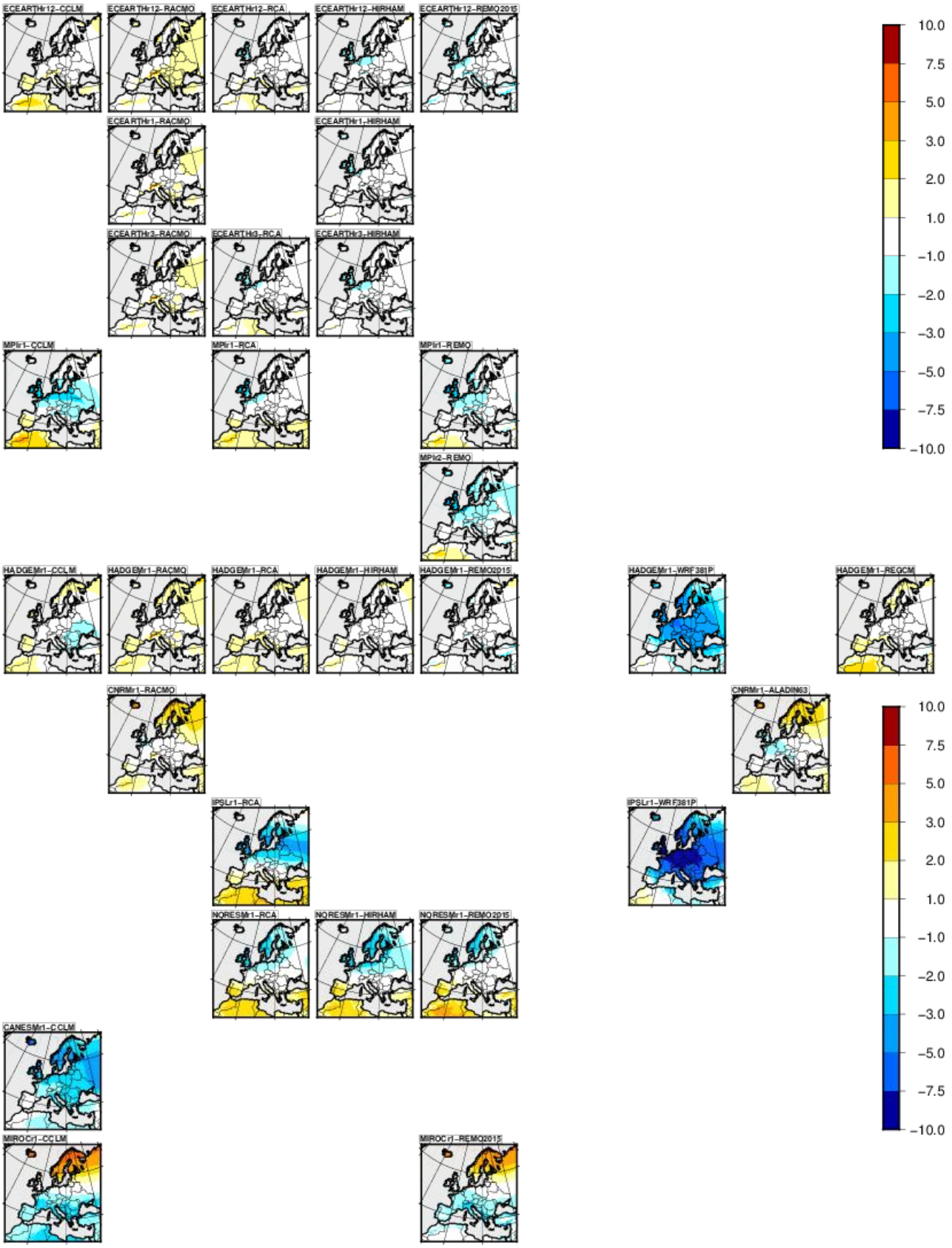

Figure 10: Bias of sea level pressure in hPa.

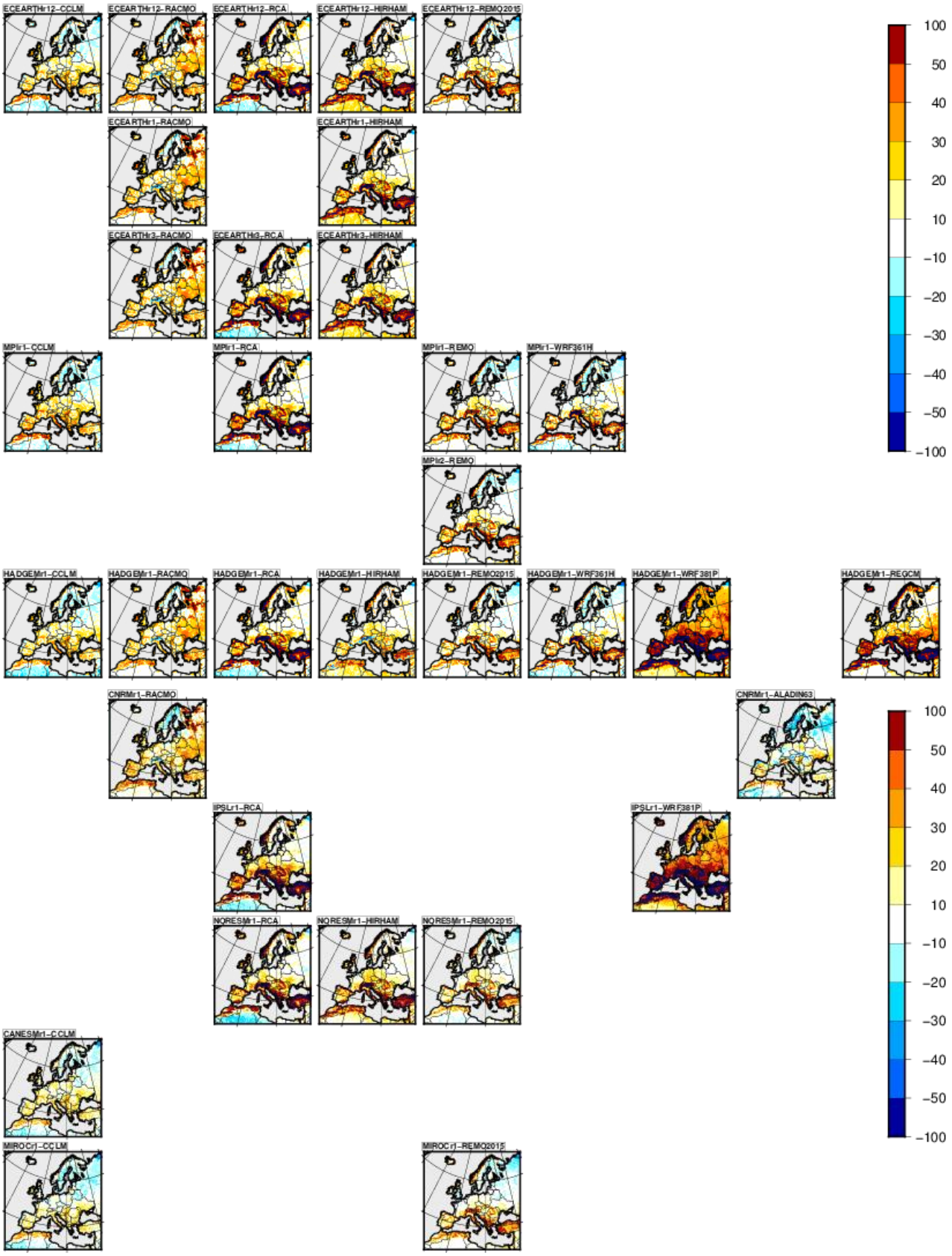

Figure 11: Bias of the mean surface wind speed in % of the ERA5 climatology.

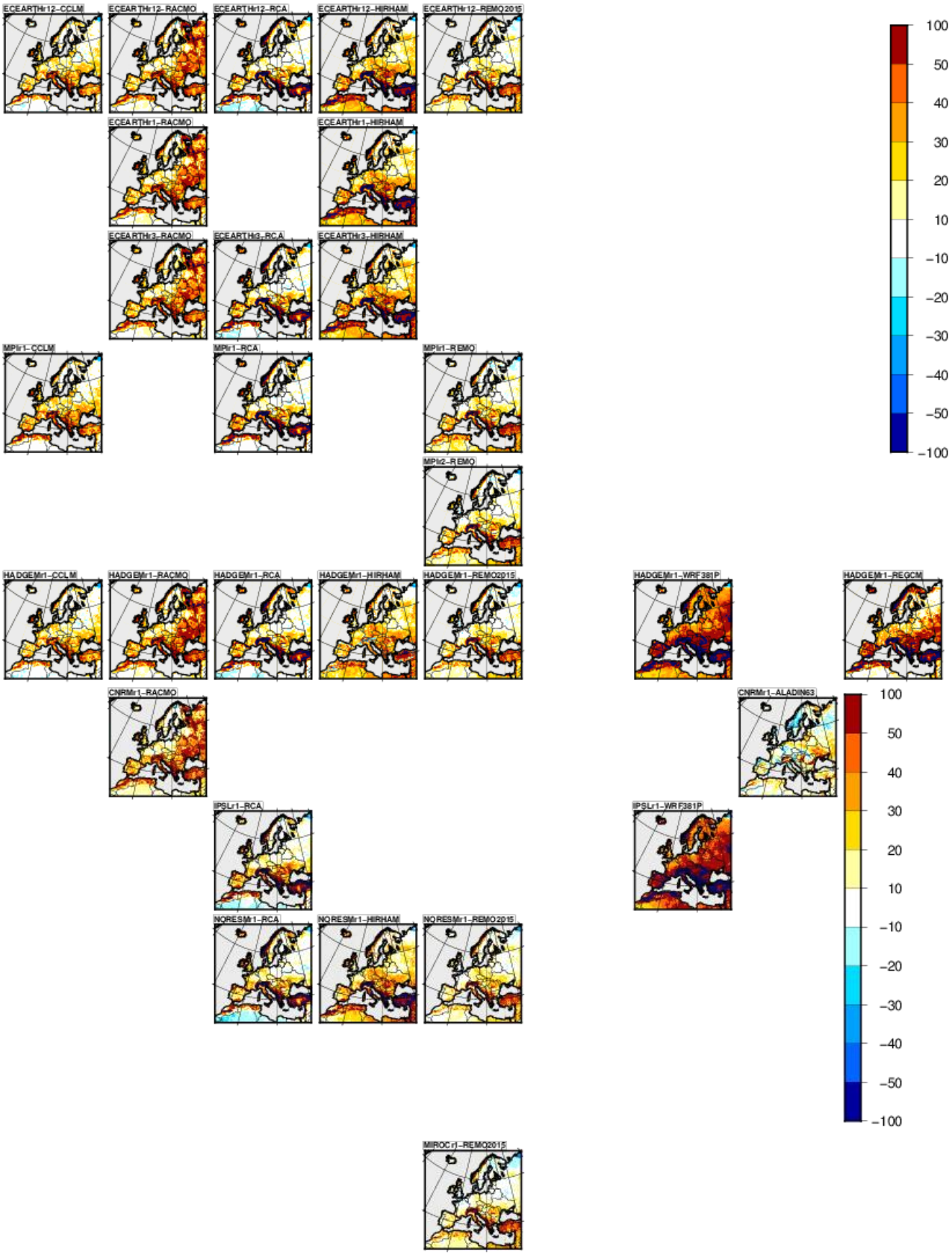

Figure 12: Same as Figure 11 for the yearly maximum wind speed.

Table 16: Bias (in %) for the mean surface wind speed. Biases larger than 20% in absolute value are colored.

	BI	IP	FR	ME	SC	AL	MD	EA
OBS (ERA5) [m s-1]	6,5	3,8	4,6	4,3	4,7	2,1	4,4	3,2
Ens Mean bias (%)	11,8	25,7	14,0	13,6	13,7	62,0	27,2	20,4
CANESMr1-CCLM	10,0	8,4	11,7	7,1	2,2	11,5	8,0	11,1
CANESMr1-REMO2105	13,3	20,3	9,2	13,1	11,4	45,7	21,5	15,8
CNRMr1-ALADIN63	-2,0	13,1	6,5	1,8	-7,1	8,1	13,8	7,1
CNRMr1-RACMO	10,2	21,8	17,9	11,0	-0,4	2,7	17,9	17,9
ECEARTHr1-HIRHAM	14,6	29,4	11,2	16,0	21,6	85,7	31,8	21,9
ECEARTHr1-RACMO	14,9	16,7	16,3	14,4	6,9	2,2	14,3	19,7
ECEARTHr12-CCLM	10,4	11,3	13,0	9,8	2,8	15,9	15,3	12,6
ECEARTHr12-HIRHAM	15,1	30,4	13,2	17,4	21,1	89,4	33,6	22,1
ECEARTHr12-RACMO	15,2	16,1	15,8	13,6	6,8	1,6	13,9	19,2
ECEARTHr12-RCA	18,2	35,4	16,5	15,2	26,3	111,3	34,5	23,6
ECEARTHr12-REMO2015	8,8	18,7	5,9	10,4	12,7	41,6	20,8	13,2
ECEARTHr3-HIRHAM	14,4	30,6	12,9	17,1	21,2	89,6	33,5	22,7
ECEARTHr3-RACMO	14,8	15,8	15,9	13,6	6,7	1,5	12,5	19,8
ECEARTHr3-RCA	16,7	36,2	16,4	14,1	25,2	112,9	34,9	24,7
HADGEMr1-CCLM	8,9	9,8	13,8	9,3	0,8	18,5	16,0	13,3
HADGEMr1-HIRHAM	12,2	13,9	8,7	13,7	13,3	3,7	17,4	15,7
HADGEMr1-RACMO	14,7	14,2	15,3	13,0	6,7	4,4	14,7	19,3
HADGEMr1-RCA	15,5	31,5	12,3	11,4	24,7	106,8	34,4	21,4
HADGEMr1-REGCM	18,9	48,6	22,4	20,4	35,7	121,2	50,3	35,3
HADGEMr1-REMO2015	8,9	14,8	3,8	8,1	11,7	42,2	19,4	12,2
HADGEMr1-WRF361H	3,5	22,0	4,2	3,8	12,9	83,8	28,8	12,1
HADGEMr1-WRF381P	17,4	72,0	36,3	36,9	37,2	182,7	69,2	59,1
IPSLr1-RCA	12,9	37,7	20,6	19,2	18,9	128,4	39,4	31,7
IPSLr1-WRF381P	19,8	86,4	47,7	44,1	40,1	204,6	82,4	67,6
MIROCr1-CCLM	2,4	7,4	7,6	1,3	-3,1	9,6	13,0	7,0
MIROCr1-REMO2015	3,6	16,5	4,1	4,8	6,5	41,8	24,6	11,0
MPIr1-CCLM	11,8	18,0	18,6	14,2	0,3	21,7	21,4	15,7
MPIr1-RCA	16,1	41,1	17,4	14,0	21,7	115,1	38,1	23,8
MPIr1-REMO	10,2	22,9	9,9	12,9	8,7	43,9	22,3	14,5
MPIr1-WRF361H	3,4	26,3	7,1	5,1	11,8	84,3	29,6	12,4
MPIr2-REMO	10,1	22,4	10,0	12,6	9,1	44,0	22,3	14,5
NORESMr1-HIRHAM	14,4	24,6	12,8	18,3	18,9	87,4	29,6	20,9
NORESMr1-RCA	14,6	27,2	14,4	14,0	20,4	105,3	30,4	21,0
NORESMr1-REMO2015	9,1	11,7	4,8	12,1	10,4	39,4	15,6	12,9

Table 17: Bias (in %) for the yearly maximum of daily maximum wind speed. Biases larger than 30% in absolute value are colored.

	BI	IP	FR	ME	SC	AL	MD	EA
OBS (ERA5) [m s-1]	18,9	13,1	15,0	13,9	14,0	8,1	14,9	10,7
Ens Mean bias (%)	21,7	29,9	19,3	17,9	21,7	94,1	36,1	28,7
CANESMr1-CCLM								
CANESMr1-REMO2105	17,6	21,1	11,0	10,5	14,9	57,0	30,8	21,1
CNRMr1-ALADIN63	5,4	10,9	8,4	5,6	2,8	22,2	16,9	16,7
CNRMr1-RACMO	15,8	26,8	18,3	12,5	11,1	48,7	28,2	30,9
ECEARTHr1-HIRHAM	32,6	36,8	23,9	27,9	32,3	129,0	48,0	33,3
ECEARTHr1-RACMO	20,8	23,8	18,2	16,3	18,7	50,3	27,7	32,8
ECEARTHr12-CCLM	23,0	21,2	22,4	17,4	15,5	46,6	30,9	21,0
ECEARTHr12-HIRHAM	30,6	35,6	22,8	23,7	31,2	127,0	47,7	33,5
ECEARTHr12-RACMO	18,2	21,1	17,5	13,7	17,3	48,4	25,9	32,0
ECEARTHr12-RCA	21,2	29,2	19,3	10,5	25,1	131,2	31,7	17,2
ECEARTHr12-REMO2015	14,3	21,5	10,0	11,7	16,0	55,6	30,8	17,6
ECEARTHr3-HIRHAM	33,2	36,9	23,3	28,1	31,7	129,3	49,0	34,7
ECEARTHr3-RACMO	21,0	23,6	19,5	16,6	17,8	49,2	26,4	32,3
ECEARTHr3-RCA	24,4	31,2	20,1	11,8	23,5	131,0	32,3	17,8
HADGEMr1-CCLM	25,8	22,7	23,2	18,1	14,6	45,7	31,0	20,0
HADGEMr1-HIRHAM	34,2	25,2	25,2	28,9	23,8	21,7	33,2	29,9
HADGEMr1-RACMO	22,8	26,9	20,7	18,2	18,4	55,2	30,7	37,6
HADGEMr1-RCA	23,3	31,4	17,7	11,9	25,4	133,4	31,8	18,1
HADGEMr1-REGCM	28,6	49,3	26,8	26,1	40,8	162,6	50,0	44,7
HADGEMr1-REMO2015	17,3	21,3	9,4	12,5	15,1	57,9	31,4	20,6
HADGEMr1-WRF361H								
HADGEMr1-WRF381P	18,9	65,6	33,2	36,7	40,1	241,6	68,1	69,7
IPSLr1-RCA	16,9	30,7	19,2	12,7	17,2	141,8	31,5	26,2
IPSLr1-WRF381P	23,6	74,0	40,4	43,6	47,2	265,5	78,0	83,5
MIROCr1-CCLM								
MIROCr1-REMO2015	12,1	16,2	6,5	8,1	11,1	52,4	32,8	14,2
MPIr1-CCLM	24,8	30,0	26,8	20,0	14,7	52,7	34,7	25,3
MPIr1-RCA	20,0	37,6	18,8	10,2	21,2	137,8	34,2	17,6
MPIr1-REMO	16,4	28,9	14,2	14,7	13,7	61,8	34,4	20,7
MPIr1-WRF361H								
MPIr2-REMO	16,8	27,0	12,7	13,0	14,5	61,1	33,9	20,2
NORESMr1-HIRHAM	32,0	30,2	21,8	26,9	32,9	125,4	44,7	33,9
NORESMr1-RCA	24,0	25,6	21,6	15,1	26,0	128,8	29,8	17,4
NORESMr1-REMO2015	15,5	15,1	7,1	13,9	17,5	53,3	27,1	20,6

8.4 Surface solar radiation biases

The 1981-2010 simulated surface shortwave downwelling radiation (rsds) annual means are evaluated against the Surface Solar Radiation Data Set - Heliosat (SARAH) (Müller *et al*., 2015). The latter has been interpolated to the common EURO-CORDEX horizontal grid for the period 1983 – 2012 (not available before). Observational uncertainty is associated with this satellite-based dataset, with 85% of absolute differences between SARAH monthly means and ground based measurements is below 10W/m². We thus recommend not to interpret model biases lower than + or - 10W/m².

Models biases, that are shown in Figure 13 and Table 18, range from -34.5W/m² in the IP box (18% of the observed climatological value) to more than +40 W/m² in the BI box (nearly 40% of the observed climatological value). Strong negative biases affect southern Europe (IP and MD boxes), which is a region with few clouds. They suggest issues in cloud modeling (too strong cloud effect, likely low level clouds) and/or in spatio-temporal variability of aerosols (too strong aerosol effect). Two RCMs (WRF381P and REGCM) present particularly strong positive biases regardless of the geographical area and of the driving GCM, suggesting a lack of simulated low clouds. Others RCMs concerned mainly by positive biases are RCA and ALADIN63. REMO, REMO2015 and HIRHAM have mainly negative biases, while RACMO and CCLM show no stringent feature. We notice no clear influence of the forcing GCM on the rsds biases.

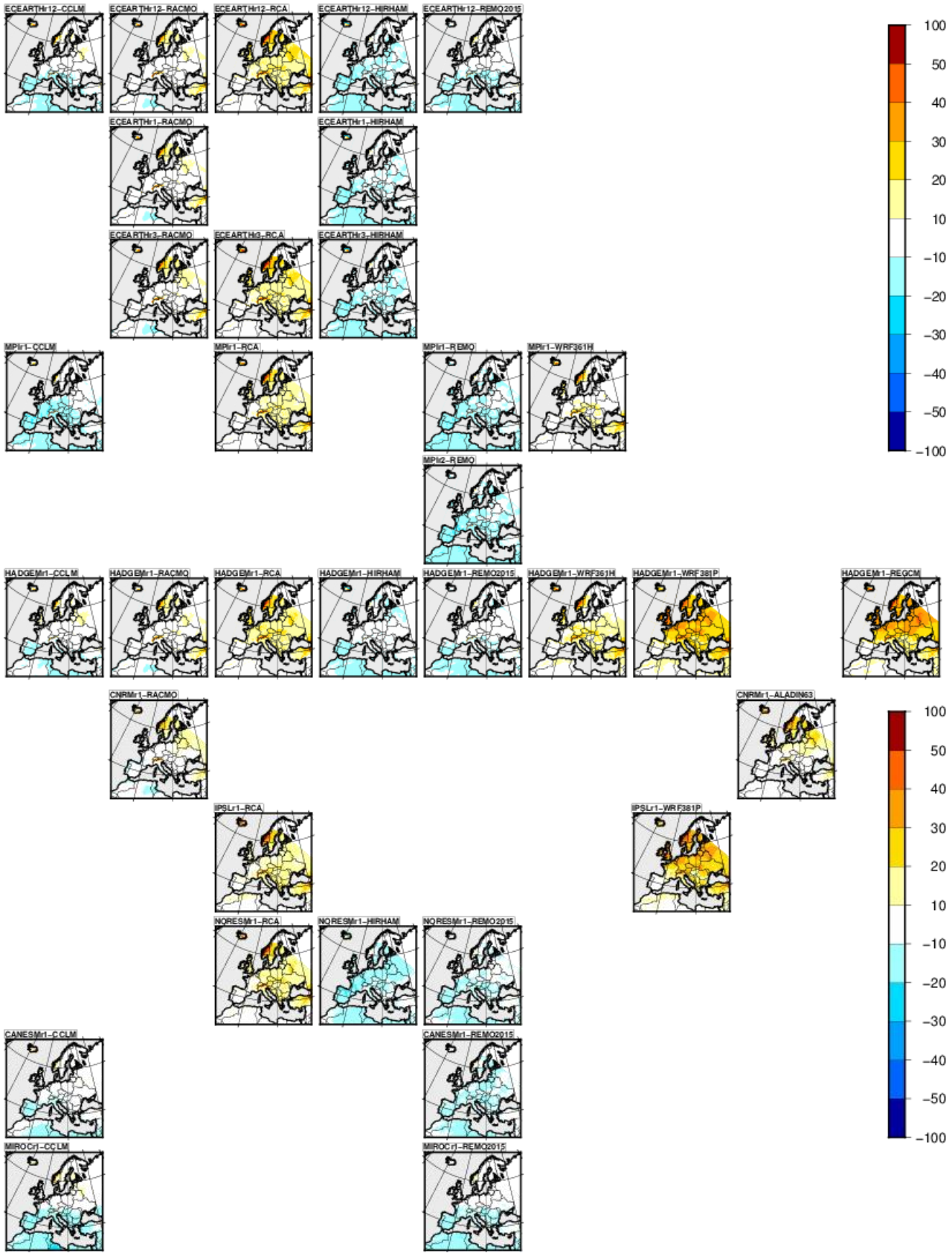

Figure 13: Surface solar radiation biases in % of the HelioSat observations.

Table 18: Same as Table 9 for radiation biases.

	BI	IP	FR	ME	SC	AL	MD	EA
OBS (W m^{-2})	107.5	196.1	144.9	127.2	100.2	153.4	188.8	141.7
Ens Mean bias (W m^{-2})	3.2	-17.2	-6.0	0.4	6.0	2.4	-9.0	3.8
CANESMr1 – CCLM	1.2	-20.0	-6.3	-3.2	3.2	-10.6	-16.7	-4.1
CANESMr1 - REMO2015	-4.7	-22.1	-16.6	-13.2	-9.4	-13.2	-20.5	-15.8
CNRMr1 - ALADIN63	17.7	-4.9	3.4	12.5	24.1	11.0	-1.8	10.5
CNRMr1 – RACMO	0.8	-15.7	-9.8	3.0	17.6	6.7	-8.7	7.3
ECEARTHr12 – CCLM	6.7	-22.6	-6.6	-1.2	8.9	-11.9	-22.9	-3.6
ECEARTHr12 - HIRHAM	-6.5	-26.9	-18.1	-12.7	-7.1	-13.1	-22.0	-14.3
ECEARTHr3 – HIRHAM	-4.5	-27.8	-16.1	-11.0	-5.3	-11.7	-22.1	-15.0
ECEARTHr1 – HIRHAM	-6.2	-27.9	-16.2	-9.6	-5.3	-11.1	-21.1	-12.9
ECEARTHr12 – RACMO	-0.6	-9.3	-4.6	2.1	12.9	9.9	-3.7	5.2
ECEARTHr1 – RACMO	0.3	-10.7	-4.1	3.2	14.5	10.4	-3.7	5.3
ECEARTHr3 – RACMO	2.4	-10.7	-0.8	6.1	16.8	12.9	-2.7	7.3
ECEARTHr12 – RCA	17.8	8.6	14.3	19.6	24.1	30.5	17.0	22.8
ECEARTHr3 – RCA	18.3	6.7	13.8	18.7	24.8	29.2	16.2	20.7
ECEARTHr12 - REMO2015	0.7	-21.5	-11.6	-5.8	-2.6	-11.6	-21.7	-10.9
HADGEMr1 – CCLM	8.1	-19.3	-0.4	3.5	9.1	-4.9	-18.3	1.1
HADGEMr1 – HIRHAM	-4.2	-24.7	-8.6	-6.1	-6.9	-5.6	-17.7	-9.7
HADGEMr1 – RACMO	1.8	-9.1	2.7	6.8	12.5	14.3	-0.7	8.7
HADGEMr1 – RCA	17.5	7.6	19.8	23.0	21.5	31.9	17.3	23.4
HADGEMr1 - REMO2015	1.6	-21.5	-5.9	-2.7	-4.7	-5.2	-18.3	-7.7
HADGEMr1 – REGCM	35.9	13.3	36.0	40.7	33.4	35.6	22.6	38.0
HADGEMr1 - WRF361H	17.1	12.4	12.9	17.9	12.5	30.5	22.4	19.4
HADGEMr1 - WRF381P	42.1	21.6	35.9	40.5	30.8	43.2	36.0	37.4
IPSLr1 – RCA	12.5	12.7	11.7	14.3	21.3	30.7	22.6	19.6
IPSLr1 - WRF381P	39.5	12.9	28.4	37.8	33.9	38.6	30.1	35.7
MIROCr1 – CCLM	5.7	-30.6	-12.8	-1.6	9.8	-16.3	-31.0	-6.6
MIROCr1 - REMO2015	1.6	-28.6	-15.1	-6.2	-2.2	-13.1	-25.1	-11.9
MPIr1 – CCLM	-4.2	-33.3	-21.0	-15.1	-1.7	-18.2	-26.2	-15.4
MPIr1 – RCA	12.1	2.7	7.5	13.8	19.0	25.9	15.0	18.7
MPIr1 – REMO	-10.7	-34.1	-22.8	-14.5	-9.0	-15.9	-25.7	-14.9
MPIr2 – REMO	-11.1	**-34.5**	-25.0	-15.6	-9.9	-17.9	-25.7	-15.6
MPIr1 - WRF361H	9.4	-0.4	-0.3	8.6	8.2	21.5	15.4	11.6
NORESMr1 – HIRHAM	-10.2	-30.1	-24.1	-17.7	-10.9	-15.7	-21.0	-16.5
NORESMr1 -REMO2015	-4.2	-24.3	-18.0	-11.7	-7.7	-13.4	-20.4	-13.4
NORESMr1 – RCA	15.8	7.2	10.5	17.3	22.2	29.0	18.8	22.8

9. Changes analysis

9.1 Temperature

Temperature changes are shown in Figures 14-18 for the five indices used. Changes in mean, maximum and minimum temperatures are rather homogeneous at yearly time scale, with larger changes in more continental Eastern Europe than in Southern and Western areas. Changes in minimum temperature are larger than those in maximum temperature, in line with IPCC assessments. The amplitude of changes are more sensitive to GCM than RCM, in line with the different sensitivity of the models. The HadGEM model has the highest sensitivity to greenhouse gases and exhibits the largest changes in temperature for the middle of the century (3-5°C) under RCP8.5.

Significant changes in the number of hot days with TX greater than 35 degrees are found along Southern European Mediterranean coasts and in South-Eastern Europe. The amplitude of changes depends again essentially on the GCM (Figure 17). Changes in freezing days are by contrast marked more over Northern Europe, with patterns and amplitude depending both on GCM and RCM. Results per PRUDENCE regions have been calculated but are not shown to avoid multiplication of tables.

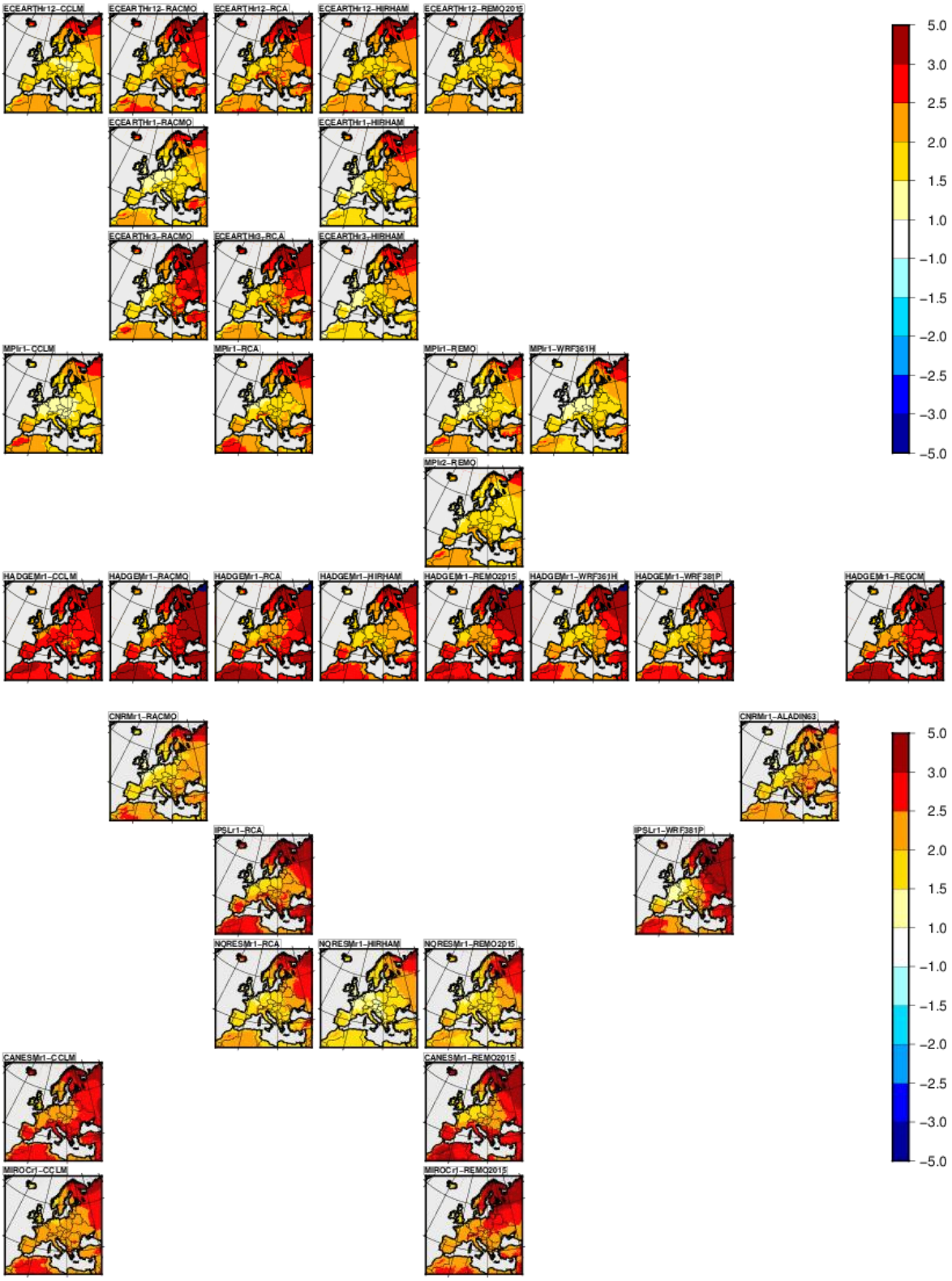

Figure 14: Changes in mean temperature (mid century – reference).

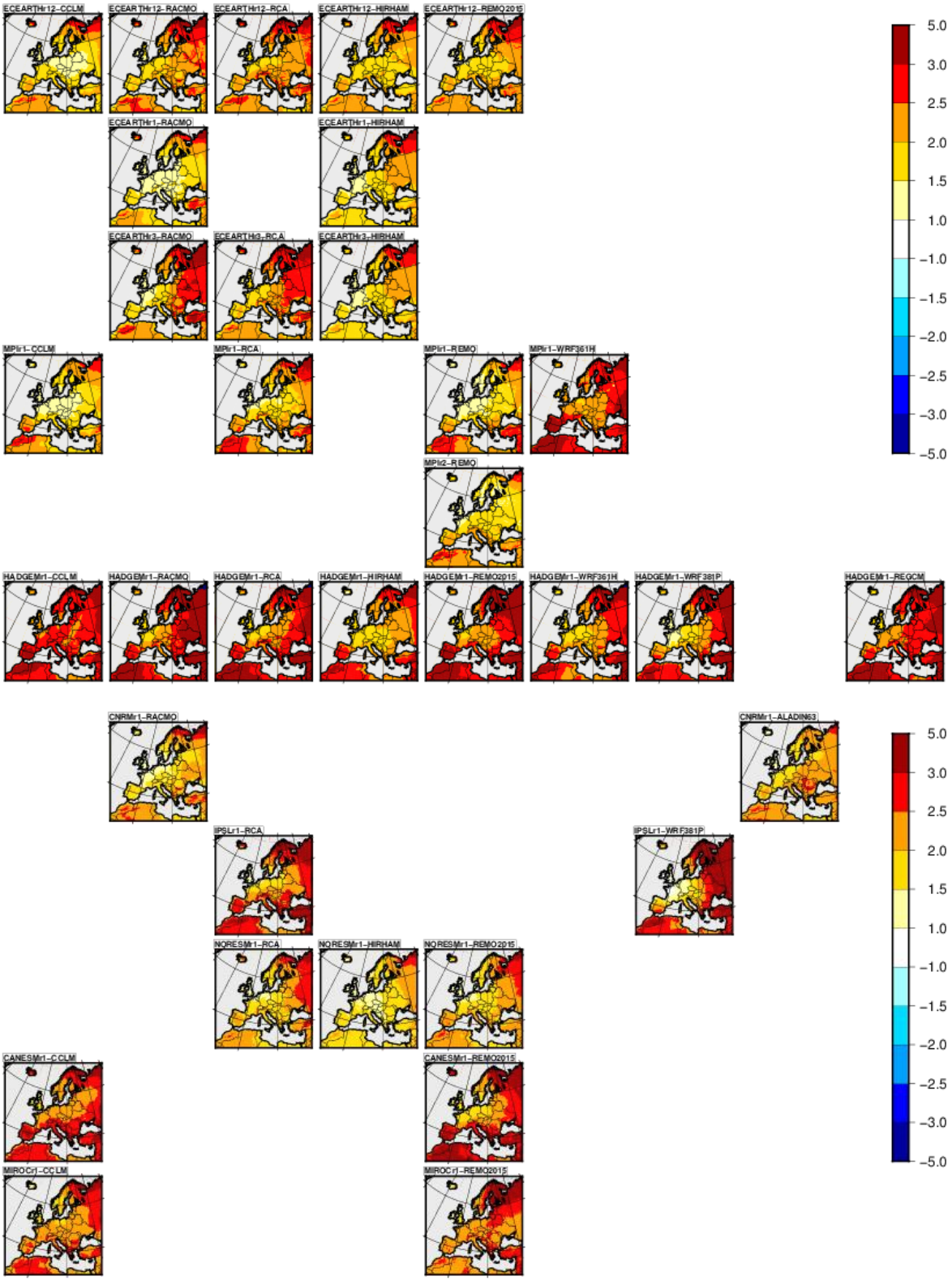

Figure 15: As in Figure 14 for the daily maximum temperature.

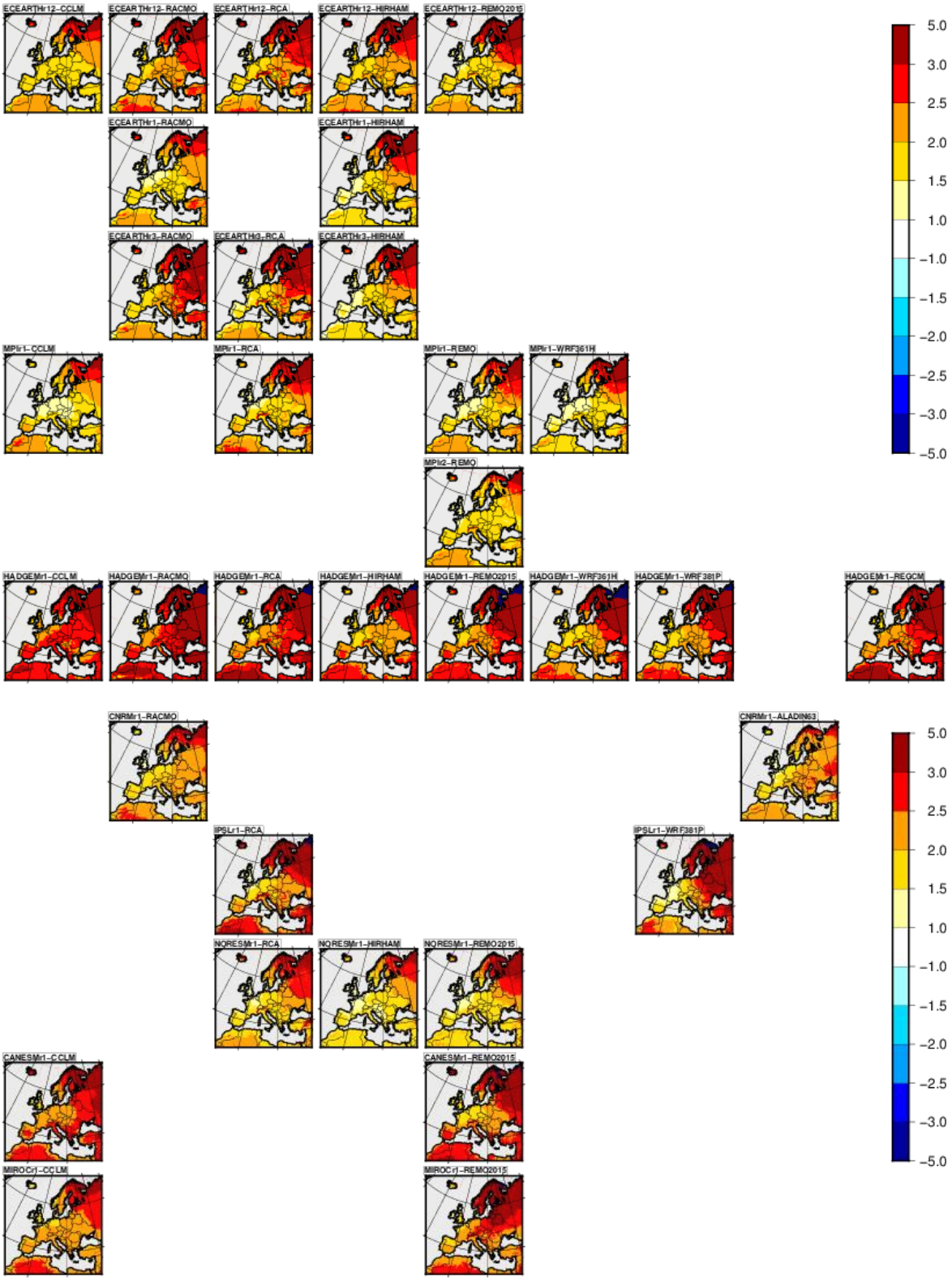

Figure 16: As in figure 14 for the daily minimum temperature

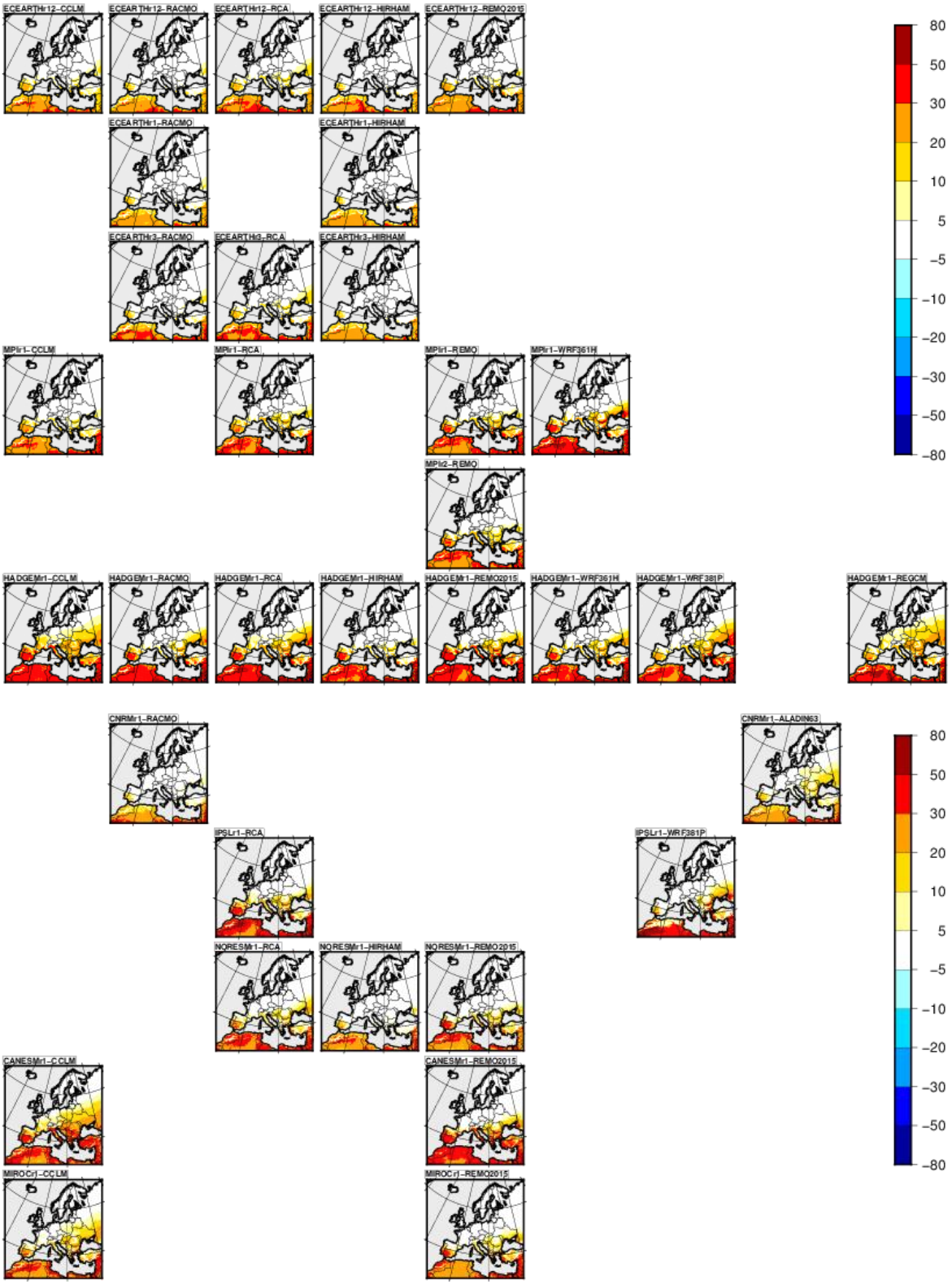

Figure 17: Changes in the number of days with temperature >35°C.

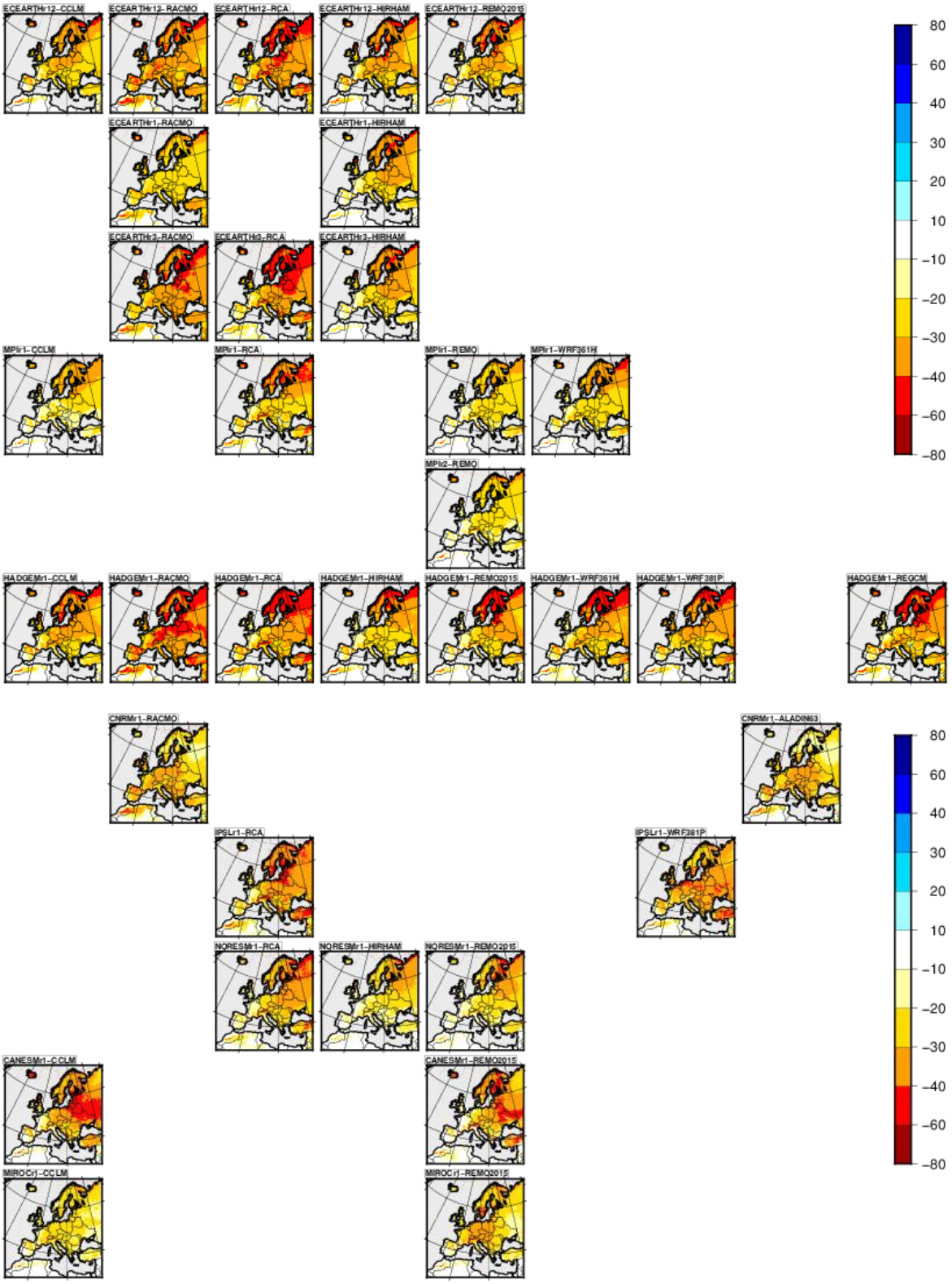

Figure 18: As in Figure 17 for the number of frost days.

9.2 Changes in precipitation

Changes in precipitation (Figure 19) expected for the middle of the century generally follow the usual pattern of increased rain amount in Northern Europe and decreased amount in Southern Europe for all models, with varying amplitude. Increases in Scandinavia range from about 5 to 20% (IPSLr1-WRF381P pattern should not be interpreted), and this response reveals a mixture of both GCM and RCM influence. Only a few simulations exhibit an increase down to the Iberian Peninsula or South-Eastern Europe.

Tables 19-20 show the distribution of changes per PRUDENCE regions and for summer and winter separately. In winter changes are in the range 0-20% depending on model and area in Northern and Central Europe while they are generally negative over the IP. In summer decrease in precipitation is widespread in Southern and central Europe and slightly positive over Scandinavia.

Changes in heavy precipitation as measured by RX1d are generalized and increasing, except over the IP where they decrease in summer (Figure 20 and Tables 21 and 22). No outlying model seems present and the ensemble looks rather homogeneous. A weak model dependence is found, indicating robust changes.

The number of wet days (Tables 23 and 24) and the extreme precipitations within these days (Tables 25 and 26) vary respectively as mean precipitation and RX1d.

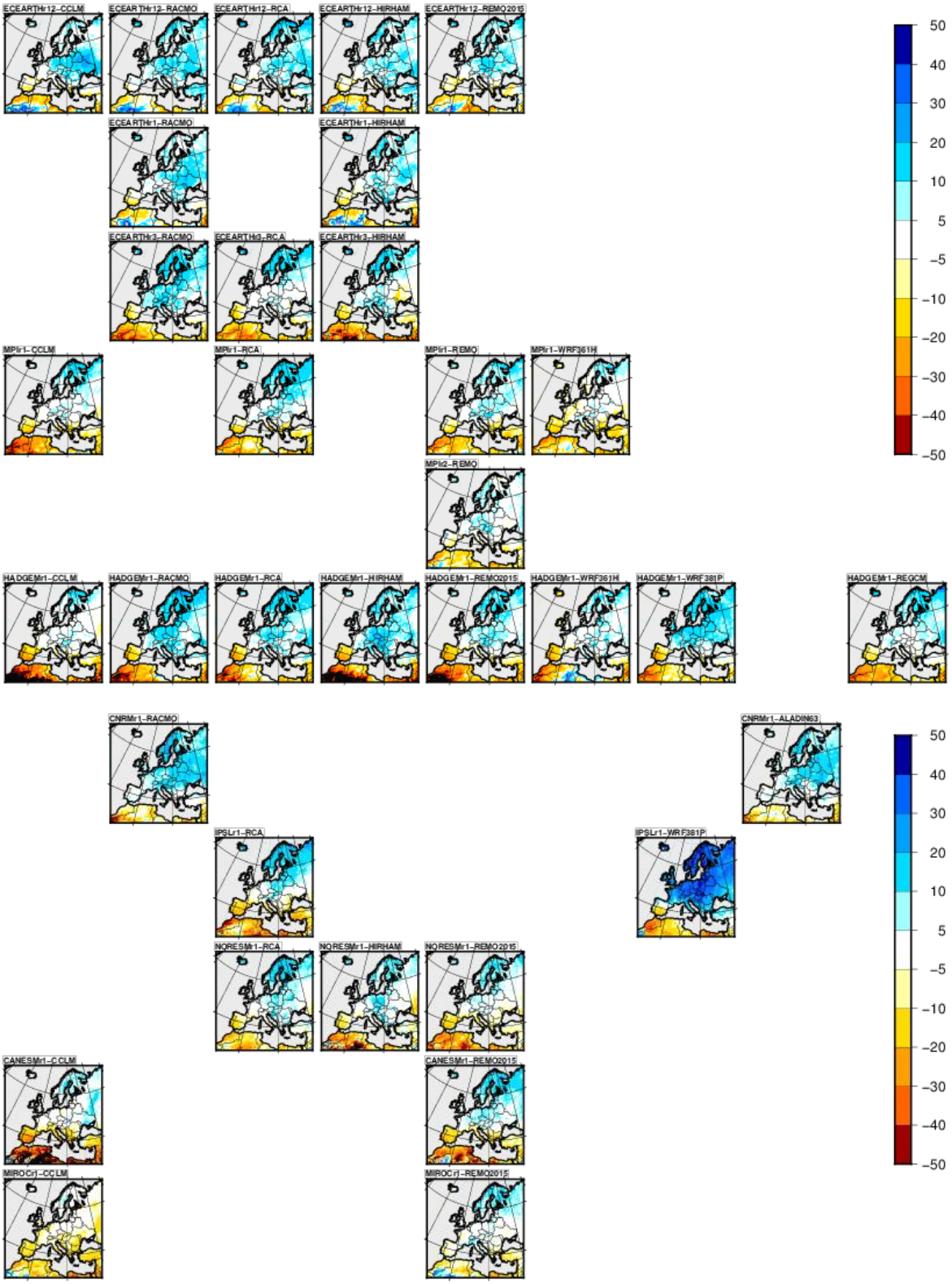

Figure 19: Change in mean precipitation (%)

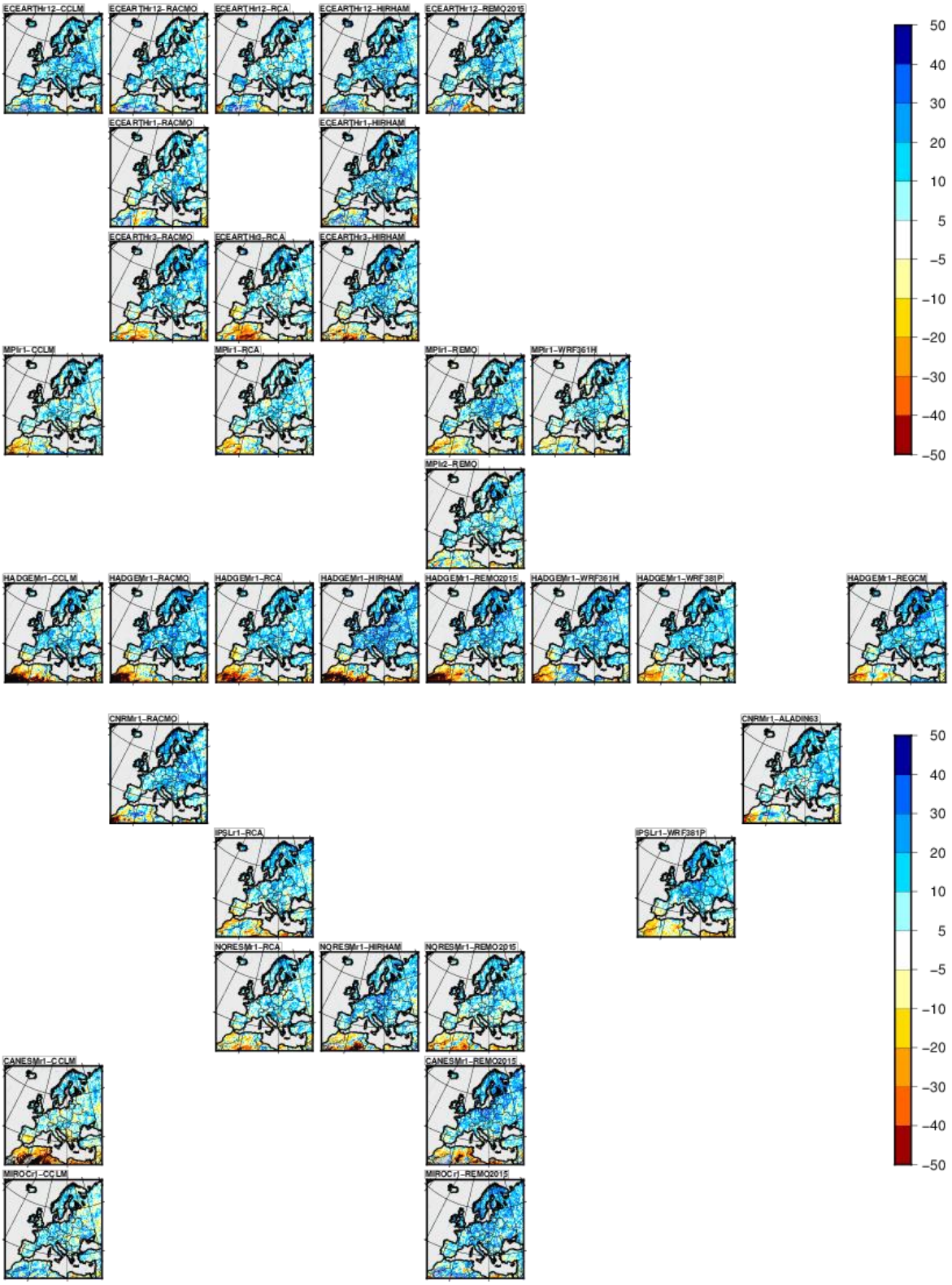

Figure 20: Changes in RX1day

Tables for precipitation changes

Table 19: Rmean for DJF

	BI	IP	FR	ME	SC	AL	MD	EA
Ens. Mean Change (%)	7	**-5**	7	11	8	8	1	13
CANESMr1-CCLM	5	**-14**	9	12	9	8	**-3**	12
CANESMr1-REMO2015	11	**-6**	14	18	12	9	**-2**	17
CNRMr1-ALADIN63	7	9	7	9	8	15	2	14
CNRMr1-RACMO	7	11	8	4	12	14	5	10
ECEARTHr12-CCLM	9	**-10**	12	21	5	13	**-5**	19
ECEARTHr12-HIRHAM	7	**-9**	8	17	10	10	**-6**	19
ECEARTHr3-HIRHAM	3	**-1**	6	4	12	16	4	9
ECEARTHr1-HIRHAM	0	2	5	6	0	2	12	12
ECEARTHr12-RACMO	9	**-8**	13	23	8	17	**-2**	26
ECEARTHr1-RACMO	4	2	10	8	**-1**	4	15	12
ECEARTHr3-RACMO	6	4	5	2	7	15	4	5
ECEARTHr12-RCA	9	**-9**	11	22	9	13	**-4**	26
ECEARTHr3-RCA	3	5	5	2	9	15	3	10
ECEARTHr12-REMO2015	6	**-8**	10	20	9	11	**-2**	20
HADGEMr1-CCLM	3	**-19**	1	12	10	3	3	13
HADGEMr1-HIRHAM	1	**-17**	**-1**	14	12	10	10	17
HADGEMr1-RACMO	7	**-14**	6	18	14	5	9	18
HADGEMr1-RCA	4	**-17**	3	14	11	3	9	16
HADGEMr1-REMO2015	6	**-13**	2	11	15	7	9	19
HADGEMr1-REGCM	8	**-10**	5	12	14	8	4	12
HADGEMr1-WRF361H	**-2**	**-19**	2	3	3	1	5	8
HADGEMr1-WRF381P	3	**-11**	7	9	6	10	5	14
IPSLr1-RCA	11	**-3**	14	12	12	11	0	12
IPSLr1-WRF381P	N/A	N/A	N/A	N/A	N/A	N/A	N/A	N/A
MIROCr1-CCLM	11	**-10**	7	4	5	5	**-5**	7
MIROCr1-REMO2015	12	**-3**	4	8	12	8	**-8**	4
MPIr1-CCLM	9	3	6	10	6	6	**-6**	7
MPIr1-RCA	9	3	10	11	8	6	**-5**	15
MPIr1-REMO	9	6	4	10	6	4	**-2**	11
MPIr2-REMO	11	7	13	18	5	8	1	19
MPIr1-WRF361H	3	**-3**	**-2**	**-3**	**-5**	**-2**	**-2**	3
NORESMr1-HIRHAM	7	**-7**	4	9	9	6	2	13
NORESMr1-REMO2015	10	**-10**	9	9	10	1	**-2**	10
NORESMr1-RCA	7	**-7**	7	10	12	2	0	14

Table 20: Rmean in JJA

	BI	IP	FR	ME	SC	AL	MD	EA
Ens. Mean Change (%)	**-8**	**-21**	**-10**	0	7	**-5**	**-15**	**-1**
CANESMr1-CCLM	**-10**	**-57**	**-33**	**-24**	**-7**	**-38**	**-56**	**-31**
CANESMr1-REMO2015	**-3**	**-37**	**-14**	3	7	**-12**	**-35**	**-4**
CNRMr1-ALADIN63	2	**-4**	**-1**	11	10	5	**-8**	5
CNRMr1-RACMO	4	**-7**	6	14	26	9	**-3**	15
ECEARTHr12-CCLM	**-6**	**-29**	**-17**	3	5	**-12**	**-24**	7
ECEARTHr12-HIRHAM	**-6**	**-16**	**-4**	3	0	**-8**	**-26**	**-4**
ECEARTHr3-HIRHAM	**-10**	**-24**	**-8**	2	10	**-2**	**-17**	3
ECEARTHr1-HIRHAM	**-13**	**-27**	**-13**	2	3	**-8**	**-12**	4
ECEARTHr12-RACMO	**-3**	**-12**	**-1**	9	5	**-2**	**-13**	4
ECEARTHr1-RACMO	**-9**	**-13**	**-11**	4	5	**-2**	6	12
ECEARTHr3-RACMO	**-5**	**-16**	2	12	18	5	**-13**	6
ECEARTHr12-RCA	**-6**	**-11**	**-11**	**-2**	6	**-14**	**-26**	**-4**
ECEARTHr3-RCA	**-7**	**-22**	**-9**	**-2**	9	**-8**	**-23**	**-5**
ECEARTHr12-REMO2015	**-12**	**-17**	**-11**	0	6	**-8**	**-16**	2
HADGEMr1-CCLM	**-18**	**-30**	**-20**	**-12**	0	**-21**	**-10**	**-16**
HADGEMr1-HIRHAM	**-5**	**-21**	**-4**	7	5	10	9	8
HADGEMr1-RACMO	**-1**	**-15**	0	12	14	8	6	12
HADGEMr1-RCA	**-3**	**-24**	**-2**	11	14	7	**-12**	2
HADGEMr1-REMO2015	**-10**	**-33**	**-8**	1	7	**-5**	**-9**	1
HADGEMr1-REGCM	**-1**	**-15**	**-1**	**-1**	7	**-2**	**-11**	**-5**
HADGEMr1-WRF361H	**-6**	**-22**	**-7**	3	10	**-1**	5	2
HADGEMr1-WRF381P	9	**-15**	12	22	18	3	**-17**	5
IPSLr1-RCA	**-7**	**-40**	**-27**	**-6**	17	**-13**	**-27**	**-2**
IPSLr1-WRF381P	N/A	N/A	N/A	N/A	N/A	N/A	N/A	N/A
MIROCr1-CCLM	**-15**	**-16**	**-21**	**-13**	**-1**	**-17**	**-26**	**-19**
MIROCr1-REMO2015	**-8**	**-8**	**-7**	**-7**	4	4	9	**-2**
MPIr1-CCLM	**-14**	**-27**	**-15**	**-8**	2	**-4**	**-22**	**-6**
MPIr1-RCA	**-13**	**-16**	**-15**	**-6**	6	0	**-22**	0
MPIr1-REMO	**-13**	**-17**	**-11**	**-6**	**-1**	**-4**	**-14**	2
MPIr2-REMO	**-11**	**-18**	**-13**	**-7**	2	**-11**	**-13**	**-7**
MPIr1-WRF361H	**-19**	**-15**	**-15**	**-8**	1	**-7**	**-27**	**-3**
NORESMr1-HIRHAM	**-11**	**-24**	**-11**	2	0	0	**-18**	**-1**
NORESMr1-REMO2015	**-13**	**-27**	**-9**	**-3**	3	**-5**	**-22**	**-4**
NORESMr1-RCA	**-13**	**-27**	**-19**	**-3**	7	**-1**	**-23**	0

Table 21: Changes in RX1d in winter

	BI	IP	FR	ME	SC	AL	MD	EA
Ens. Mean Change (%)	8	1	9	10	11	9	7	15
CANESMr1-CCLM	9	**-5**	13	9	13	12	5	13
CANESMr1-REMO2015	7	0	15	12	14	10	3	14
CNRMr1-ALADIN63	8	7	7	11	8	11	6	16
CNRMr1-RACMO	6	8	10	7	12	9	6	13
ECEARTHr12-CCLM	8	3	14	16	11	11	4	14
ECEARTHr12-HIRHAM	8	6	9	13	14	10	2	16
ECEARTHr3-HIRHAM	5	6	6	5	15	13	8	14
ECEARTHr1-HIRHAM	4	1	5	11	7	1	11	11
ECEARTHr12-RACMO	7	3	8	12	13	13	2	22
ECEARTHr1-RACMO	11	2	9	10	5	1	10	11
ECEARTHr3-RACMO	7	9	8	3	10	11	7	11
ECEARTHr12-RCA	8	3	10	14	13	10	3	19
ECEARTHr3-RCA	5	9	9	5	11	14	8	16
ECEARTHr12-REMO2015	5	3	10	15	12	12	1	15
HADGEMr1-CCLM	9	**-6**	11	15	13	13	14	17
HADGEMr1-HIRHAM	7	**-7**	7	10	13	12	11	19
HADGEMr1-RACMO	9	**-7**	10	15	13	6	14	21
HADGEMr1-RCA	6	**-11**	9	15	9	6	12	16
HADGEMr1-REMO2015	9	**-4**	6	12	15	11	10	18
HADGEMr1-REGCM	10	**-5**	12	16	18	13	10	17
HADGEMr1-WRF361H	6	**-8**	11	8	11	11	10	15
HADGEMr1-WRF381P	5	**-5**	14	10	12	14	9	17
IPSLr1-RCA	11	2	18	10	10	10	14	16
IPSLr1-WRF381P	N/A	N/A	N/A	N/A	N/A	N/A	N/A	N/A
MIROCr1-CCLM	7	**-2**	8	5	9	11	7	9
MIROCr1-REMO2015	9	0	4	6	13	9	3	7
MPIr1-CCLM	12	11	8	11	10	8	3	11
MPIr1-RCA	11	9	10	13	9	10	3	13
MPIr1-REMO	8	11	3	10	8	3	2	8
MPIr2-REMO	6	6	5	10	9	3	3	15
MPIr1-WRF361H	15	6	4	8	6	4	3	10
NORESMr1-HIRHAM	10	2	6	11	12	8	8	17
NORESMr1-REMO2015	10	0	6	8	13	7	6	12
NORESMr1-RCA	8	1	10	12	13	6	7	21

Table 22: Changes in RX1d in JJA

	BI	IP	FR	ME	SC	AL	MD	EA
Ens. Mean Change (%)	5	**-8**	6	11	12	5	**-3**	10
CANESMr1-CCLM	1	**-40**	**-16**	**-7**	3	**-16**	**-39**	**-13**
CANESMr1-REMO2015	8	**-18**	3	23	19	2	**-15**	15
CNRMr1-ALADIN63	8	5	8	13	12	6	**-1**	8
CNRMr1-RACMO	9	**-1**	15	14	20	14	7	19
ECEARTHr12-CCLM	5	**-10**	**-1**	13	11	2	**-8**	11
ECEARTHr12-HIRHAM	10	**-3**	14	16	10	4	**-11**	10
ECEARTHr3-HIRHAM	0	**-11**	11	12	16	7	**-2**	17
ECEARTHr1-HIRHAM	4	**-12**	7	20	13	5	**-3**	14
ECEARTHr12-RACMO	3	**-1**	11	10	8	1	**-9**	6
ECEARTHr1-RACMO	2	**-5**	0	5	7	3	12	12
ECEARTHr3-RACMO	0	**-5**	13	13	15	3	1	12
ECEARTHr12-RCA	6	**-4**	**-1**	3	9	**-8**	**-17**	3
ECEARTHr3-RCA	2	**-18**	8	4	10	**-7**	**-15**	3
ECEARTHr12-REMO2015	1	**-4**	8	10	11	**-1**	**-3**	14
HADGEMr1-CCLM	4	**-12**	5	7	12	2	7	2
HADGEMr1-HIRHAM	10	**-2**	16	23	16	24	23	24
HADGEMr1-RACMO	11	3	14	14	18	15	17	23
HADGEMr1-RCA	5	**-7**	9	14	13	15	**-1**	12
HADGEMr1-REMO2015	12	**-14**	14	17	18	12	3	15
HADGEMr1-REGCM	11	8	10	12	21	10	11	13
HADGEMr1-WRF361H	8	**-6**	9	15	20	14	16	15
HADGEMr1-WRF381P	14	0	9	18	16	12	**-1**	9
IPSLr1-RCA	0	**-24**	**-10**	4	15	**-4**	**-12**	6
IPSLr1-WRF381P	N/A	N/A	N/A	N/A	N/A	N/A	N/A	N/A
MIROCr1-CCLM	4	0	2	11	9	2	**-9**	**-1**
MIROCr1-REMO2015	14	0	8	13	19	14	13	14
MPIr1-CCLM	**-1**	**-14**	5	3	6	9	**-3**	2
MPIr1-RCA	**-3**	**-15**	2	2	6	3	**-9**	9
MPIr1-REMO	0	**-8**	3	7	3	2	**-3**	17
MPIr2-REMO	5	**-4**	8	6	9	**-1**	**-5**	3
MPIr1-WRF361H	1	**-9**	10	7	6	1	**-14**	9
NORESMr1-HIRHAM	12	**-8**	13	23	13	11	**-7**	18
NORESMr1-REMO2015	6	**-10**	4	11	14	3	**-13**	10
NORESMr1-RCA	0	**-17**	**-7**	7	11	5	**-18**	5

Table 23: Change in the number of wet days in DJF

	BI	IP	FR	ME	SC	AL	MD	EA
Ens. Mean Change (%)	1	**-7**	1	4	1	1	**-4**	5
CANESMr1-CCLM	**-2**	**-11**	2	4	1	0	**-7**	4
CANESMr1-REMO2015	5	**-5**	6	11	3	4	**-4**	11
CNRMr1-ALADIN63	1	4	1	2	2	4	**-3**	4
CNRMr1-RACMO	2	5	2	**-1**	5	4	0	2
ECEARTHr12-CCLM	2	**-14**	5	12	0	4	**-9**	11
ECEARTHr12-HIRHAM	1	**-13**	3	9	3	1	**-8**	11
ECEARTHr3-HIRHAM	0	**-3**	0	2	3	6	**-2**	3
ECEARTHr1-HIRHAM	**-2**	2	3	0	**-4**	1	8	5
ECEARTHr12-RACMO	3	**-10**	8	14	2	7	**-3**	15
ECEARTHr1-RACMO	**-1**	2	7	2	**-5**	4	9	5
ECEARTHr3-RACMO	2	**-1**	**-1**	**-2**	1	3	**-2**	**-1**
ECEARTHr12-RCA	3	**-11**	7	13	2	5	**-6**	15
ECEARTHr3-RCA	**-1**	1	**-1**	**-2**	3	4	**-3**	2
ECEARTHr12-REMO2015	2	**-10**	5	12	2	2	**-6**	12
HADGEMr1-CCLM	**-5**	**-20**	**-5**	3	1	**-4**	**-7**	4
HADGEMr1-HIRHAM	**-2**	**-14**	**-3**	6	3	1	2	6
HADGEMr1-RACMO	1	**-12**	2	9	5	1	1	7
HADGEMr1-RCA	**-1**	**-12**	1	6	4	**-1**	0	7
HADGEMr1-REMO2015	0	**-12**	**-2**	5	5	**-1**	1	7
HADGEMr1-REGCM	1	**-10**	**-1**	5	5	0	**-2**	4
HADGEMr1-WRF361H	**-9**	**-17**	**-6**	**-4**	**-7**	**-7**	**-3**	**-3**
HADGEMr1-WRF381P	**-2**	**-8**	1	3	**-1**	3	1	4
IPSLr1-RCA	2	**-8**	2	4	5	2	**-7**	3
IPSLr1-WRF381P	N/A	N/A	N/A	N/A	N/A	N/A	N/A	N/A
MIROCr1-CCLM	5	**-11**	1	**-1**	**-1**	**-1**	**-11**	2
MIROCr1-REMO2015	5	**-4**	2	2	3	1	**-12**	0
MPIr1-CCLM	**-1**	**-6**	**-1**	1	1	0	**-9**	0
MPIr1-RCA	1	**-4**	3	4	4	1	**-9**	6
MPIr1-REMO	1	**-1**	2	4	2	3	**-3**	6
MPIr2-REMO	6	1	7	10	**-1**	5	**-1**	11
MPIr1-WRF361H	**-8**	**-9**	**-8**	**-10**	**-11**	**-6**	**-8**	**-5**
NORESMr1-HIRHAM	2	**-7**	**-1**	2	2	2	**-2**	4
NORESMr1-REMO2015	4	**-10**	3	4	1	**-3**	**-6**	3
NORESMr1-RCA	2	**-8**	1	4	3	**-1**	**-4**	4

Table 24: Changes in the number of wet days in summer

	BI	IP	FR	ME	SC	AL	MD	EA
Ens. Mean Change (%)	**-10**	**-23**	**-13**	**-5**	0	**-8**	**-17**	**-7**
CANESMr1-CCLM	**-15**	**-58**	**-34**	**-26**	**-11**	**-37**	**-57**	**-37**
CANESMr1-REMO2015	**-5**	**-36**	**-13**	**-4**	0	**-15**	**-35**	**-10**
CNRMr1-ALADIN63	**-1**	**-8**	**-6**	4	2	0	**-10**	**-1**
CNRMr1-RACMO	1	**-8**	1	8	15	1	**-7**	3
ECEARTHr12-CCLM	**-10**	**-36**	**-19**	**-4**	0	**-13**	**-25**	1
ECEARTHr12-HIRHAM	**-12**	**-22**	**-9**	**-5**	**-4**	**-9**	**-26**	**-6**
ECEARTHr3-HIRHAM	**-10**	**-26**	**-13**	**-3**	3	**-4**	**-20**	**-5**
ECEARTHr1-HIRHAM	**-16**	**-28**	**-16**	**-6**	**-3**	**-8**	**-15**	**-1**
ECEARTHr12-RACMO	**-4**	**-14**	**-4**	2	0	**-2**	**-11**	**-1**
ECEARTHr1-RACMO	**-9**	**-12**	**-11**	**-1**	1	**-2**	**-2**	4
ECEARTHr3-RACMO	**-4**	**-16**	**-2**	6	10	1	**-15**	**-2**
ECEARTHr12-RCA	**-8**	**-13**	**-12**	**-5**	1	**-10**	**-21**	**-4**
ECEARTHr3-RCA	**-8**	**-18**	**-12**	**-5**	3	**-6**	**-18**	**-8**
ECEARTHr12-REMO2015	**-12**	**-18**	**-14**	**-4**	1	**-9**	**-18**	**-3**
HADGEMr1-CCLM	**-24**	**-41**	**-30**	**-22**	**-7**	**-28**	**-22**	**-24**
HADGEMr1-HIRHAM	**-10**	**-30**	**-12**	**-4**	**-2**	**-4**	**-6**	**-4**
HADGEMr1-RACMO	**-4**	**-22**	**-7**	4	5	**-1**	**-2**	1
HADGEMr1-RCA	**-4**	**-25**	**-5**	3	7	**-4**	**-15**	**-6**
HADGEMr1-REMO2015	**-13**	**-35**	**-14**	**-5**	**-2**	**-11**	**-13**	**-6**
HADGEMr1-REGCM	**-5**	**-18**	**-5**	**-7**	**-1**	**-7**	**-14**	**-12**
HADGEMr1-WRF361H	**-14**	**-27**	**-15**	**-7**	**-4**	**-10**	**-8**	**-9**
HADGEMr1-WRF381P	4	**-19**	7	12	8	**-3**	**-19**	**-1**
IPSLr1-RCA	**-5**	**-37**	**-23**	**-7**	10	**-11**	**-24**	**-5**
IPSLr1-WRF381P	N/A	N/A	N/A	N/A	N/A	N/A	N/A	N/A
MIROCr1-CCLM	**-19**	**-24**	**-27**	**-22**	**-7**	**-19**	**-28**	**-25**
MIROCr1-REMO2015	**-13**	**-10**	**-12**	**-12**	**-3**	**-4**	2	**-8**
MPIr1-CCLM	**-15**	**-27**	**-19**	**-11**	**-1**	**-7**	**-25**	**-9**
MPIr1-RCA	**-10**	**-10**	**-14**	**-7**	2	**-2**	**-18**	**-6**
MPIr1-REMO	**-11**	**-14**	**-10**	**-7**	**-2**	**-4**	**-12**	**-5**
MPIr2-REMO	**-11**	**-17**	**-13**	**-9**	**-2**	**-10**	**-12**	**-8**
MPIr1-WRF361H	**-22**	**-12**	**-22**	**-14**	**-5**	**-8**	**-20**	**-10**
NORESMr1-HIRHAM	**-16**	**-28**	**-18**	**-9**	**-6**	**-6**	**-20**	**-8**
NORESMr1-REMO2015	**-13**	**-27**	**-12**	**-7**	**-4**	**-6**	**-18**	**-8**
NORESMr1-RCA	**-10**	**-25**	**-16**	**-7**	1	**-5**	**-18**	**-4**

Table 25: Change in R99w in winter

	BI	IP	FR	ME	SC	AL	MD	EA
Ens. Mean Change (%)	7	4	8	9	11	9	9	14
CANESMr1-CCLM	9	**-1**	11	8	13	14	10	12
CANESMr1-REMO2015	6	3	14	7	14	11	5	10
CNRMr1-ALADIN63	7	5	8	11	8	11	6	17
CNRMr1-RACMO	6	9	10	8	11	10	7	14
ECEARTHr12-CCLM	7	10	13	12	11	11	9	13
ECEARTHr12-HIRHAM	5	13	8	10	13	11	5	12
ECEARTHr3-HIRHAM	5	5	8	4	15	12	9	13
ECEARTHr1-HIRHAM	4	1	4	10	9	1	8	10
ECEARTHr12-RACMO	4	9	8	11	12	12	4	19
ECEARTHr1-RACMO	12	1	4	10	6	**-1**	9	10
ECEARTHr3-RACMO	4	7	8	5	11	10	11	13
ECEARTHr12-RCA	5	9	8	13	11	11	6	14
ECEARTHr3-RCA	4	7	9	7	10	12	10	17
ECEARTHr12-REMO2015	3	10	9	12	13	12	5	14
HADGEMr1-CCLM	11	**-1**	11	10	13	12	18	14
HADGEMr1-HIRHAM	7	**-6**	6	8	13	11	11	15
HADGEMr1-RACMO	9	**-5**	7	10	13	7	12	19
HADGEMr1-RCA	8	**-10**	6	12	10	7	13	14
HADGEMr1-REMO2015	9	**-3**	6	8	13	13	11	18
HADGEMr1-REGCM	12	**-3**	12	11	18	15	12	16
HADGEMr1-WRF361H	8	**-6**	11	8	13	11	10	16
HADGEMr1-WRF381P	6	**-5**	10	8	10	12	9	16
IPSLr1-RCA	8	10	18	8	9	10	19	14
IPSLr1-WRF381P	N/A	N/A	N/A	N/A	N/A	N/A	N/A	N/A
MIROCr1-CCLM	7	4	9	5	9	10	11	8
MIROCr1-REMO2015	10	5	4	7	14	9	8	7
MPIr1-CCLM	10	13	7	11	9	7	8	11
MPIr1-RCA	8	10	8	10	6	6	6	13
MPIr1-REMO	6	9	2	6	7	0	5	7
MPIr2-REMO	6	9	4	8	9	1	4	12
MPIr1-WRF361H	14	9	6	8	9	4	6	11
NORESMr1-HIRHAM	7	6	6	9	12	8	9	15
NORESMr1-REMO2015	8	4	5	6	12	9	11	11
NORESMr1-RCA	7	6	8	9	13	6	7	21

Table 26: Change in R99w in summer

	BI	IP	FR	ME	SC	AL	MD	EA
Ens. Mean Change (%)	9	11	14	14	13	9	9	15
CANESMr1-CCLM	8	5	1	9	9	2	2	18
CANESMr1-REMO2015	13	8	9	21	19	8	8	19
CNRMr1-ALADIN63	8	9	11	13	12	7	7	10
CNRMr1-RACMO	8	4	14	12	15	15	14	19
ECEARTHr12-CCLM	10	24	10	16	11	6	9	11
ECEARTHr12-HIRHAM	14	25	21	18	12	8	13	13
ECEARTHr3-HIRHAM	3	12	22	14	14	11	14	19
ECEARTHr1-HIRHAM	10	13	18	22	14	8	13	14
ECEARTHr12-RACMO	5	10	12	9	8	3	**-5**	8
ECEARTHr1-RACMO	8	1	4	5	6	4	19	13
ECEARTHr3-RACMO	3	8	17	13	13	4	12	12
ECEARTHr12-RCA	11	11	6	5	9	**-2**	**-7**	5
ECEARTHr3-RCA	6	**-6**	16	7	10	**-4**	**-6**	6
ECEARTHr12-REMO2015	6	9	11	10	12	3	9	16
HADGEMr1-CCLM	12	31	31	21	15	20	34	19
HADGEMr1-HIRHAM	13	43	27	26	17	27	45	27
HADGEMr1-RACMO	11	30	20	15	15	17	19	23
HADGEMr1-RCA	6	10	17	15	11	21	16	19
HADGEMr1-REMO2015	16	14	22	19	19	16	11	20
HADGEMr1-REGCM	11	14	11	17	21	12	12	19
HADGEMr1-WRF361H	13	17	19	17	21	19	25	19
HADGEMr1-WRF381P	13	12	8	14	12	12	9	10
IPSLr1-RCA	2	**-4**	0	5	12	**-3**	1	7
IPSLr1-WRF381P	N/A	N/A	N/A	N/A	N/A	N/A	N/A	N/A
MIROCr1-CCLM	13	27	17	24	13	13	14	14
MIROCr1-REMO2015	18	5	12	17	19	14	14	17
MPIr1-CCLM	4	9	12	7	6	10	12	7
MPIr1-RCA	0	**-11**	6	4	6	5	**-2**	14
MPIr1-REMO	1	4	10	12	3	2	3	22
MPIr2-REMO	8	7	15	11	10	6	1	7
MPIr1-WRF361H	7	0	20	14	8	4	**-9**	13
NORESMr1-HIRHAM	18	13	27	28	15	18	10	23
NORESMr1-REMO2015	10	4	11	13	15	6	**-2**	14
NORESMr1-RCA	2	**-4**	0	9	11	11	**-8**	8

9.3 Dynamics

Change in sea level pressure (Figure 21) is generally small, not exceeding a few hPa for the middle of the century. However a few models exhibit some patterns with a mixture of RCM and GCM dependence, such as the WRF381P downscaling of IPSLr1 or, to a lesser extent, of HadGEM, and CanESMr1-CCLM or IPSLr1-RCA. For winds, widespread small-amplitude decreases are found for the mean wind (Figure 22) and for extreme winds (Figure 23). Such decreases are more robust in the IP, consistent with Tobin *et al*. (2015).

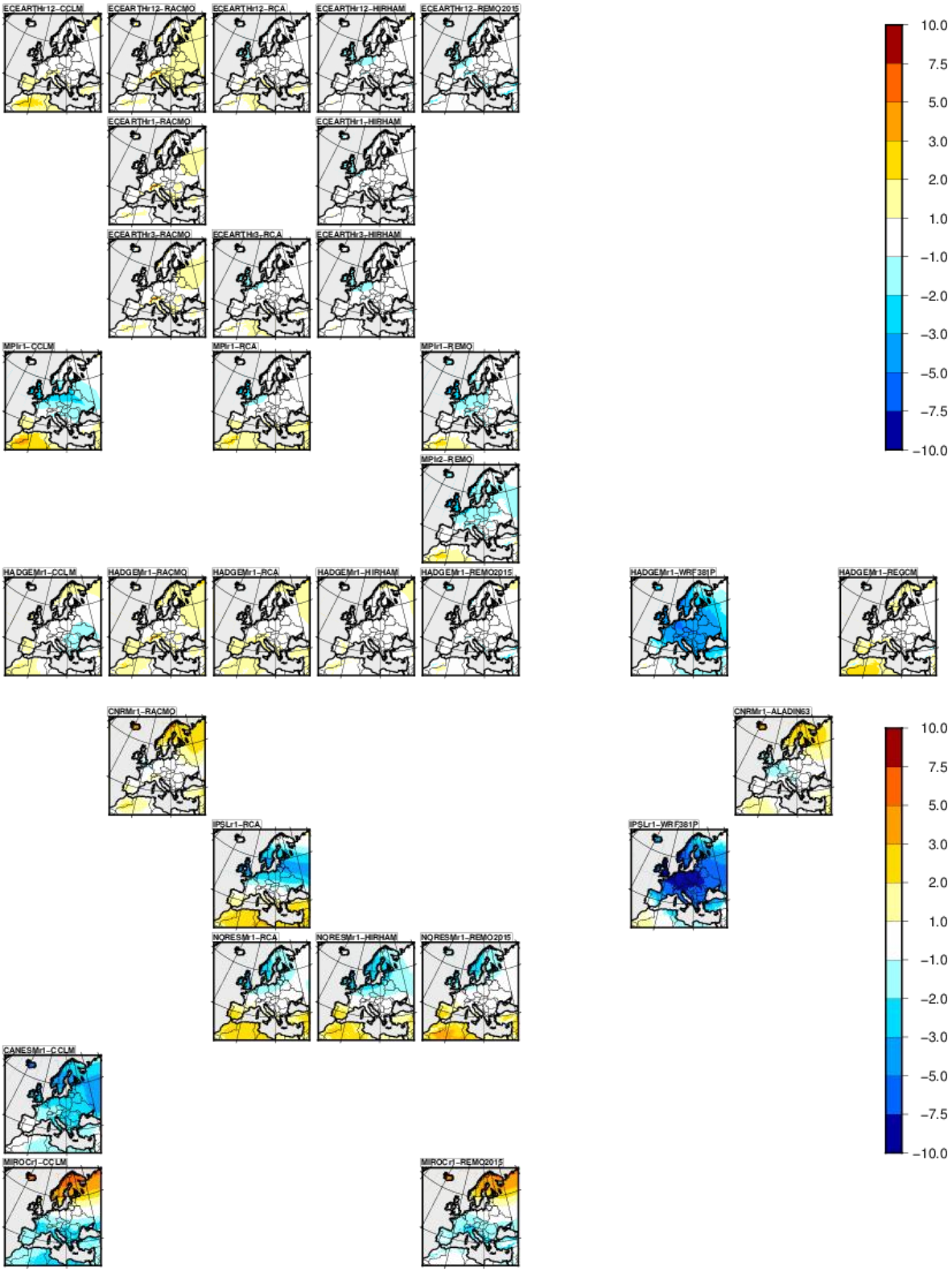

Figure 21: Changes in mean sea level pressure (hPa).

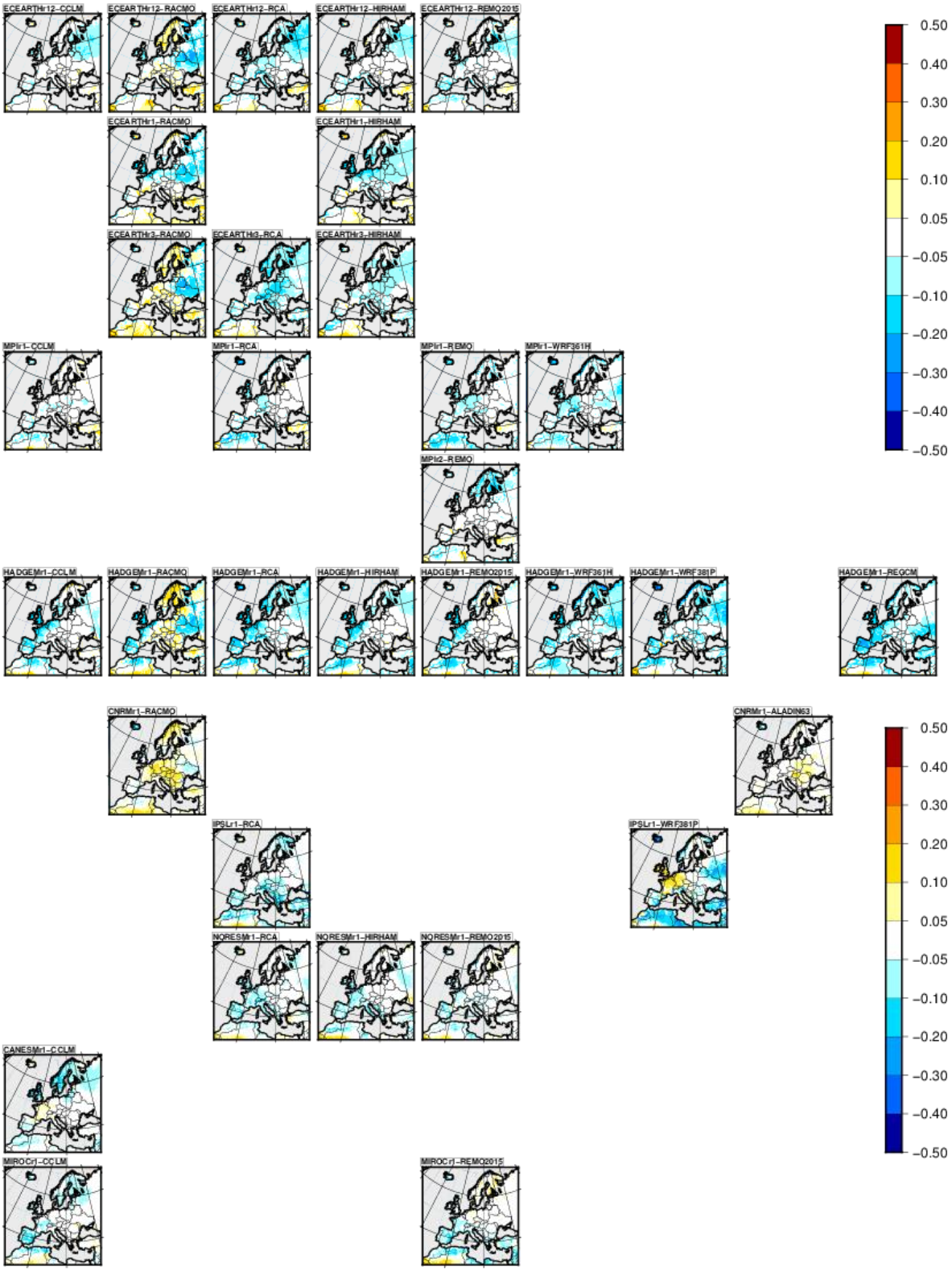

Figure 22: Changes in mean surface wind.

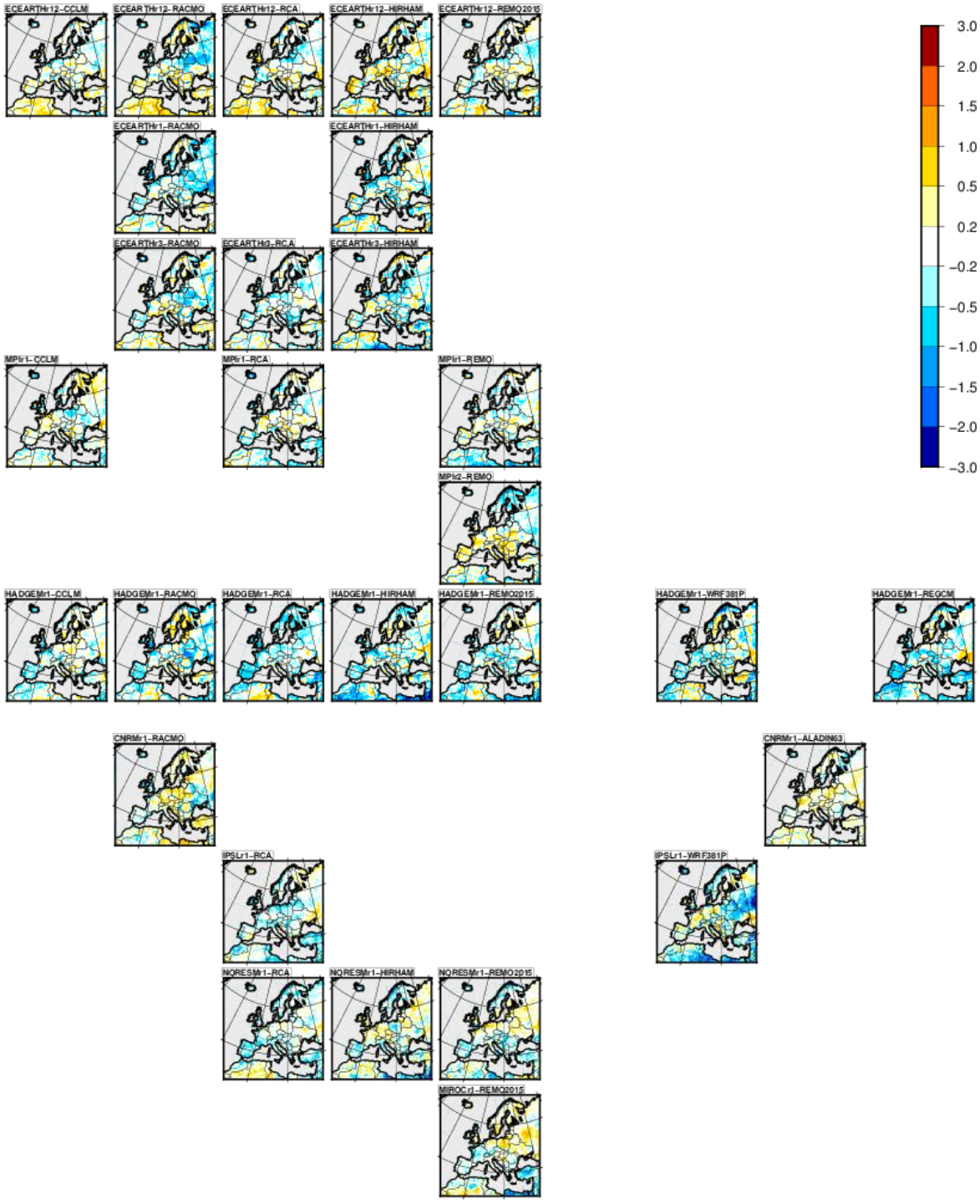

Figure 23: Changes in the annual maximal wind speed.

9.4 Radiation

The ensemble mean rsds changes between 1981-2010 and 2036-2065 range from -1.6 to -3.9 W/m² for the BI, ME, SC, AL and EA boxes (Table 26 and Figure 24). It is lower than + or -1W/m² in the IP, FR and MD boxes. Changes simulated by individual models are also rather weak, with absolute change lower than 5W/m². Two exceptions are WRF361H and ALADIN63. The first simulates negative changes ranging from -10 to -20W/m². Note that these changes cannot be explained by the choice of the forcing GCMs as the same GCMs associated with other RCMs provide different results, including in terms of sign. On the opposite side, ALADIN63 forced by CNRM-CM5 gives positive changes from 2 to 7W/m². Changes are most pronounced over central and eastern Europe (boxes ME, MD and EA), which is the European region where anthropogenic aerosols decreased more over the last decades (Gutiérrez *et al*., 2018). While most RCMs use constant aerosol forcings, only ALADIN63 and RACMO take into account a transient aerosol forcing for both the historical and the scenario periods:
(https://docs.google.com/document/d/1UCCv-DU8hLlZaSPkcndnM0SrJHoX4cvG-yqxbIDZlRc/edit).

Previous work based on former version of the same model has shown that realistic aerosol forcings should be applied in models in order to reproduce observed radiation trend (Nabat *et al*., 2015). Our results suggest that it may also influence the sign of the future rsds changes. Sensitivity experiments in the framework of the CORDEX-FPS aerosol are ongoing to assess the role of the regional aerosol load in the future evolution of the regional climate (see https://www.hymex.org/cordexfps-aerosol/wiki/doku.php?id=protocol1b for more details about the sensitivity experiments protocol).

Table 26: Changes in surface solar radiation (mid century – reference).

	BI	IP	FR	ME	SC	MD	AL	EA
Ens Mean change	-2.9	0.9	-0.8	-2.5	-3.9	-1.6	0.1	-2.0
CANESMr1 – CCLM	-2.1	3.3	1.0	-0.8	-3.8	1.7	1.8	-1.3
CANESMr1 - REMO2015	-3.2	1.3	-1.7	-3.4	-3.1	0.1	0.9	-2.4
CNRMr1 - ALADIN63	3.2	4.9	5.7	6.3	2.1	5.1	7.3	6.9
CNRMr1 - RACMO	-2.8	1.7	-0.7	-1.3	-2.7	-1.0	3.9	0.3
ECEARTHr12 - CCLM	-4.0	-0.1	-1.7	-4.5	-5.7	-2.1	-0.7	-5.6
ECEARTHr12 - HIRHAM	-0.2	1.2	0.8	-0.3	-1.4	0.6	1.0	-1.0
ECEARTHr3 - HIRHAM	-2.3	2.1	-1.2	-1.7	-3.2	-1.8	0.3	0.0
ECEARTHr1 - HIRHAM	-0.2	2.4	1.4	-1.5	-3.1	-0.0	-0.2	-2.0
ECEARTHr12 - RACMO	-1.3	1.2	0.7	0.6	-0.5	1.0	4.1	2.6
ECEARTHr1 - RACMO	-2.8	3.1	1.3	-0.7	-2.4	1.0	3.4	0.4
ECEARTHr3 - RACMO	-2.6	3.6	-2.3	-2.4	-2.7	-2.0	4.2	1.8
ECEARTHr12 - RCA	-1.4	0.5	0.9	-1.7	-4.3	-1.4	0.4	-3.0
ECEARTHr3 -RCA	-1.6	1.8	0.4	-0.7	-4.7	-1.4	0.2	-1.2
ECEARTHr12 - REMO2015	-1.8	-0.2	-0.4	-2.4	-2.0	-0.3	-0.7	-2.9
HADGEMr1 - CCLM	-1.6	1.4	0.4	-0.6	-5.3	-0.5	-1.0	-2.7
HADGEMr1 - HIRHAM	-0.2	3.3	0.2	-2.0	-1.8	-0.9	0.3	-1.7
HADGEMr1 - RACMO	-1.5	3.7	0.9	-1.3	-2.0	0.0	2.5	2.1
HADGEMr1 -RCA	-2.5	1.9	-1.3	-4.0	-5.2	-1.9	-0.4	-2.9
HADGEMr1 - REMO2015	-1.4	0.6	-1.0	-2.3	-1.8	-0.9	-0.3	-3.0
HADGEMr1 - REGCM	-1.8	1.7	-0.6	-0.4	-1.6	0.2	1.5	0.4
HADGEMr1 - WRF361H	-17.4	-11.4	-10.3	-13.9	-16.9	-11.4	-13.2	-13.1
HADGEMr1 - WRF381P	-4.0	0.2	-3.4	-4.3	-1.5	-3.3	-0.8	-1.8
IPSLr1 -RCA	-4.4	0.1	1.9	-2.6	-6.8	-0.3	1.3	-2.7
IPSLr1 - WRF381P	-5.0	-0.5	-5.4	-6.1	-2.9	-5.8	-1.3	-3.6
MIROCr1 -CCLM	-2.5	1.1	1.9	0.1	-3.9	0.1	0.4	-0.8
MIROCr1 - REMO2015	-2.5	0.3	0.4	-1.5	-1.9	-1.9	-0.9	-1.4
MPIr1 -CCLM	-4.3	1.8	-1.3	-3.3	-5.8	-3.0	0.4	-3.5
MPIr1 -RCA	-2.9	2.5	-0.9	-2.8	-6.0	-1.7	1.4	-2.1
MPIr1 -REMO	-3.6	0.4	-2.9	-4.0	-4.5	-3.9	-0.6	-3.8
MPIr2 -REMO	-3.3	-0.1	-1.8	-3.5	-3.0	-0.6	-0.5	-2.1
MPIr1 -WRF361H	-19.7	-11.0	-13.5	-16.5	-17.6	-12.9	-12.6	-13.6

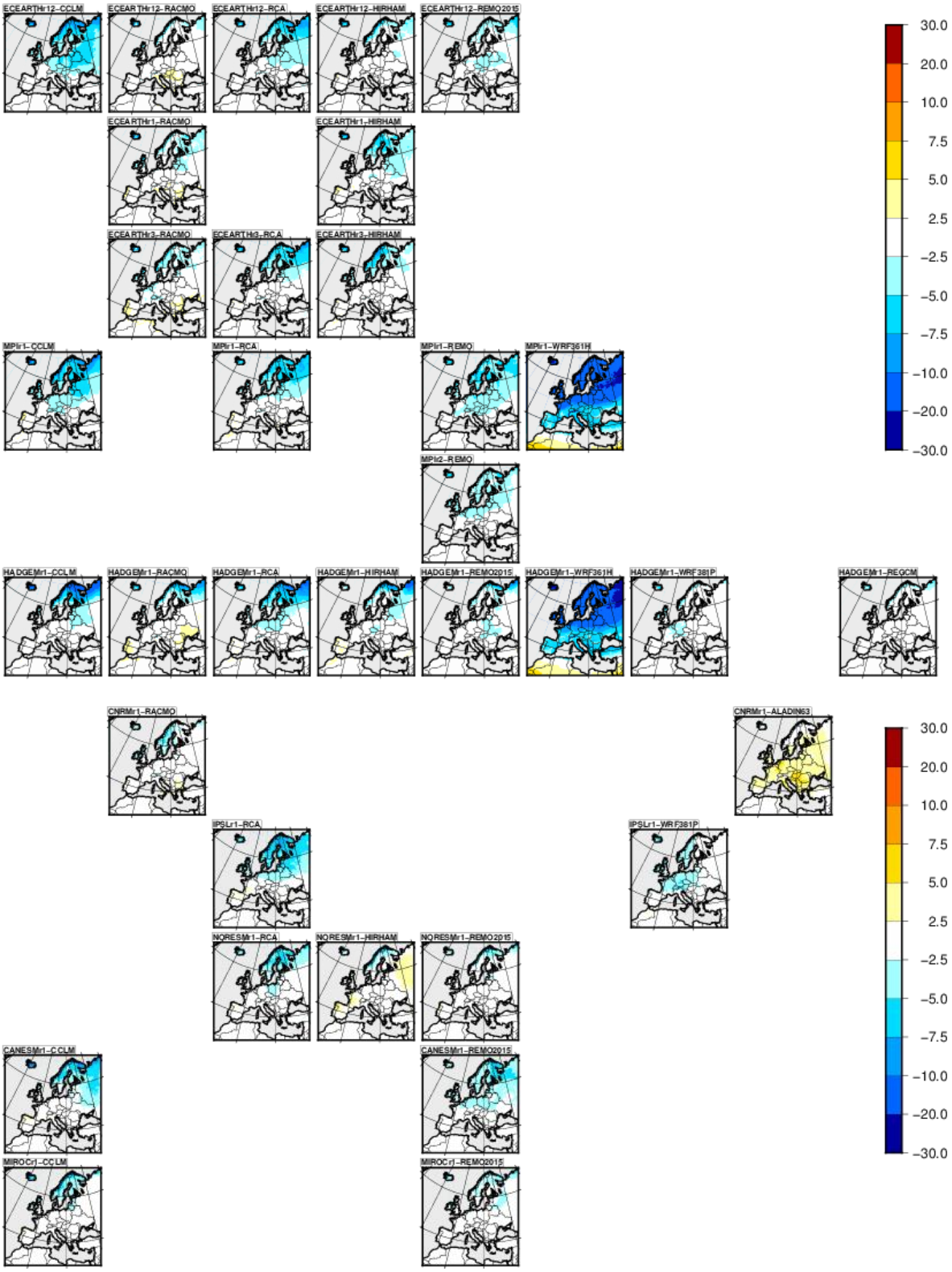

Figure 24: Changes in surface radiation (mid century – reference).

10. Specific analyses

10.1 Added value of RCMs relative to GCMs

A new method for calculating the Spatial Added Value of a variable is being developed. This method stems from the spatial downscaling signal described by Giorgi *et al.* (2016) and the spatial correlation skill mentioned in Rummukainen (2016). Other studies (Kanamitsu & DeHaan, 2011; Torma *et al.*, 2015; Fantini *et al.*, 2016) use different metrics to describe the difference between modelled and observed PDFs, however, these describe only parts of the distribution. The method presented below, describes an attempt to quantify a Spatial Added Value by accounting for the full difference between PDF distributions.

For a variable of interest, the method requires data from a RCM, the corresponding GCM, and an observation (OBS) source (of high resolution). Once the three data-sets are interpolated to a common grid, the PDF data is calculated for the 3 data sets for each grid cell (with identical bins), in order to perform a fair comparison.

The resulting PDF data for the GCM is compared to the PDF of the OBS by calculating the Relative Probability Difference, *D* (shown in the equation below) where *P* is the Probability, *F* is the Frequency, and *v* is the variable value. This process (shown in Figure 5) is repeated for the RCM and is done to account for all the discrepancies throughout the distribution. The resulting plots describe the spatial distribution of D_{MOD} from the observation. The Added Value, A_v is thus obtained by comparing D_{GCM} to D_{RCM} where positive quantities describe an improvement of the RCM over the GCM.

$$D_{MOD} = \frac{\sum_v |F_{MOD} - F_{OBS}|}{\sum_v F_{OBS}}$$

$$D_{MOD} = \frac{|P_{MOD} - P_{OBS}|}{P_{OBS}}$$

$$A_v = D_{GCM} - D_{RCM}$$

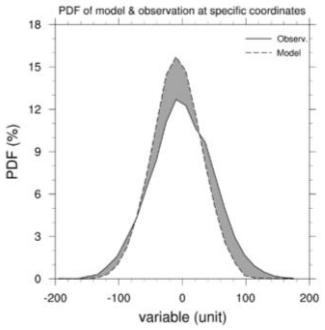

Figure 25. An imitation PDF of a single grid cell comparing the distributions of a model and an observation source for a particular variable. The shaded area represents the Relative Probability Difference of the model (D_{MOD}).

The final aim of this method is to quantify the RCM added value for a projected signal and assess how different are the two distributions for a future time slice. In an analogous way as above, we can then define a Downscaling Signal, A_{DS} (as shown in the equation below), similar to the method described by Giorgi *et al.* (2016). The larger the value, the more different the two projected PDFs are and the magnitude of A_{DS} is proportional to this difference.

$$A_{DS} = \frac{|P_{RCM} - P_{GCM}|}{P_{GCM}}$$

The CORDEX ensemble of 34 EUR-11 simulations was used to test this method as well as assess the added value provided by each member. The analysis was focused on 3 variables (precipitation, maximum winter temperatures, and maximum summer temperatures) and repeated for two grids one representative of the RCM resolution and the other representing the GCM resolution (0.11° and 2.00°) for the time period of 1981-2010. The E-OBS data set was used as a reference and interpolated over both analysis grids.

The A_v plots (Figure 26 to Figure) reveal an improvement of the variable distribution for the majority of the models, especially for precipitation (Figure 25 and Figure) and the added value is retained also when the models are upscaled to the lower resolution. Areas of complex topography and coastal regions also tend to have a greater added value. The maximum temperature plots (Figure 7, Figure 8, Figure 30, and Figure 31) sometimes display a negative A_v in areas of higher topography, which may be attributed the station availability of the E-OBS in those regions and also to the lower resolution of the OBS compared to the RCMs.

A similar analysis was performed for the downscaling signal for the 2036-2065 future time slice of the RCP 8.5 scenario (Figure to Figure 7). There is an average difference around 40% between RCM and GCM projections for precipitation and the difference is up to 200% for maximum temperature especially over the topography. Also, for the A_{DS} (Figure 5 to Figure 7) the added value is retained at a lower resolution, especially in coastal regions.

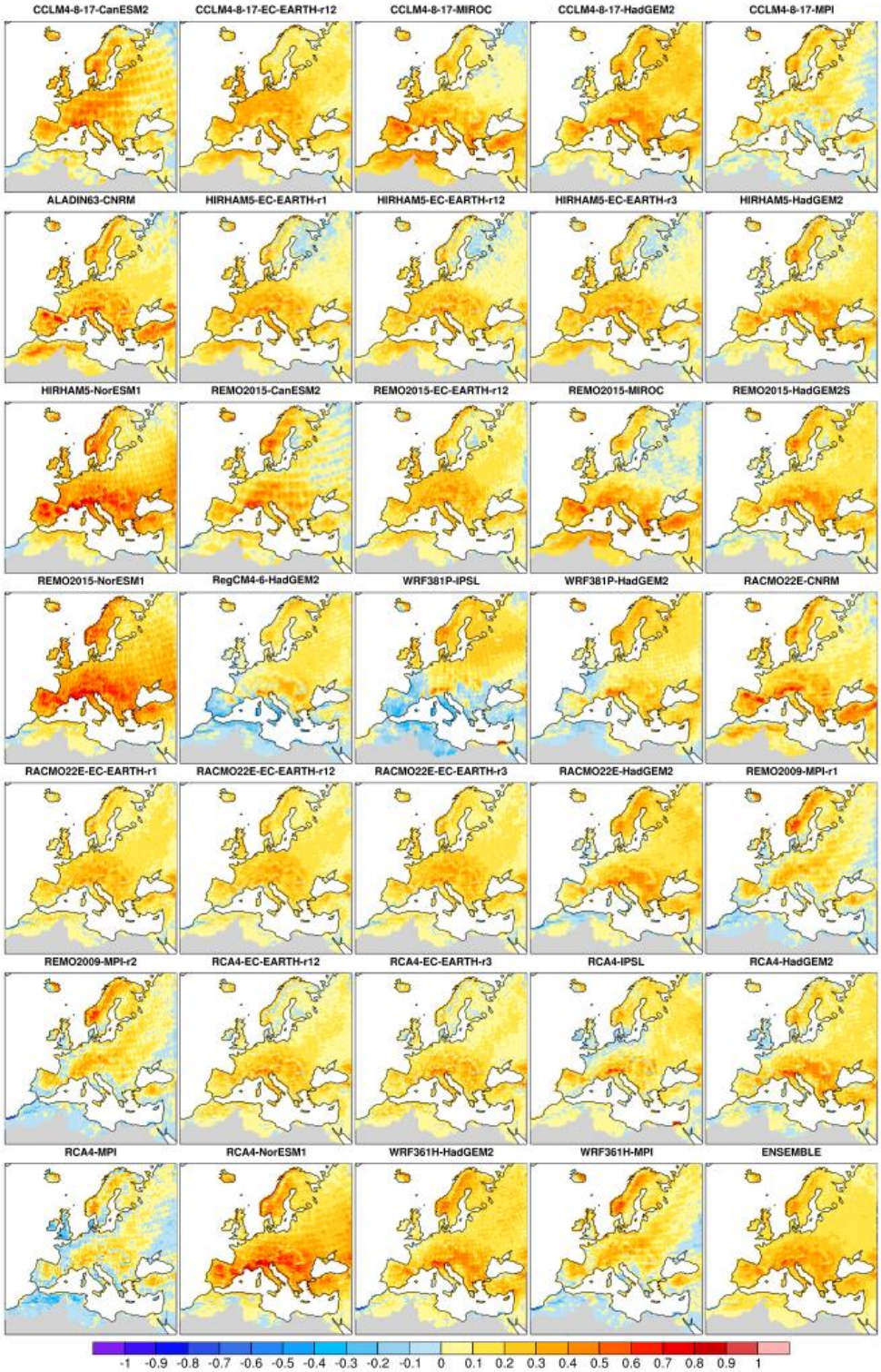

Figure 26. Spatial Added Value, A_v (expressed as fractions, where 1 corresponds to 100%) for the RCM ensemble members and the ensemble mean on the 0.11° grid for precipitation for the period of 1981-2010.

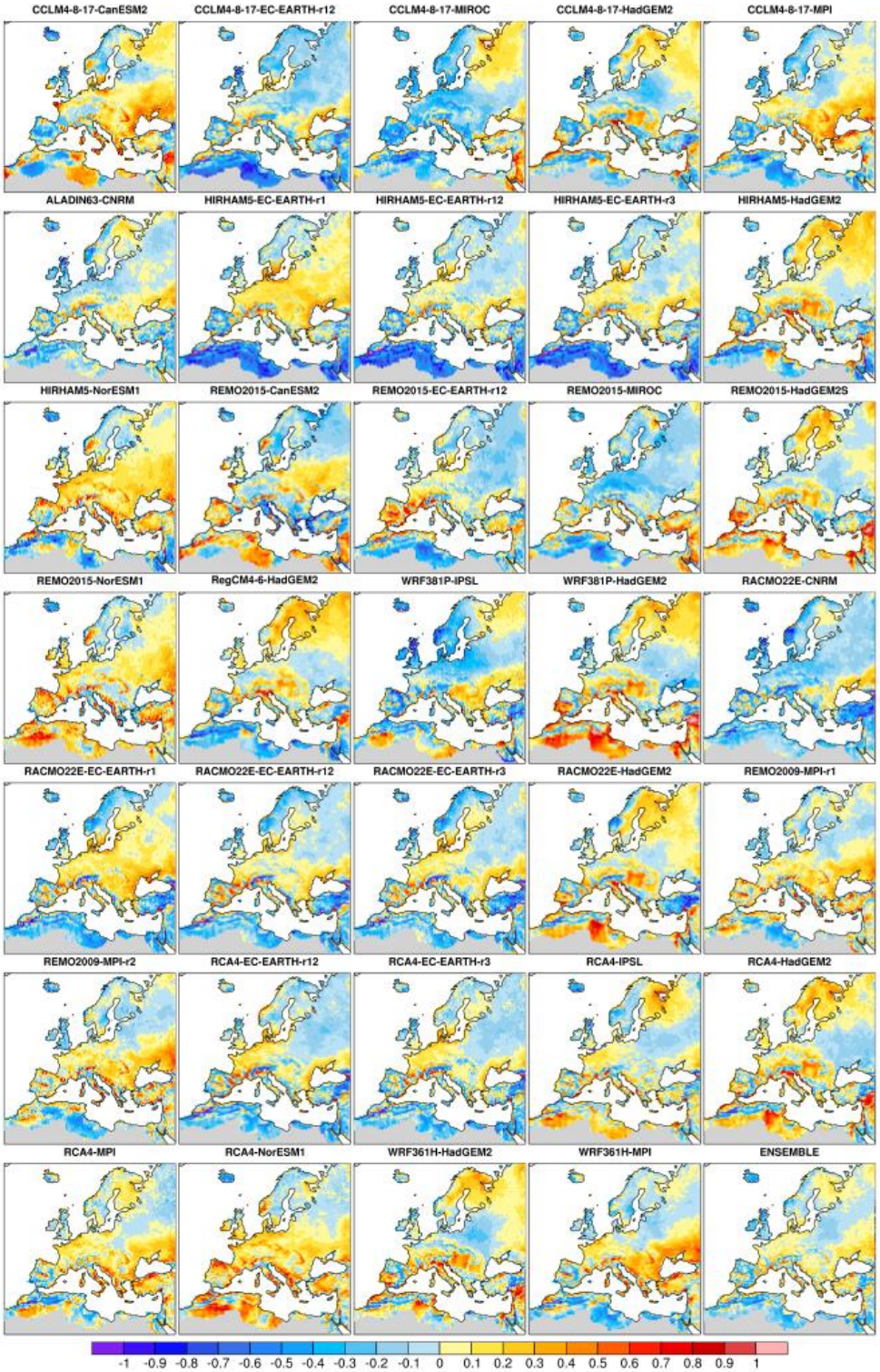

Figure 27. Spatial Added Value, A_v (expressed as fractions, where 1 corresponds to 100%) for the RCM ensemble members and the ensemble mean on the 0.11° grid for maximum air temperature during DJF for the period of 1981-2010.

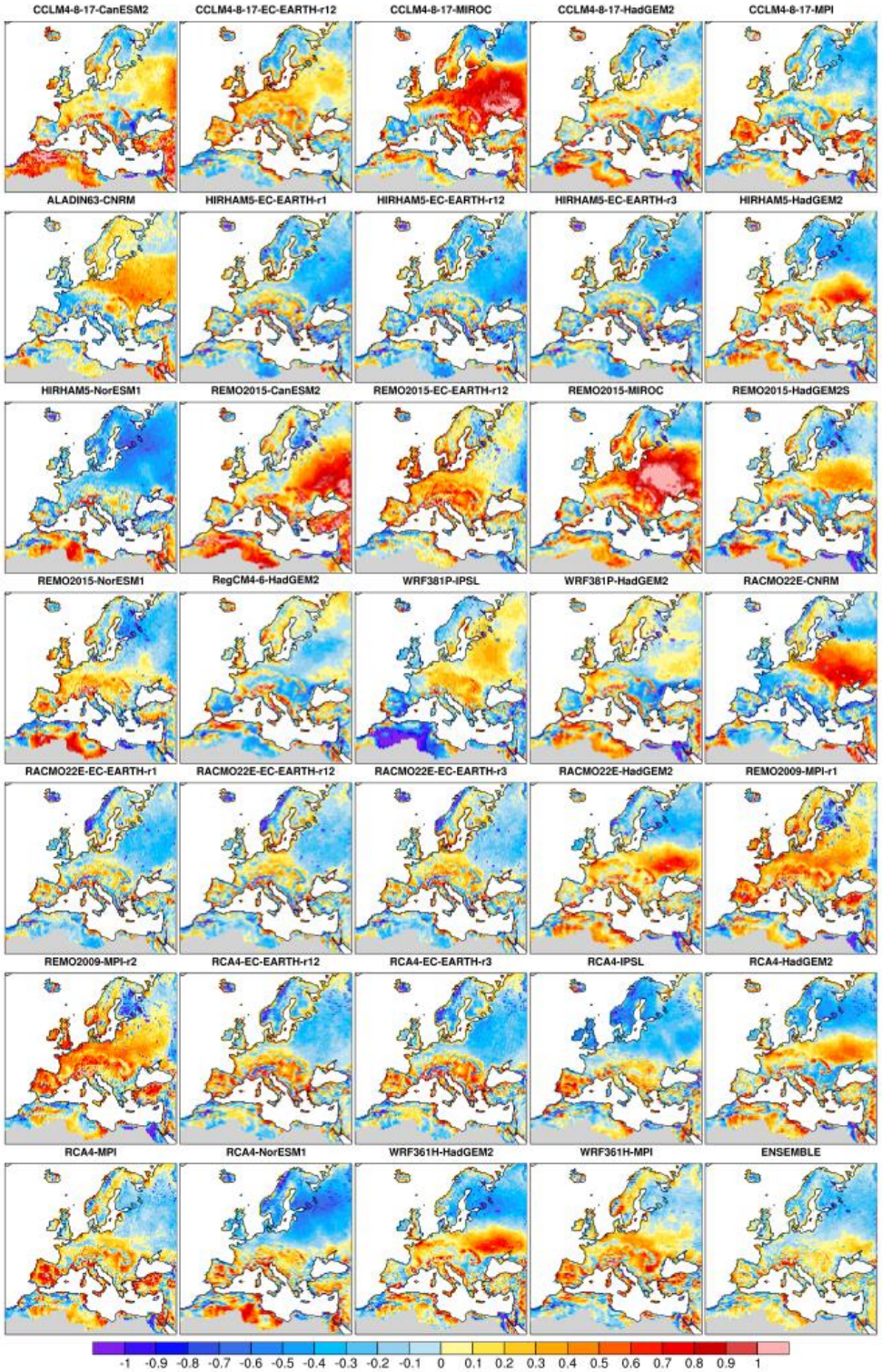

Figure 28. Spatial Added Value, A_v (expressed as fractions, where 1 corresponds to 100%) for the RCM ensemble members and the ensemble mean on the 0.11° grid for maximum air temperature during JJA for the period of 1981-2010.

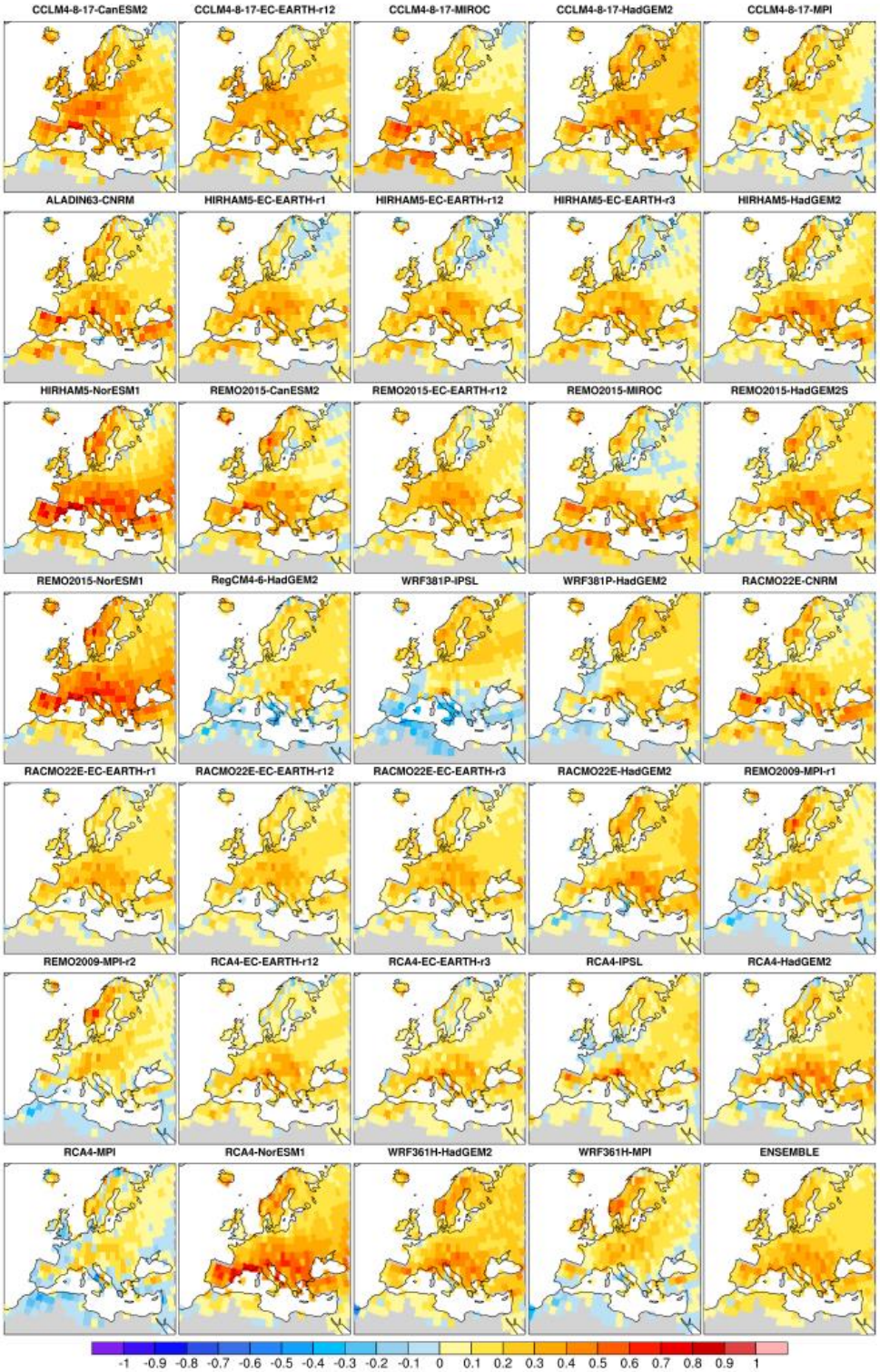

Figure 29. Spatial Added Value, A_v (expressed as fractions, where 1 corresponds to 100%) for the RCM ensemble members and the ensemble mean on the 2.0° grid for precipitation for the period of 1981-2010.

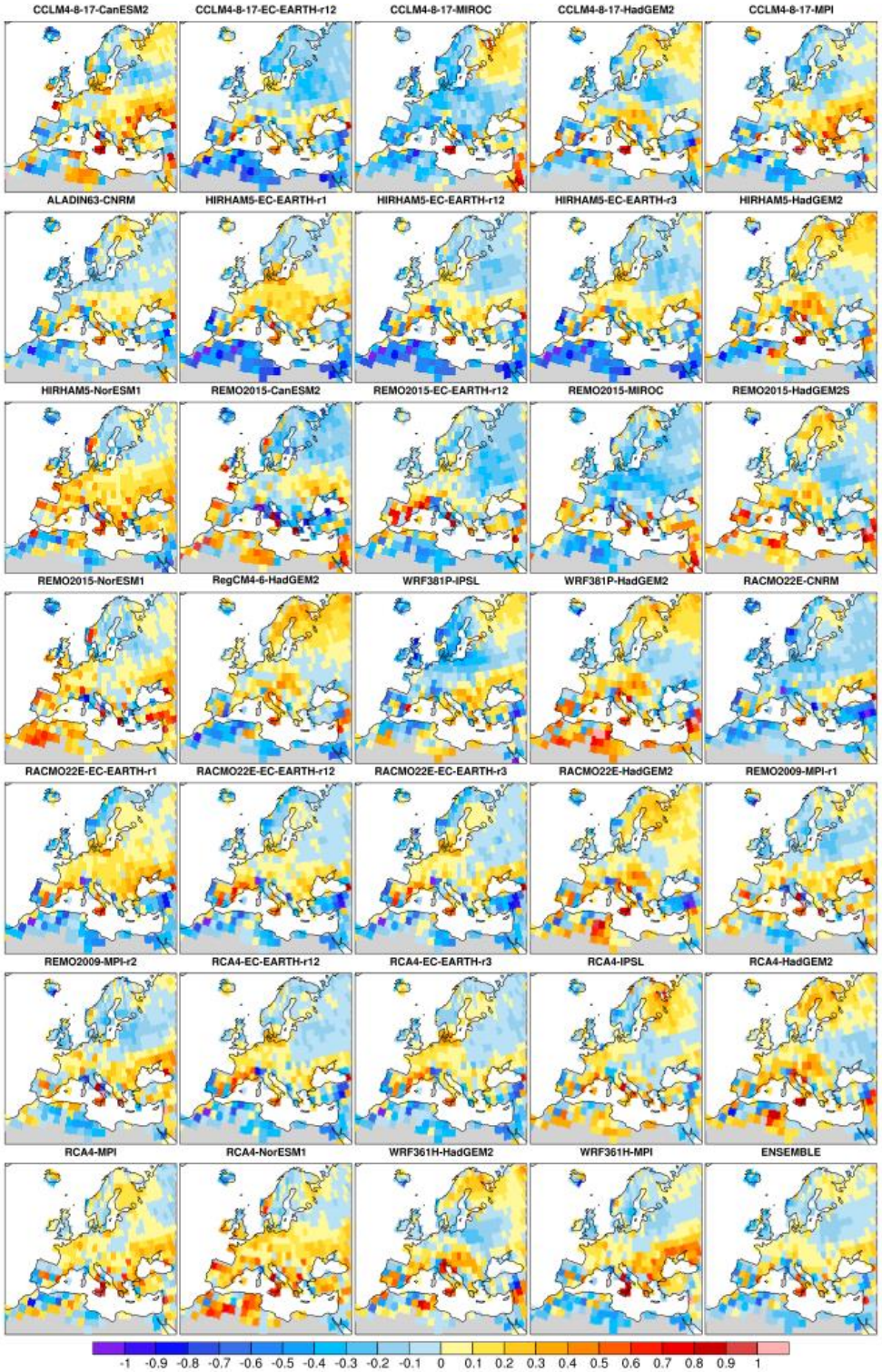

Figure 30. Spatial Added Value, A_v (expressed as fractions, where 1 corresponds to 100%) for the RCM ensemble members and the ensemble mean on the 2.0° grid for maximum air temperature during DJF for the period of 1981-2010.

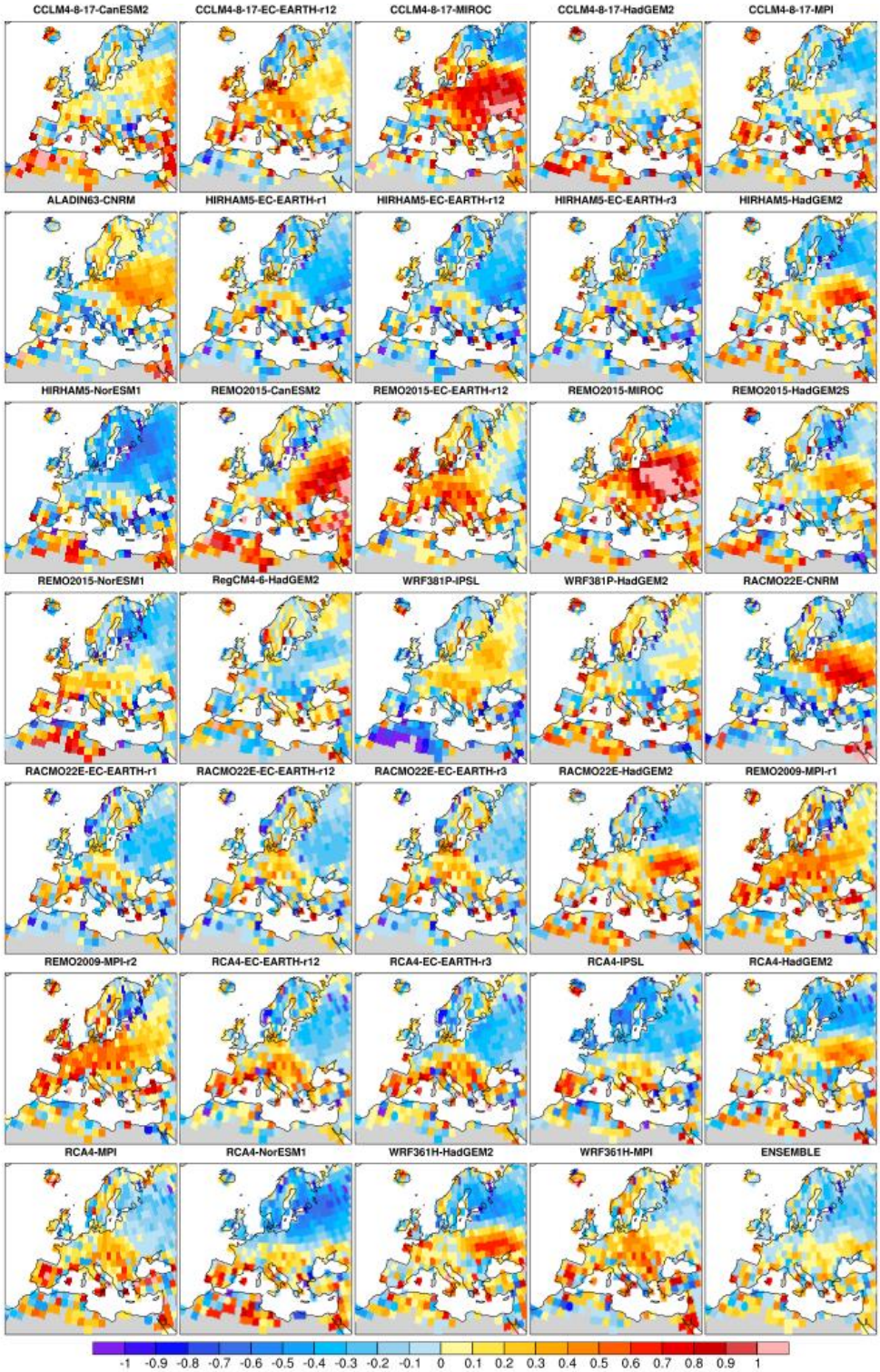

Figure 31. Spatial Added Value, A_v (expressed as fractions, where 1 corresponds to 100%) for the RCM ensemble members and the ensemble mean on the 2.0° grid for maximum air temperature during JJA for the period of 1981-2010.

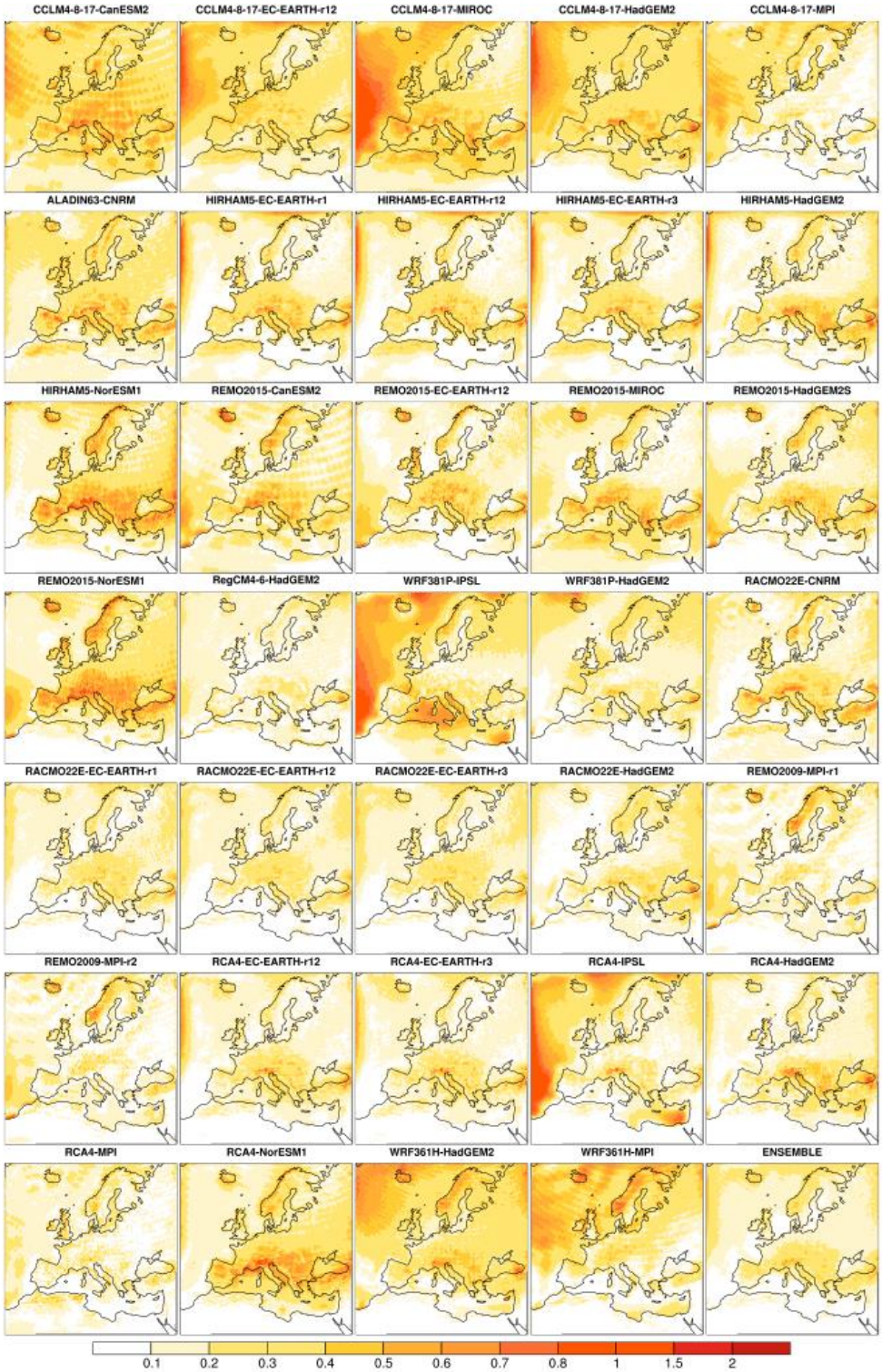

Figure 32. Downscaling Signal, A_{DS} (expressed as fractions, where 1 corresponds to 100%) for the RCM ensemble members and the ensemble mean on the 0.11° grid for precipitation for the period of 2036-2065 at RCP 8.5.

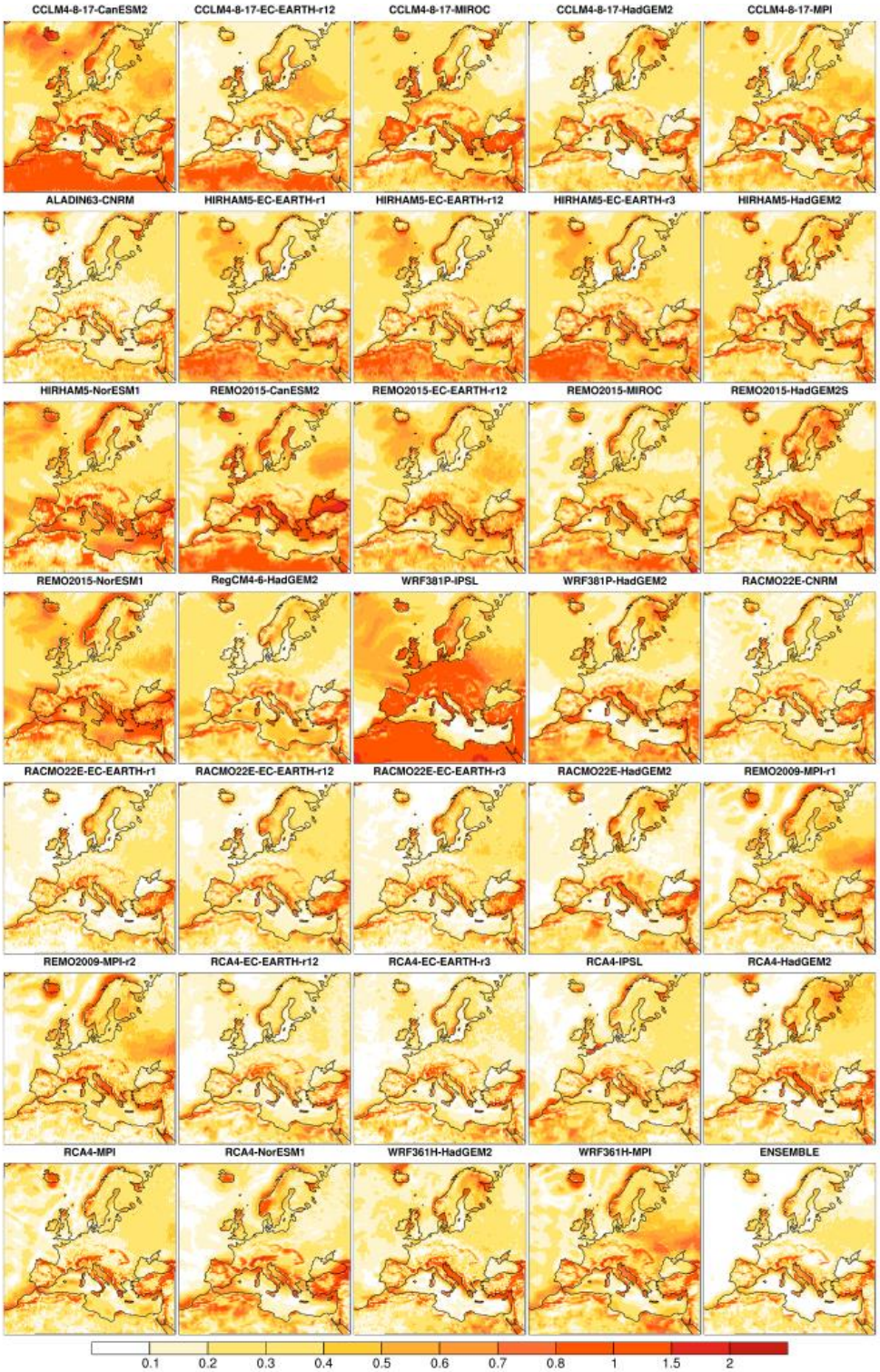

Figure 33. Downscaling Signal, A_{DS} (expressed as fractions, where 1 corresponds to 100%) for the RCM ensemble members and the ensemble mean on the 0.11° grid for maximum air temperature during DJF for the period of 2036-2065 at RCP8.5.

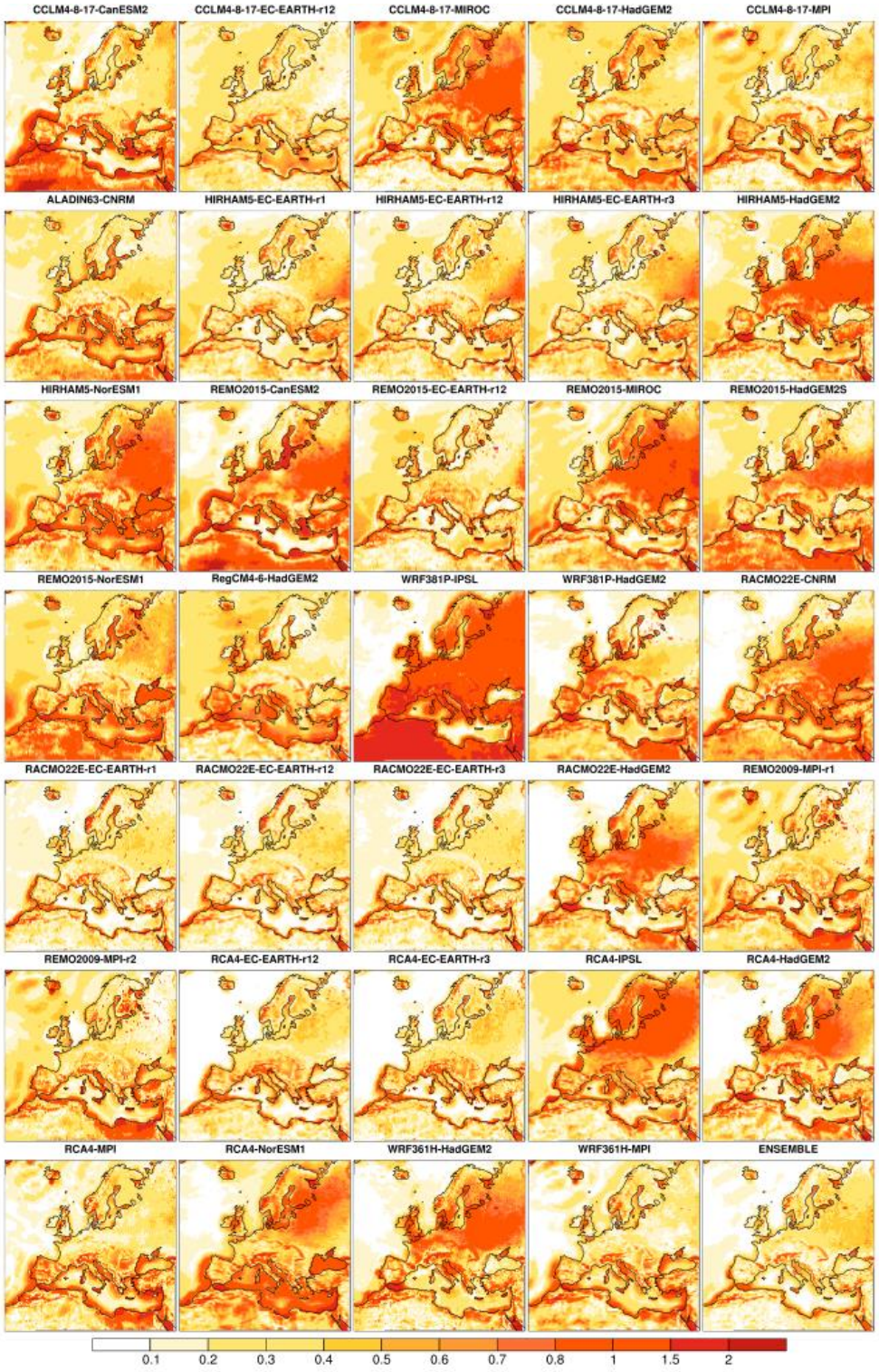

Figure 34. Downscaling Signal, A_{DS} (expressed as fractions, where 1 corresponds to 100%) for the RCM ensemble members and the ensemble mean on the 0.11° grid for maximum air temperature during JJA for the period of 2036-2065 at RCP8.5.

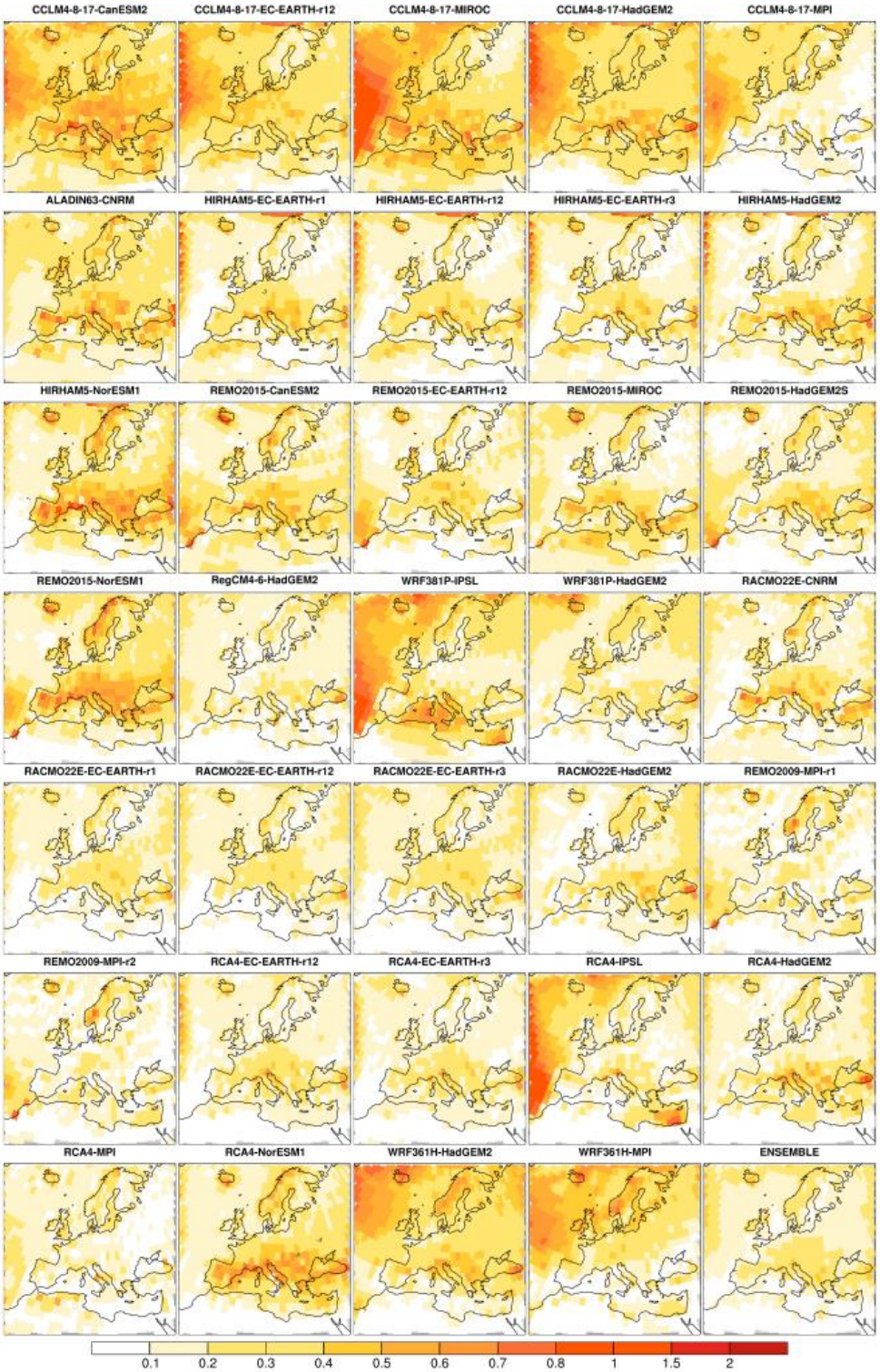

Figure 35. Downscaling Signal, A_{DS} (expressed as fractions, where 1 corresponds to 100%) for the RCM ensemble members and the ensemble mean on the 2.0° grid for precipitation for the period of 2036-2065 at RCP 8.5.

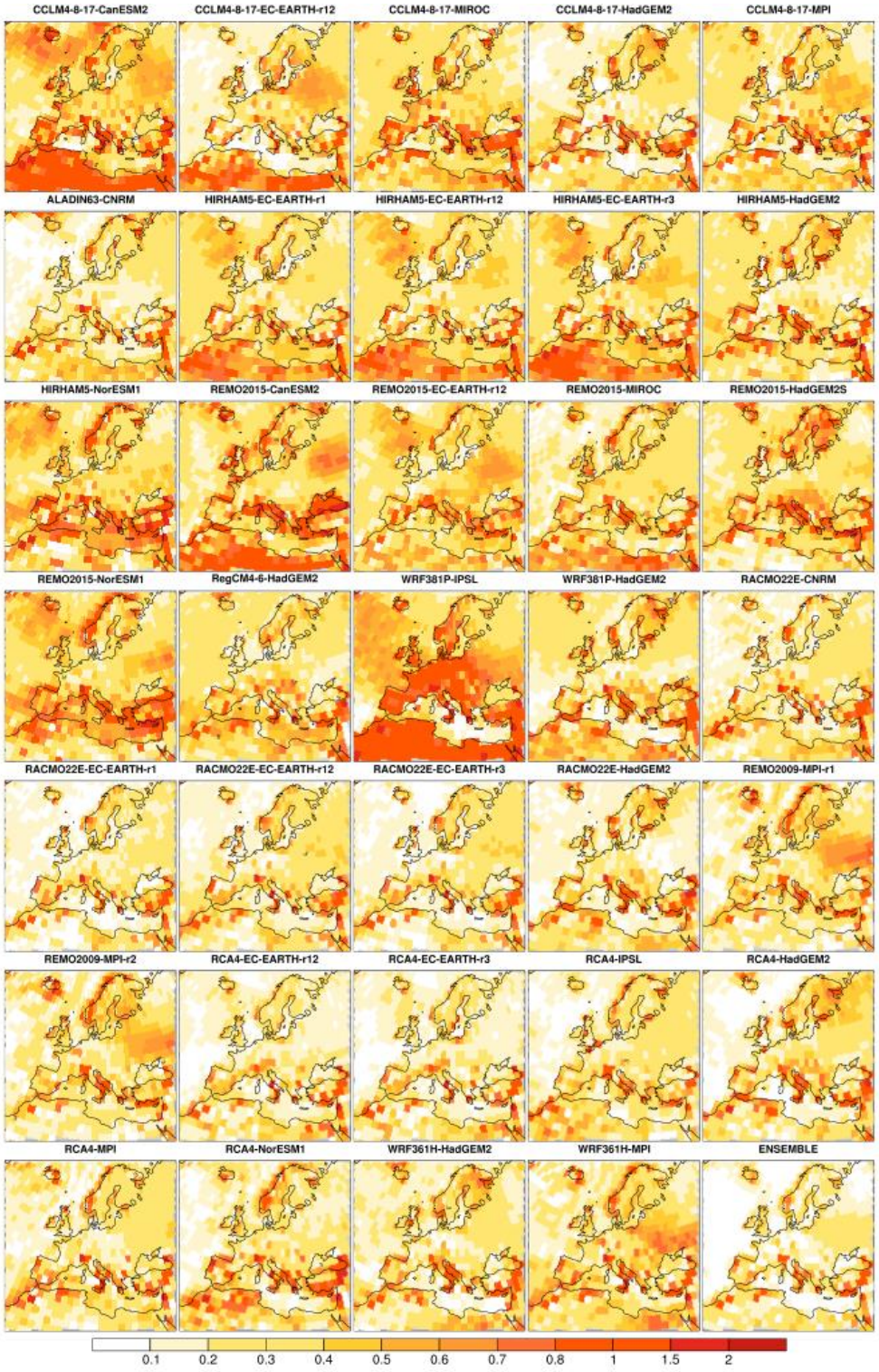

Figure 36. Downscaling Signal, A_{DS} (expressed as fractions, where 1 corresponds to 100%) for the RCM ensemble members and the ensemble mean on the 2.0° grid for maximum air temperature during DJF for the period of 2036-2065 at RCP8.5.

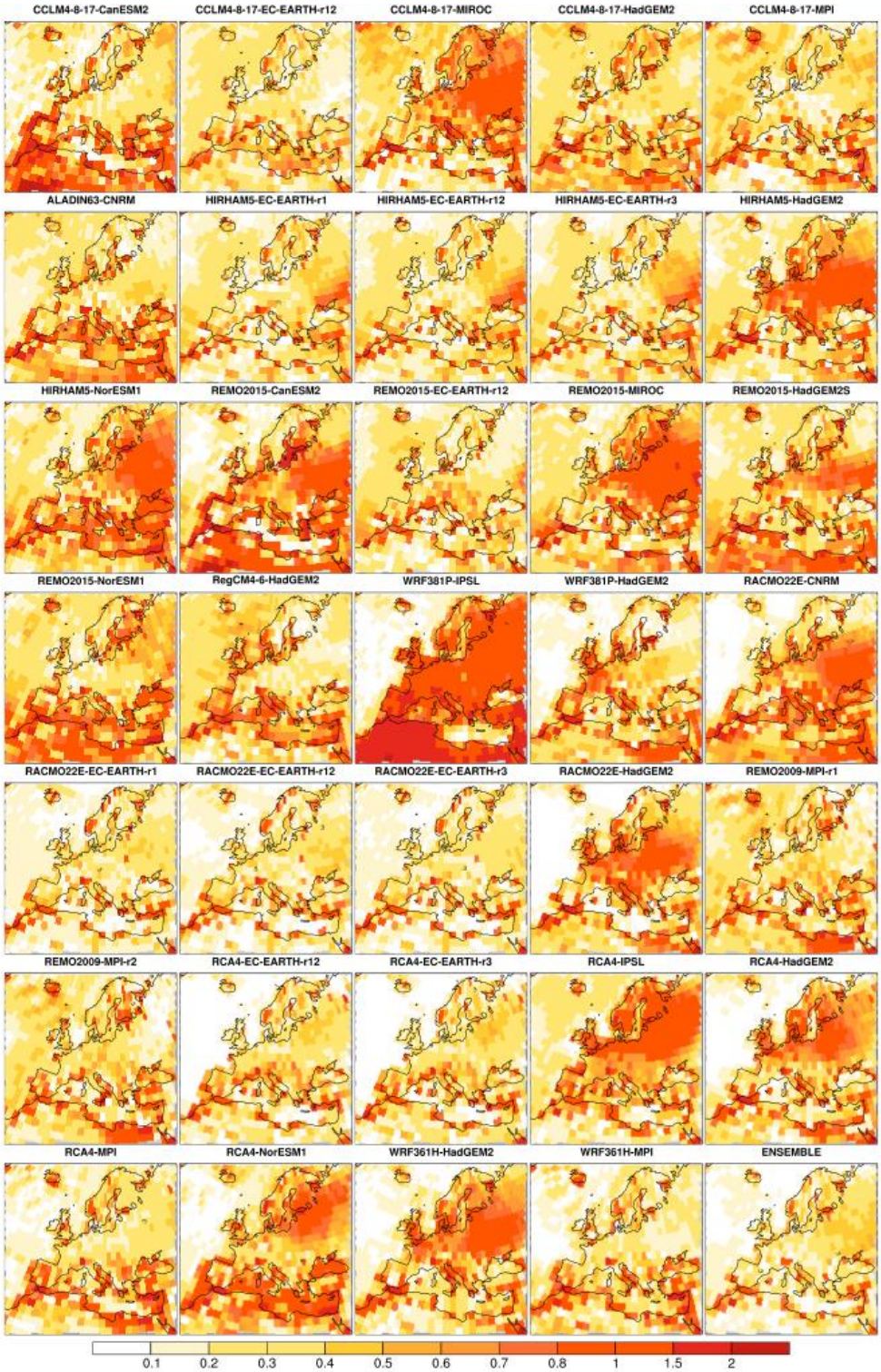

Figure 37. Downscaling Signal, A_{DS} (expressed as fractions, where 1 corresponds to 100%) for the RCM ensemble members and the ensemble mean on the 2.0° grid for maximum air temperature during JJA for the period of 2036-2065 at RCP8.5.

10.2 GCM and RCM spread of climate change signals

Here we present results where the RCMs are compared with the driving GCM. We are comparing the model spread in the RCM ensemble with the GCM ensemble, in addition to see how the temperature and precipitation climate change signal is modulated by the RCMs from the GCM. The climate change signal is calculated for the end of century (2071-2100) with respect to the historical period (1981-2010). The bivariate (near surface temperature and precipitation) climate change signals for the 34 RCMs simulations are compared with the corresponding 10 GCM simulations (Note that there are 11 GCM simulations, but the EC-EARTH r3 is not available on the ESGF node, and is therefore not included). To visualize the climate change signal, a probability ellipse for the bivariate climate change signal is calculated, where the data are assumed to have a normal distribution. The covariance of the data determines the angle of the ellipse, and the contour of the ellipse represents the confidence interval, which spans $\pm$ one standard deviation, thus the probability ellipse covers 68.2% of the data. Note that the probability ellipses are merely meant to guide the eye when considering the figure, rather than providing a probabilistic assessment. The probability ellipse is calculated separately for the RCMs (34 simulations, full lines) and the GCMs (10 simulations, dashed lines). The RCM and GCM are compared by aggregating the results over the eight PRUDENCE regions for the summer (JJA) and winter (DJF) season.

For the summer season (Figure 38), the RCMs are substantially modulating the projected temperature and precipitation changes. The temperature change is often reduced by the RCMs compared to the GCMs, especially over Scandinavia, eastern Europe and the Alps, while over the Iberian Peninsula the temperature reductions by the regional models are not so strong. For GCMs that predict a comparatively low temperature change, the RCMs do not reduce the temperature change much, or they may even increase it. However, when a GCM predict a high temperature change, the RCMs tend to systematically reduce the change signal. This is seen in particular for the HadGEM2-ES, which has the highest climate sensitivity of the different GCMs (see e.g. Andrews *et al*. 2012). 8 RCMs have downscaled this particular GCM, and for all the regions, the RCMs are reducing the temperature change by 0.5 and up to 4°C. The change in the precipitation is more complex, but there is a tendency of the RCMs to reduce the projected drying over the Alpine and Mediterranean regions, and to increase precipitation over Scandinavia, compared to the driving GCMs. For a few GCMs the regional models are actually changing the sign of the projected precipitation change compared with the GCMs. There is a tendency that the RCM ensemble has a smaller model spread then the GCM ensemble, epically for the spread in the temperature change signal. However, as discussed above, much of the change in the summer temperature comes from the very high temperature change predicted by the HadGEM2-ES, which is reduced by all the RCMs.

For the winter season (Figure 39), the RCMs are not modulating the climate change signal in a systematic way as seen for the summer season. In general, the bivariate climate change signal in the RCMs does not differ so much from the driving GCMs. Thus, in winter the RCMs seems to be strongly driven by the GCMs, while in summer the RCMs make the climate change response quite different compared to the driving GCMs. These results are in line with Sørland *et al*. (2018) and Kjellström *et al*. (2016), which also found that RCMs in EURO-CORDEX simulations are modifying the climate change signal compared to the driving GCMs. Sørland *et al*. (2018) suggested that one of the

reasons for the lowered temperature projections in summer is that RCMs are better at representing near-surface processes that are important for e.g. reducing the drying feedback.

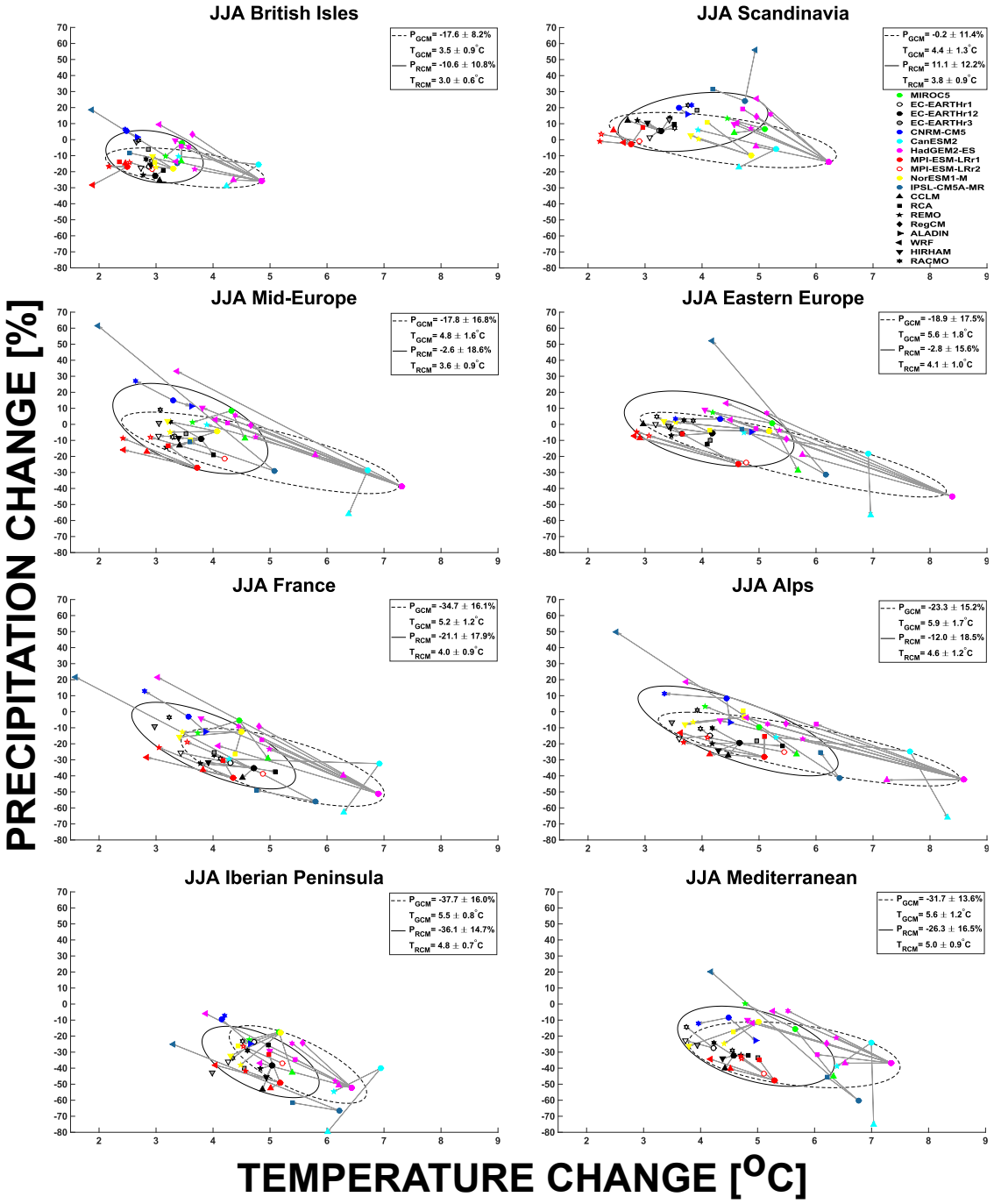

Figure 38: Panels show the bivariate climate change signal in terms of projected summer (JJA) temperature and precipitation changes for 2070-2099 versus 1981-2010 assuming the RCP8.5 emissions scenarios. The circles show the GCM results, the other symbols indicate the different GCM-RCMs and colours the driving GCMs. The dashed (solid) line indicates the probability ellipse for the GCM (RCM) results, covering 68.2 % of the data. The grey arrow is pointing from the driving GCM to the corresponding GCM-RCM simulation. The mean precipitation (P, %) and temperature (T, °C) changes together with the standard deviations (mean ± σ), for the GCM and RCM ensemble, respectively, is given in the top right corner of each sub-figure. Note that the GCM data for the member EC-EARTH r3 was not available and is therefore not included in the analysis.

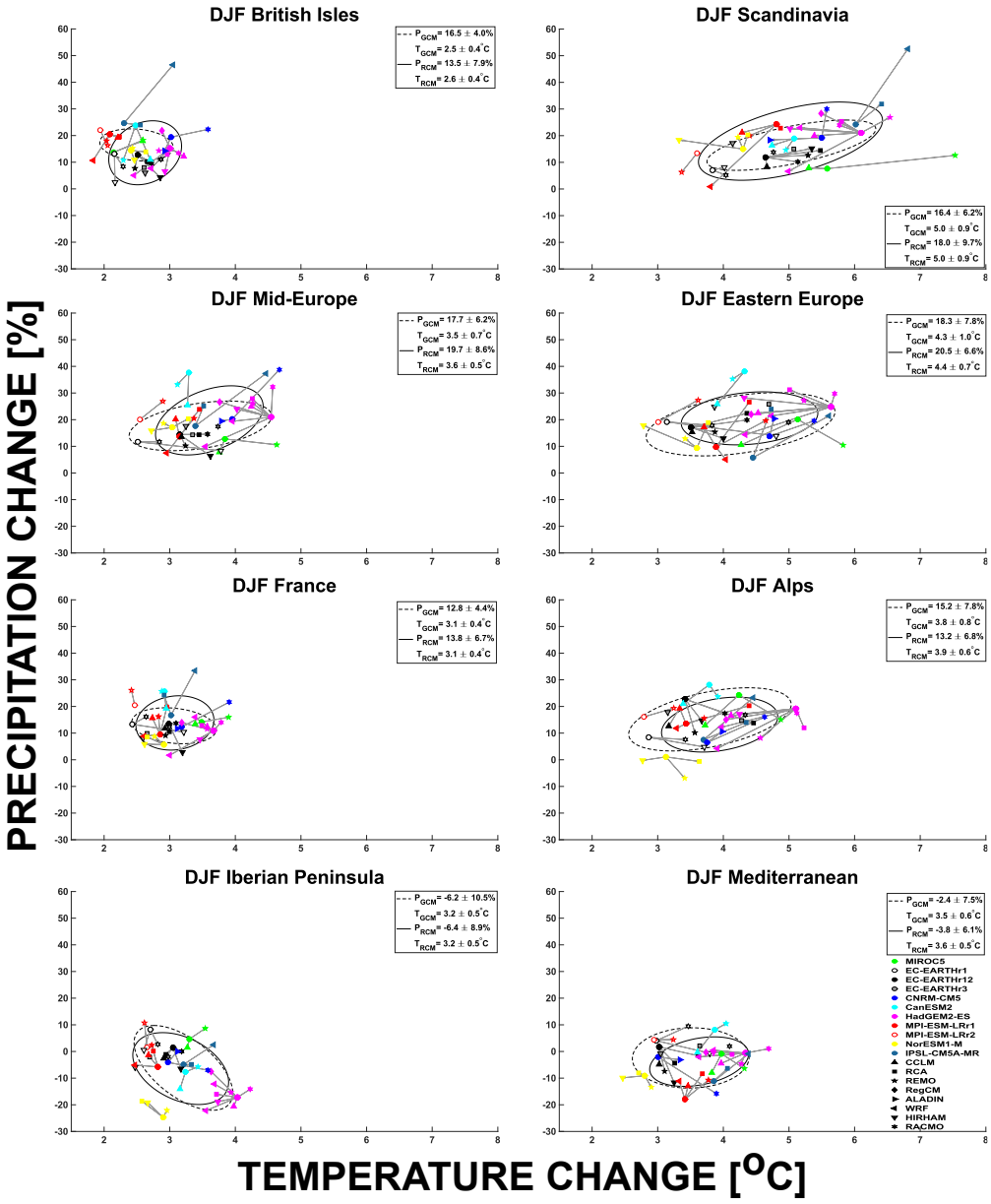

Figure 39: Same as Figure 38, but for DJF.

10.3 Precipitation scaling

This section reports an innovative investigation on hourly precipitation. It is based on a simple scaling analysis to derive the covariation between dew point (as a measure of near surface absolute humidity) and the hourly precipitation extremes. This provides information on the dependency of hourly extremes on humidity and therefore could provide information on the trustworthiness of future predictions. The method is applied to two modeling streams to illustrate its potential: NCC-NorESM1-M-r1i1p1-SMHI-RCA4 (hereafter RCA4r1) and MPI-M-MPI-ESM-LR-MPI-CSC-REMO2009 (hereafter REMOr1).

Hourly data from the simulations is first re-gridded in block of 4x4 grid points (i.e. 50 by 50 km^2). In these blocks we output the mean and the maximum value over these 16 grid points, as well as a sample grid point in the middle of the box. Here, we used the maximum hourly value of precipitation of these 16 grid points. Each hourly value is paired with the dew point temperature (in this case the mean over 16 grid points) from 4 hours before the event (Lenderink *et al* 2011). When dew points are at 3 hourly interval we took the closest value in time. This data set is divided based on the dew point temperature in bins with 2 degrees, and overlapping bins with 1 degree steps are used following Lenderink and van Meijgaard (2008). From the binned data we computed three percentiles (90^{th}, 99^{th} and 99.9^{th}) based on wet events only. The results presented here are based on data for the period May to September only.

In addition to the EURO-CORDEX modeling stream we also compared outputs of a mesoscale run driven by ERA-interim (HCLIM38h1_CXFPS). In this case, the 2.5 km is first re-gridded to 5x5 blocks (almost equal to the EURO-CORDEX resolution) and the mean hourly precipitation is computed. Hereafter, the data is treated in the same way as the EURO-CORDEX simulations.

Data is pooled over relatively large areas, e.g. covering a square area over the Netherlands, Belgium and Luxemburg (BENELUX), Germany (GERL), western part of France (FRANCEWEST) and southern part of France (FRANCESOUTH).

10.3.1 Results

Figure 40 shows as a reference the results for the convective permitting model simulation (HCLIM38h1_CXFPS). A rather regular scaling behavior is obtained with the three different percentiles showing a similar dependency. In general, the dependencies in the lower percentiles are higher than that of the 99.9^{th} percentiles, which is probably partly related to statistical artifacts as suggested in (Haerter and Berg 2009). The highest percentiles show a regular scaling behavior of close to two times the Clausius-Clapeyron (CC) relationship. For the high humidity regime (above 16 degrees dew point) there is a tendency to fall back to the CC rate, e.g. for the data over Germany.

Results for RCA4r1, now derived for the period 1981-1990, show a rather different behavior (Figure 41). In general, the intensities are much lower, in particular for dewpoints above 10 degrees. Also, the dependency is generally close to the CC rate, or below, and appears to fall off at high dew points (above 16 degrees). The results for a 10 year later period, 1991-2000, show a very similar behavior,

with the exception for the high humidity regime in the BENELUX area. This indicates that a 10 year time period is providing sufficient statistics to estimate the scaling relations. It is not clear at the moment whether this unsatisfactory behavior is due to the RCM or whether it originates from the driving GCM boundaries.

Finally, results for REMOr1 (Figure 3) do show more convincing behavior compared to the convective permitting results. Intensities are more realistic when comparing to Figure 40, with dependencies reasonably close to the 2CC relation. However, in comparison, dependencies are less regular in REMOr1, and also the intensities appear to strongly decrease beyond 18 degrees dew point for all areas considered.

10.3.2 Outlook

Results presented are based on an initial analyses. This work will be extended further

- Investigation of the other existing model simulations
- Investigation of the role of the boundaries as well as the role of the RCM
- Investigation of the sensitivity to the time period
- Investigation of other seasons and analysis domains.

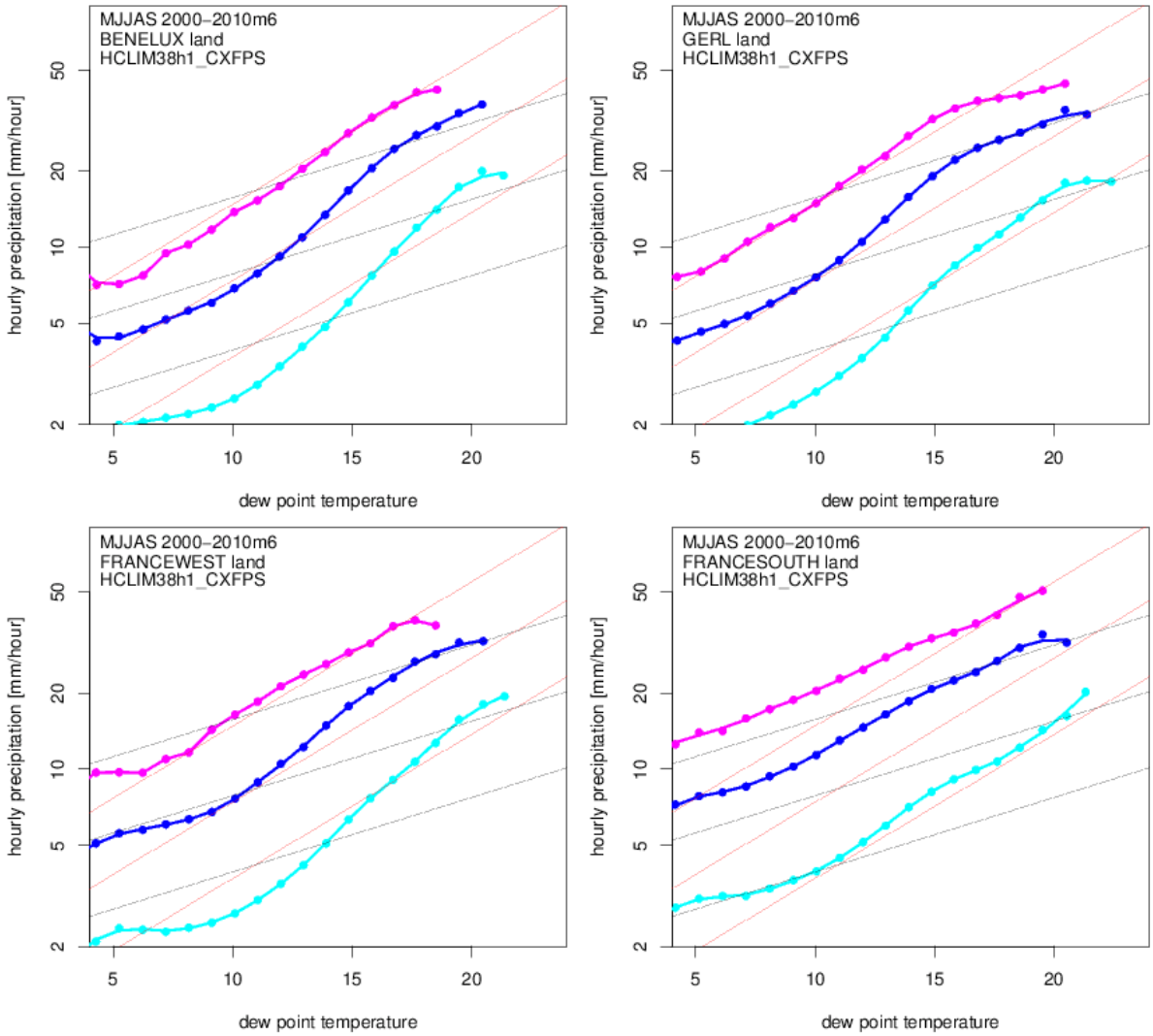

Figure 40. Intensity of hourly rainfall as a function of near surface temperature derived from data in 4 different areas, Benelux, Germany, Western France, and Southern France. Three percentiles are show: 90th (cyan), 99th (blue), and 99.9th (magenta). Black thin dashed lines are exponential lines following a 7% per degree dependency (Clausius-Clapeyron relation), whereas the red dashed lines follow a 14 % per degree dependency. Data of the period 2000 until 2009 is used (the year 2006 is neglected due to data issues, which will be corrected in the next update).

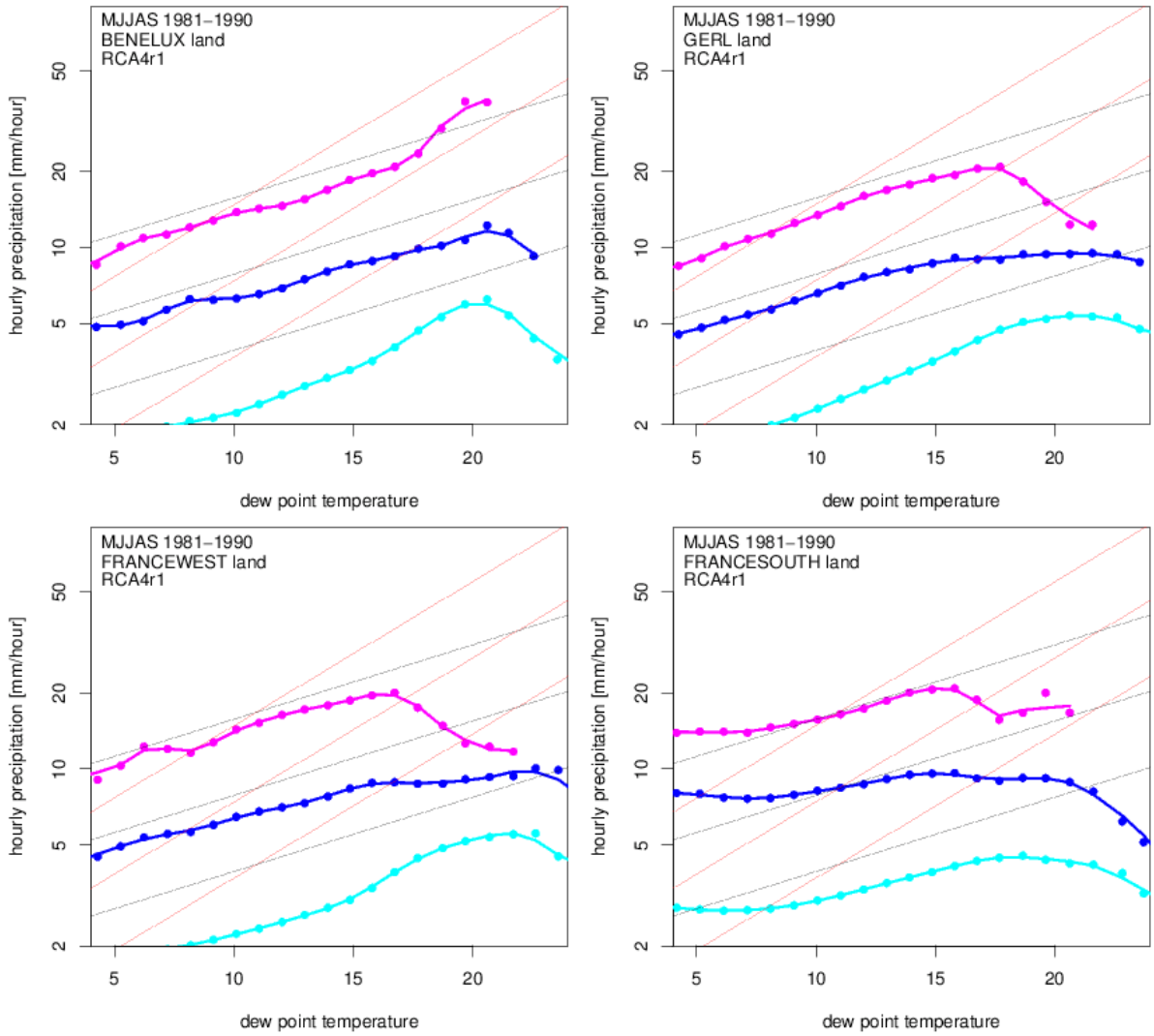

Figure 41. Same as Figure 40, but now for RCA4r1 and the period 1981-1990.

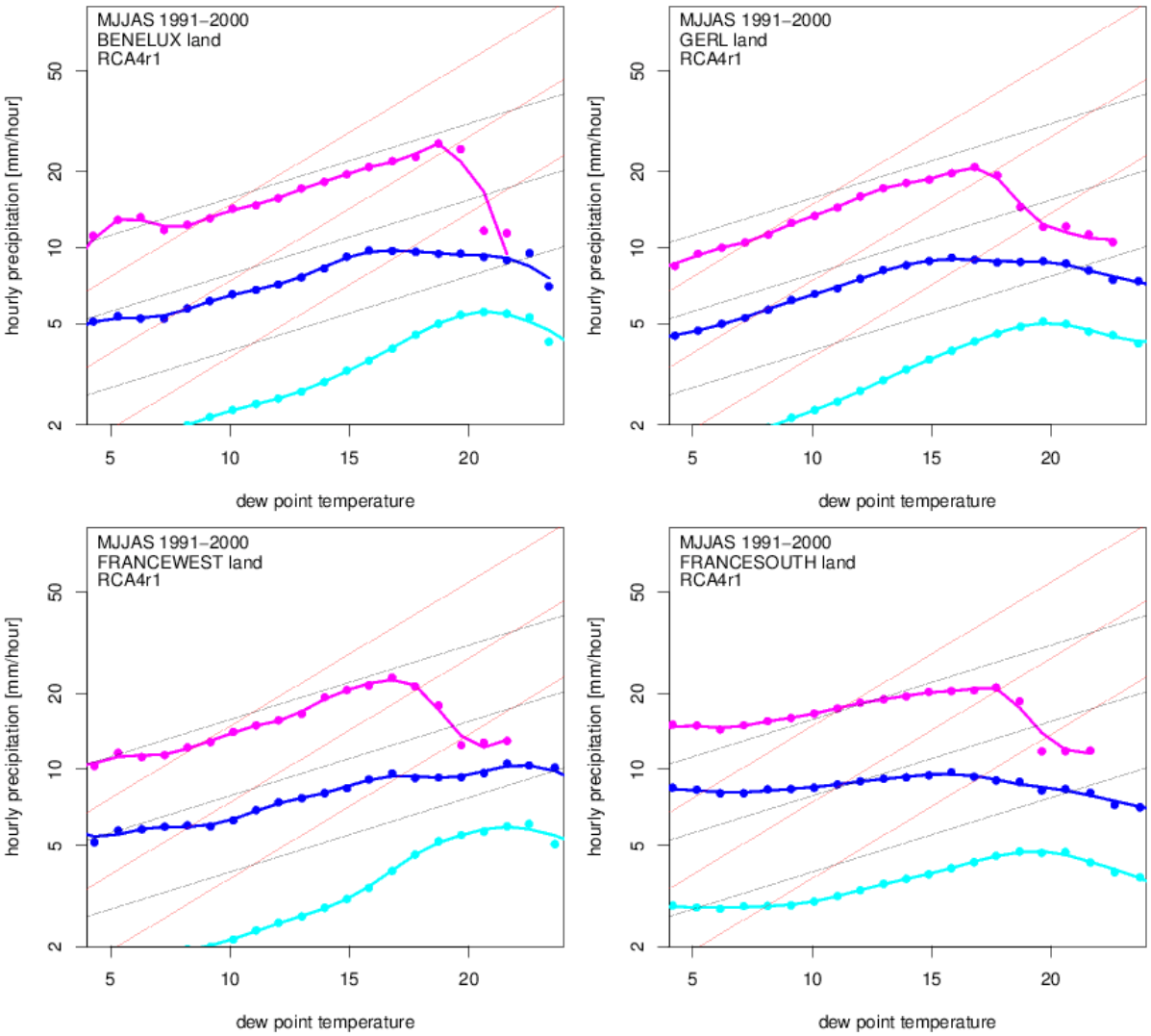

Figure 42. Same as Figure 40, but now for RCA4r1 and the period 1991-2000.

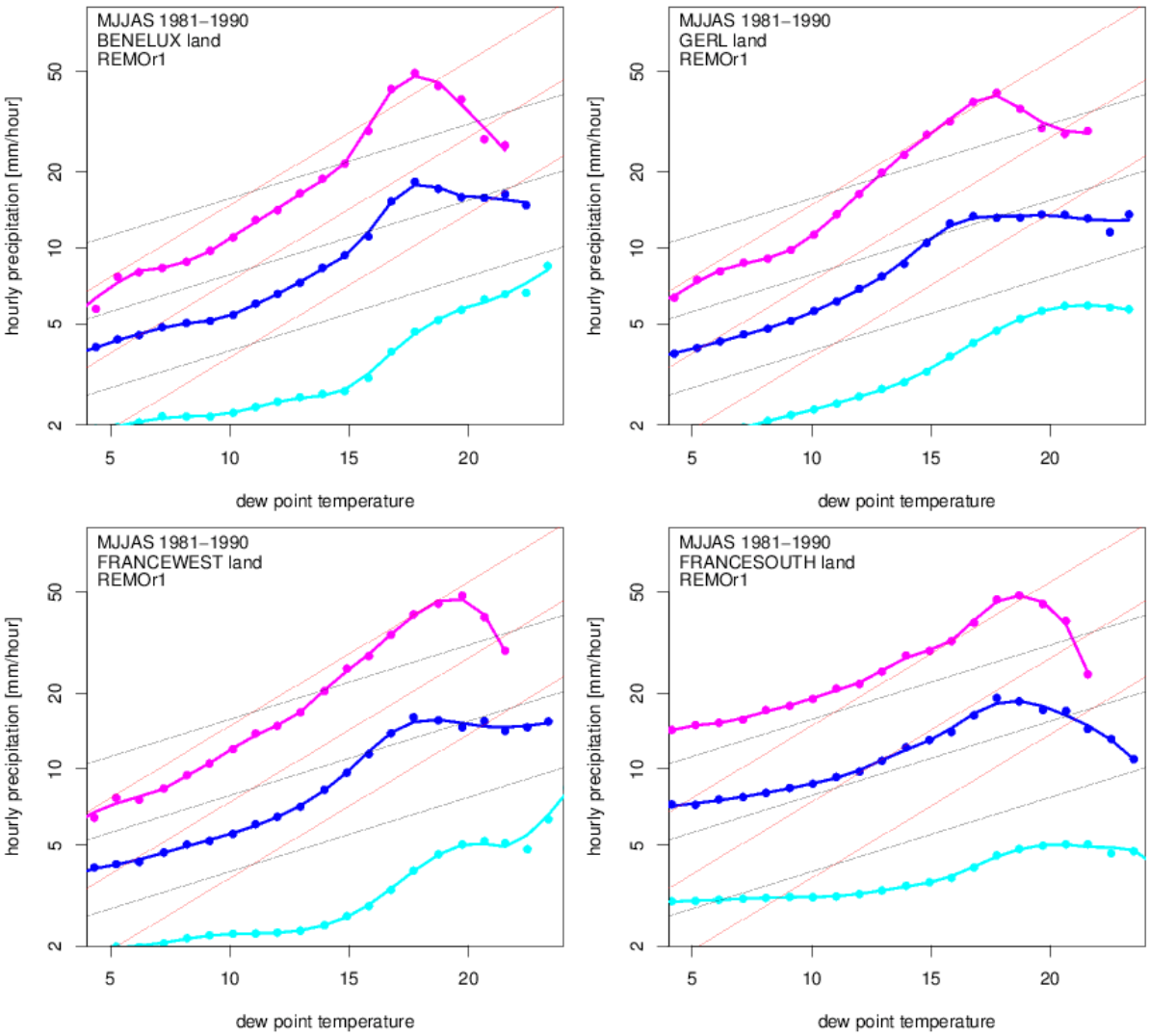

Figure 43. Same as Figure 40, but now for REMOr1 and the period 1981-1990.

10.4 Water balance

10.4.1 Key message

By comparing seasonal means of precipitation for 30 GCM driven RCMs for eight European sub-regions for 1981-2010 with observations, we see that most models have a wet bias, especially for the winter period. The level of bias seems to be determined to a large extent by the RCM. Similar patterns are seen when comparing absolute values of precipitation, evaporation, runoff and soil moisture. When analyzing relative changes of hydrological fields for the RCP 8.5 scenario (2036-2065) relative to the historical period 1981-2010 we notice that the pattern of precipitation change in the GCM/RCM matrix is less structured and it is difficult to determine whether it is the GCM or the RCM determining the level of change. Variables like evaporation, runoff, and soil moisture show changes, which generally depend on the RCM to the largest extent.

10.4.2 Baseline evaluation

Seasonal means (DJF and JJA) of precipitation (pr), total runoff (mrro), evaporation (evspsbl) and soil moisture (mrso) for the period 1981-2010 have been calculated for 30 regional climate model simulations together with observed precipitation taken from E-OBS data version 16. The WRF simulations intended to be analysed did not provide the necessary variables. The 30 RCM simulations are driven by different GCMs and can be divided into a GCM/RCM matrix consisting of 8 GCMs and 8 RCMs:

Table 27: Summary of GCM driven RCM simulations used in this evaluation. A total of 30 simulations are included, divided on 8 RCMs and 8 GCMs.

	RCM / GCM	1 CLMcom-CCLM	2 CNRM-ALADIN63	3 SMHI-RCA	4 KNMI-RACMO	5 DMI-HIRHAM	6 MPI-CSC-REMO	7 GERICS-REMO	8 ICTP-RegCM
8	NorESM1-M			r1		r1		r1	
7	MPI-ESM-LR	r1		r1			r1,r2		
6	HadGEM2-ES	r1		r1	r1	r1		r1	r1
5	MIROC5	r1						r1	
4	IPSL-CM5A-MR			r1					
3	EC-EARTH	r12		r3,r12	r1,r3,r12	r1,r3,r12		r12	
2	CNRM-CM5		r1		r1				
1	CanESM2	r1						r1	

The RCM data and the observations are divided into the PRUDENCE regions. The sub-region model means of seasonal precipitation are then compared with observations for winter (DJF, Figure 44, top panel) and summer (JJA, Figure 44, bottom panel). For DJF, most models (SMHI-RCA and DMI-HIRHAM in particular) show a large (positive) bias for sub-regions IP, FR, AL and MD. Almost all models and for almost all sub-regions show a positive bias for DJF. For JJA, the number of sub-regions and simulations with a negative bias is relatively high although the (negative) values are not as high as the values for the wet bias sub-regions and simulations. For JJA, models GERICS-REMO and SMHI-RCA show large wet biases for region IP and to some extent BI, FR, ME, SC and MD. Furthermore, RCMs driven by the GCM CNRM-CM5 show large JJA wet biases for regions IP, FR and

MD. We also note that RCMs driven by the GCM HadGEM2-ES give more negative biases for JJA relative to RCMs driven by other GCMs.

Absolute values for the 8 sub-regions for the variables precipitation (pr), evaporation (evspsbl), runoff (mrro) and soil moisture (mrso) are shown in Figure 45. For precipitation, we see some well-known patterns across the matrix. Regions IP and MD are dry for the JJA period while regions BI and AL are wet for the DJF period and to some extent also for the JJA period. As expected, evaporation is low for all models in DJF and then much higher in JJA for all regions except sub-regions IP and MD. Again, models SMHI-RCA, DMI-HIRHAM and GERICS-REMO show high values for JJA. For total runoff, we see high values for sub-region BI in DJF and sub-region AL in JJA. For total soil moisture content, we notice some every large differences between RCMs. SMHI-RCA and GERICS-REMO show small values for all sub-regions and both seasons while CLMcom-CCLM show large values, especially for sub-region IB for both seasons. This large difference between RCMs can probably be ascribed to different definitions on how the soil moisture is defined in these three models.

In summary, almost all model combinations, seasons, and areas show positive precipitation bias when compared with observations. Only summer precipitation in Southern Europe is an exception.

10.4.3 Future changes

Figure 46 shows relative changes in the hydrological fields under investigation for 2036-2065 for the RCP 8.5 scenario relative to the baseline period 1981-2010. Here we notice that the precipitation pattern in the GCM/RCM matrix is less structured and it is difficult to tell if it is the GCM or the RCM that dominates the outcome of the model run. For DJF, the changes are dominantly positive for all sub-regions except IP and MD. All six RCMs driven by the GCM HadGEM2-ES show negative values for sub-region IP for DJF. For JJA, sub-regions BI, IP, FR and MD show negative changes, the sub-region SC shows positive values while for the other sub-regions we see models giving precipitation changes with both signs.

In winter we see the more intense hydrological cycle reflected in generally higher evaporation and runoff. During summer, the smaller amount of precipitation leads to drier soil, less evaporation in spite of higher temperatures, and generally less runoff.

Structures in the GCM-RCM matrix for evaporation, runoff and soil moisture are mostly vertical, indicating that the RCM model plays a large role in the way precipitation changes manifest themselves.

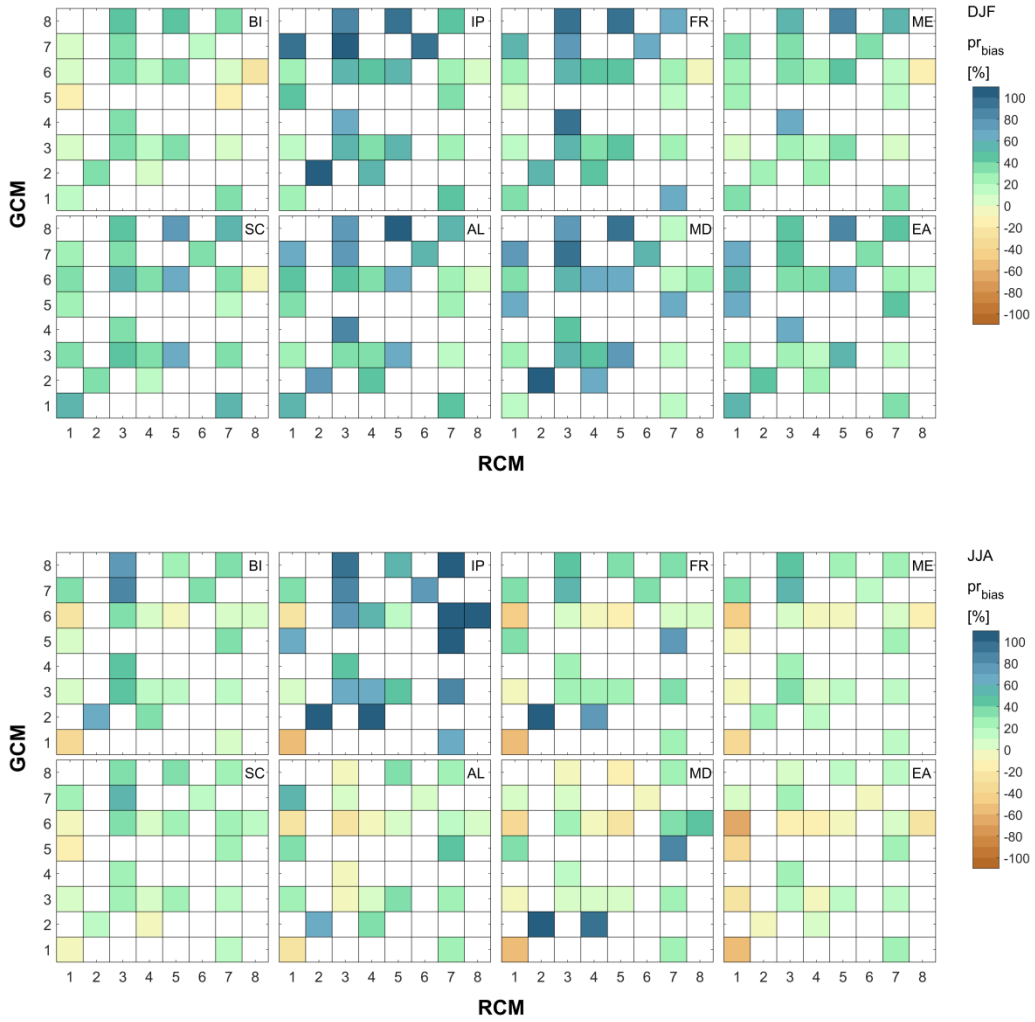

Figure 44: 1981-2010 precipitation bias (relative to E-OBS v16) for 30 RCM simulations divided into a GCM/RCM matrix. Top panel is for DJF and bottom panel for JJA. For those GCM/RCM combinations with more than one realization, we present the mean bias.

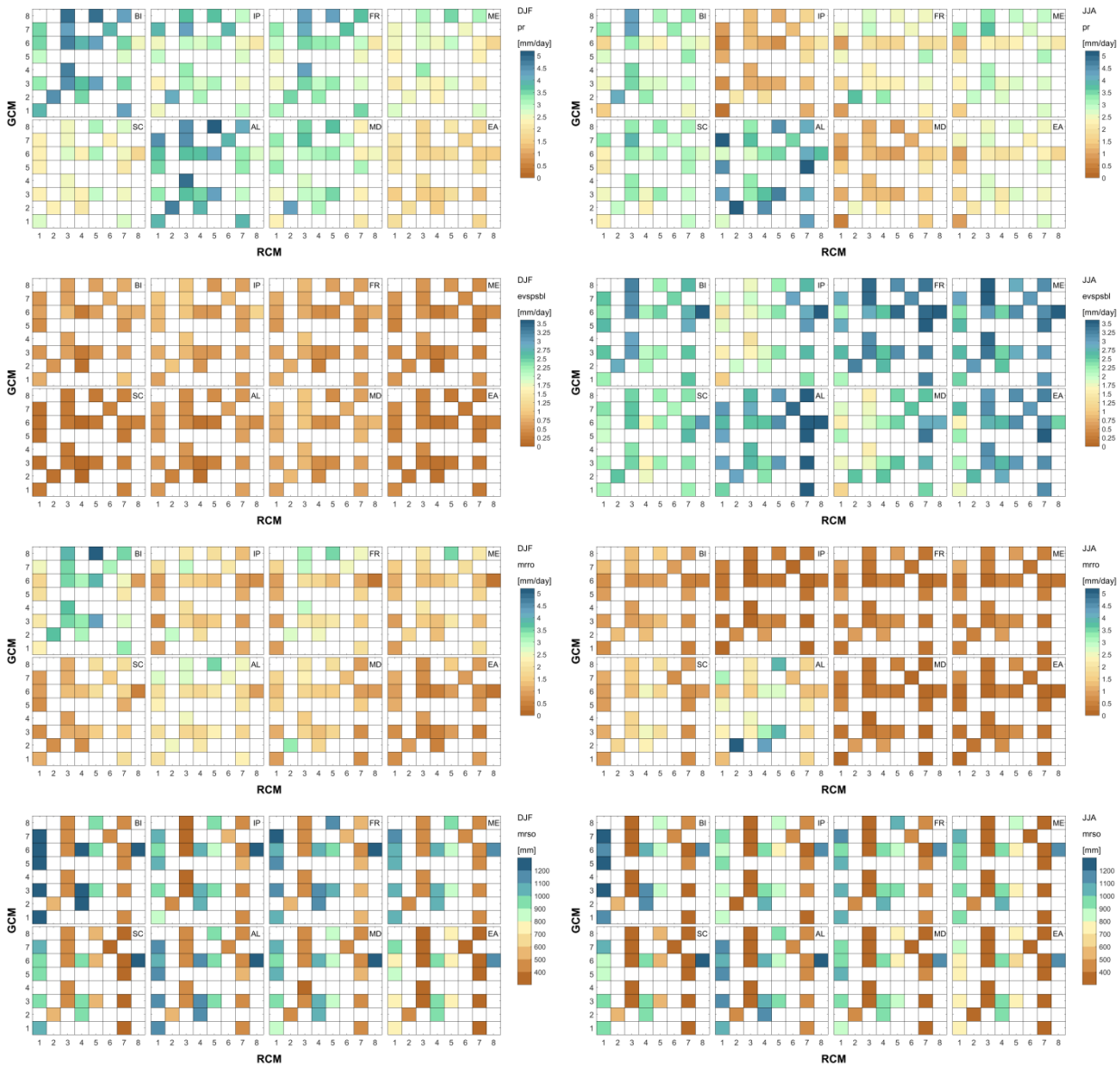

Figure 45: 1981-2010 means for 30 RCM simulations divided into a GCM/RCM matrix. Left column of panels is for DJF and right column for JJA. The variables shown are precipitation (first row), evaporation (second row), runoff (third row) and soil moisture (fourth row).

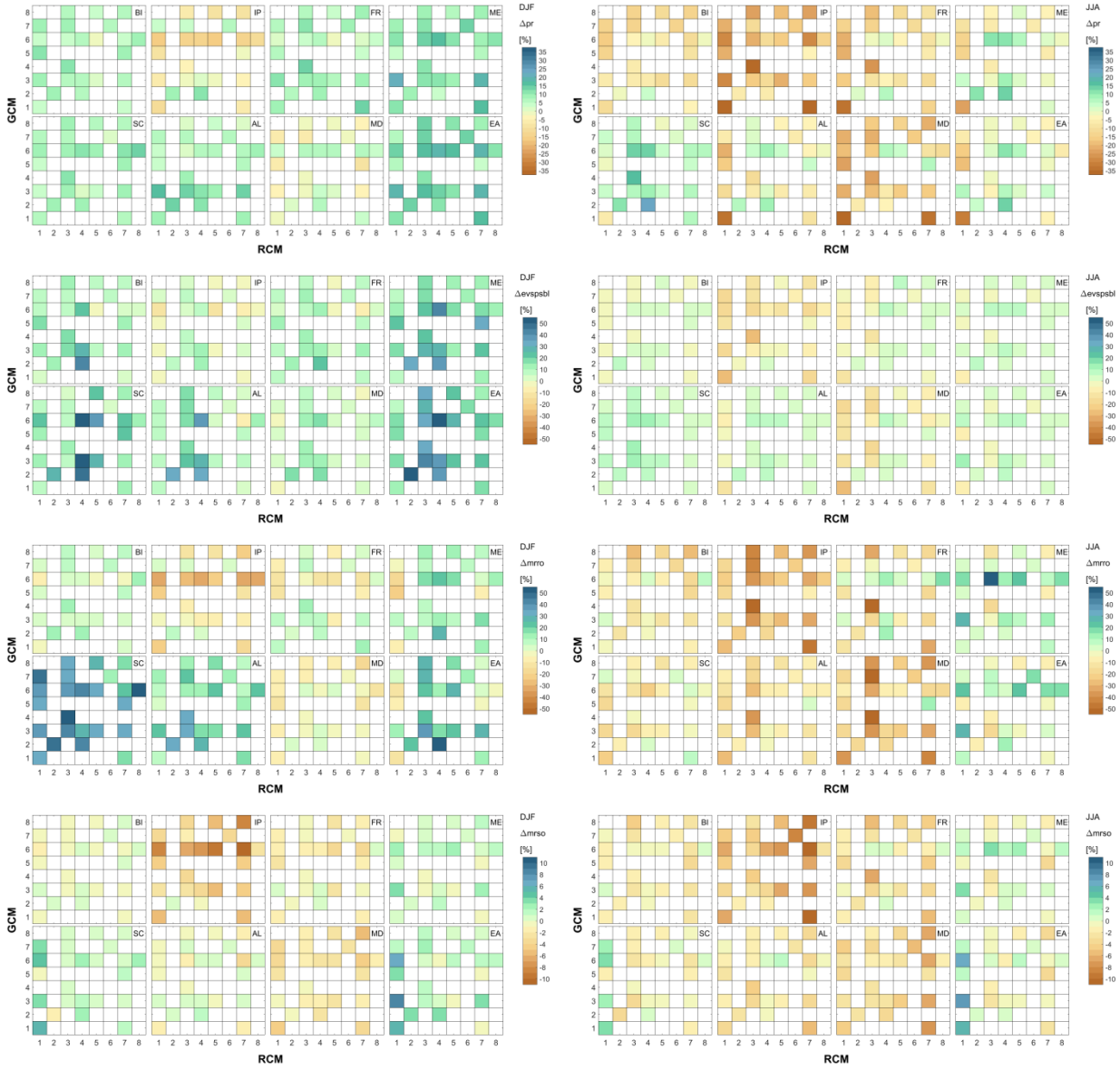

Figure 46: Relative change in the fields of Fig. 43 for 2036-2065 (RCP 8.5) relative to 1981-2010 for 30 RCM simulations divided into a GCM/RCM matrix. Left column is for DJF and right column for JJA.

10.5 GCM-RCM spatial correlation analysis

Regional climate model integrations depend on the validity on the "one-way" nesting approach, i.e. by assuming that the large scale dynamical forcing imposed at the boundary of the RCM domain are not altered by the interaction with the local scale forcings due to the refinement in the description of phisiography, and by the improved description of faster dynamical processes due to the increased resolution, and smaller time step, used in RCM integrations.
An assessment of the consistency between GCM and RCM large scale circulation, therefore, can be considered one of the basic checks to test the validity of RCM simulations. The most relevant time scale for this analysis is diurnal, since it considers the scale at which RCMs at 0.11^0 resolution are producing valuable output which could not be obtained directly from their driving GCMs. Day-to-day consistency of the large scale circulation between RCMs and their driving GCMs has been assessed from the correlation of spatial patterns of daily averaged mean sea level pressure (mslp). 9 RCMs (CCLM4-8.17, REMO2009, REMO2015, ALADIN63, RACMO22E, HIRHAM5, RCA4, RegCM4-6, and WRF381P) driven by 8 GCMs (CanESM2, EC-EARTH r1 and r12, HadGEM2-ES, IPSL-CM5-MR, MIROC5, MPI-ESM-LR, and NorESM1) have been included in this study, with 20 RCM integrations under the historical and RCP8.5 forcings, and 11 under RCP2.6. The period 1980-2005 has been used for the historical period, 2036-2065 for the future scenarios. Both RCM and GCM mpsl have been interpolated on a 0.75^0 regular grid using a bilinear interpolation; this process is practically equivalent to filtering the largest scales from both sets of simulations. The results have been analysed by seasons and summarised as box plots (Figure 47).

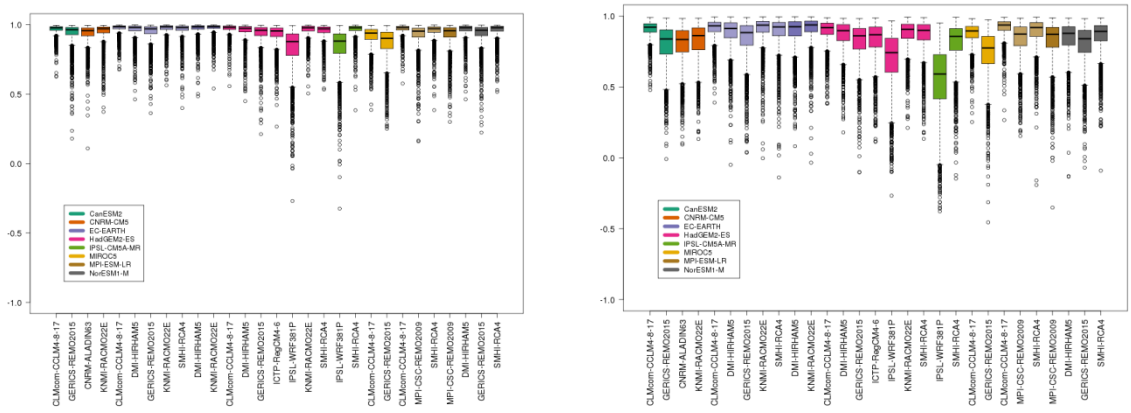

Figure 47: Distribution of mean sea level pressure spatial correlation between RCMs and driving GCMs, for simulation in the historical period (1976-2005). Left panel, winter (DJF): right panel, summer (JJA). Different GCM realisations are indicated by box plots of different colour intensities.

The analysis shows the expected result of a very high correlation in winter for all the models, with all the median values larger than 0.9, while in summer the intermodel spread is larger (0.6-0.9 for medians). The results of the intermediate seasons, not shown, are, halfway between the winter and summer results. The seasonal differences for a given RCM simulation can be explained by the strength of the dynamical forcing from the GCM in each season, which ultimately determines the intensity of the constraint on the circulation over the RCM domain (e.g. Sanchez-Gomez *et al.*, 2009).

Figure 48 shows the summary statistics for the RCP8.5 simulations.

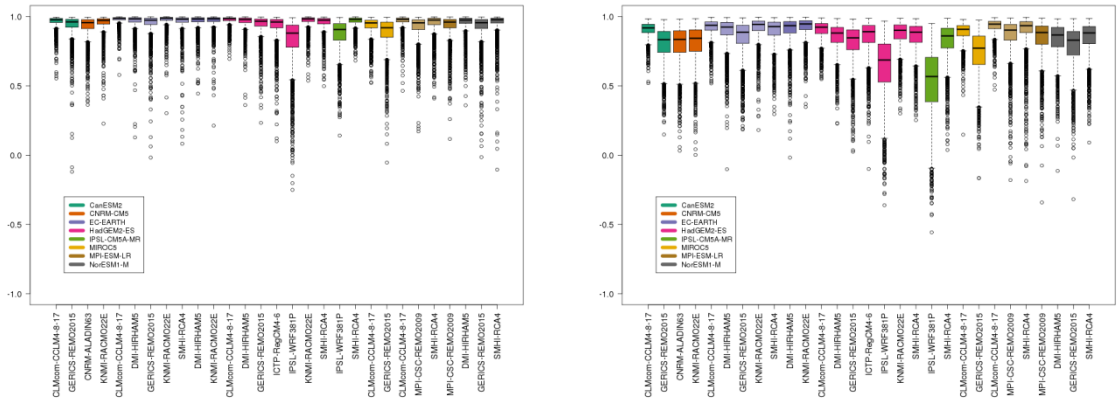

Figure 48: Same as figure 45, for the RCP8.5 simulations, 2036-2065. Left panel, winter (DJF); right panel, summer (JJA).

The results for the RCP8.5 simulations are very similar to those obtained for the historical period, and to those, not shown, from the RPC2.6 simulations. The main purpose of this study is a basic assessment of the RCM/GCM large scale consistency, and the analysis confirms that all the RCM integrations give reasonably good statistics for the chosen RCM/GCM consistency measure. It is also worth noting that the RCM integrations driven by CNRM-CM5 for the historical period, which are driven by lateral boundary conditions from prognostic variables on pressure levels, give the same consistency as the RCP8.5 simulations driven by the same GCM, which are driven by prognostic variables on model hybrid pressure levels directly from CNRM-CM5. This outcome supports the choice of the approach used for the new historical CNRM-CM5-driven simulations, which had to be used as a result of the lack of model levels 6-hourly data for the GCM realisation used in this project.

The figures in this study also show rather large model differences, in particular in the lower tail of the correlation distributions; these differences are not necessarily an indication of different RCM skill in reproducing the driving large scale circulation. Factors which may contribute to these differences include the size of the domain used in RCM simulations, which might explain the results from the WRF381P integrations for which a larger domain has been used (offsetting the EURO-CORDEX domain by about 500km on each side), GCM resolution, and strength of the driving circulation (e.g. Laprise *et al*, 2008). Additional analysis will be needed to clarify these aspects.

11. Summary of biases and changes

11.1 Biases

We have analyzed biases for temperature, precipitation, dynamical quantities and solar radiation. Based on this analysis we establish a qualitative table on strengths and weaknesses of the simulations based on expert judgement. Table 28 summarizes this information. It highlights the models having substantial or generalized biases. Two levels of bias intensity/extent are proposed. This analysis is supported by Figure 49 below which summarizes the main biases per region, and by tables in Section 4.

Table 28: Qualitative evaluation of models biases. A color is set when the model appears to have a bias that is systematic, or substantial in a large region. Orange stands for positive bias and blue for negative. Intensity stands for the intensity of the bias.

GCM-RCM	Temperature	Precipitation (TBD)	Winds	Radiation
CANESMr1 – CCLM				
CANESMr1 - REMO2015				
CNRMr1 - ALADIN63				
CNRMr1 – RACMO				
ECEARTHr12 – CCLM				
ECEARTHr12 – HIRHAM				
ECEARTHr3 – HIRHAM				
ECEARTHr1 – HIRHAM				
ECEARTHr12 – RACMO				
ECEARTHr1 – RACMO				
ECEARTHr3 – RACMO				
ECEARTHr12 – RCA				
ECEARTHr3 – RCA				
ECEARTHr12 - REMO2015				
HADGEMr1 – CCLM				
HADGEMr1 – HIRHAM				
HADGEMr1 – RACMO				
HADGEMr1 – RCA				
HADGEMr1 - REMO2015				
HADGEMr1 – REGCM				
HADGEMr1 - WRF361H				
HADGEMr1 - WRF381P				
IPSLr1 – RCA				
IPSLr1 - WRF381P		N/A		
MIROCr1 – CCLM				
MIROCr1 - REMO2015				
MPIr1 – CCLM				
MPIr1 – RCA				
MPIr1 – REMO				
MPIr2 – REMO				
MPIr1 - WRF361H				
NORESMr1 – HIRHAM				
NORESMr1 -REMO2015				
NORESMr1 – RCA				

Figure 49 (that is a repetition of Figure 1) shows the diversity of GCM-RCM results and the fact that no single model is biased on all parameters. Some GCM-RCM combinations turn out to have large biases for precipitation but not for temperature and vice versa.

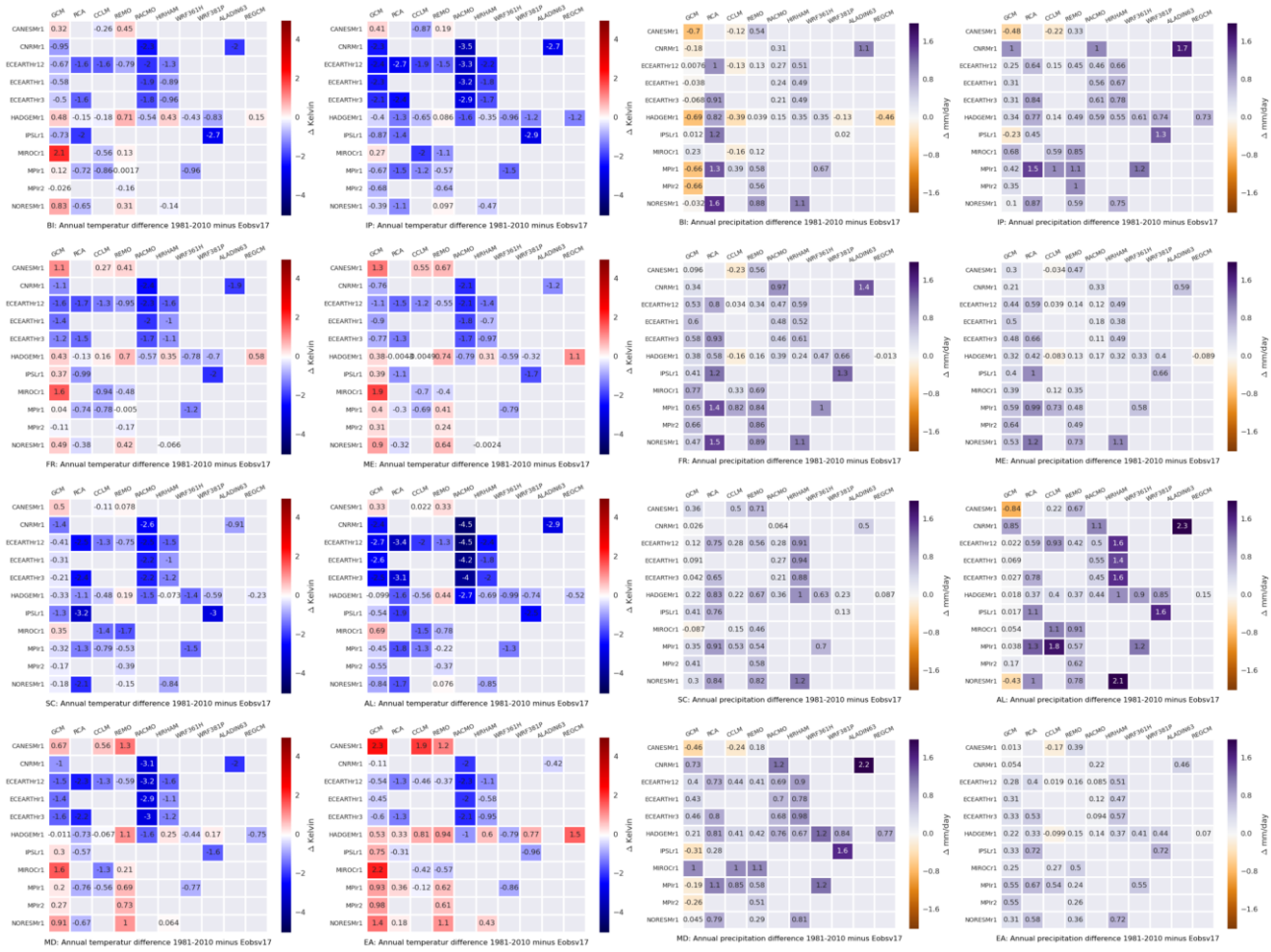

Figure 49: Annual mean temperature [K] (left 8 panels) and precipitation [mm/day] (right 8 panels) differences over 1981-2010 between each GCM/RCM and EOBSv17 averaged over each Prudence Region.

11.2 Changes

Figure 50 (that is a repetition of Figure 2) is similar to Figure 49 for changes instead of biases. It shows the homogeneity of the climate change signals for temperature and to a large extent for precipitation. In some regions, however, models disagree, such as for FR and BI.

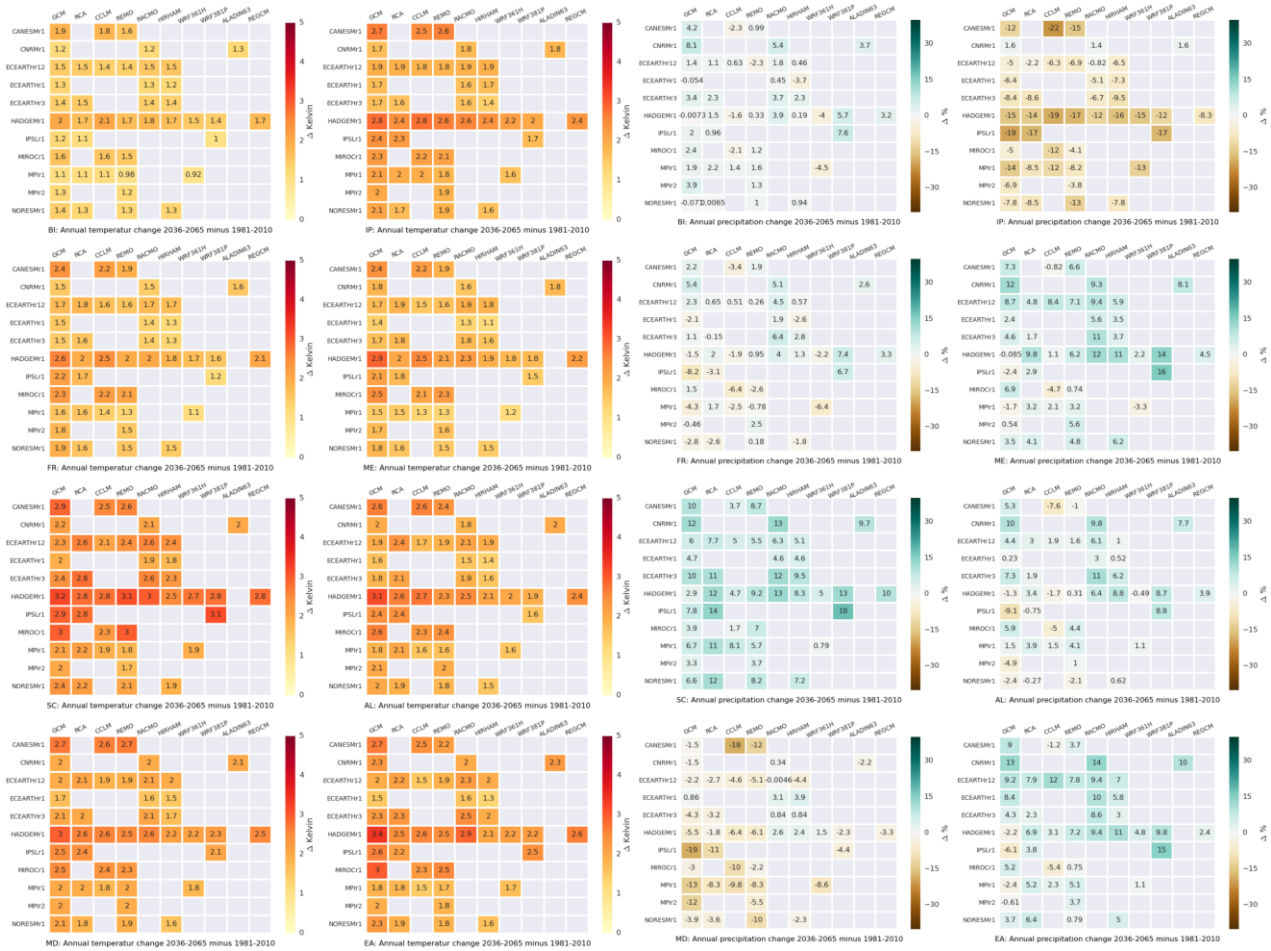

Figure 50: same as Figure 49 for changes (2050-ref) instead of biases.

12. Acknowledgements

E-OBS temperature and precipitation v17 were used: We acknowledge the E-OBS dataset from the EU-FP6 project ENSEMBLES (http://ensembles-eu.metoffice.com) and the data providers in the ECA&D project (http://www.ecad.eu)" (Haylock *et al*., 2008)

For the WRF381P simulations the TGCC supercomputer centre graciously provided the computer time required for the simulations of the PRINCIPLES project.

13. References

Andrews, T., Gregory, J. M., Webb, M. J., Taylor, K. E. (2012). Forcing, feedbacks and climate sensitivity in CMIP5 coupled atmosphere-ocean climate models. Geophys. Res. Lett. 39, L09712, doi:10.1029/2012GL051607.

Chatterjee, C., Cremer, R., Trentmann, J., Hollmann, R. (2015). Surface Solar Radiation Data Set - Heliosat (SARAH) - Edition 1. EUMETSAT Satellite Application Facility on Climate Monitoring (CM SAF). https://doi.org/10.5676/EUM_SAF_CM/SARAH/V001.

Christensen, J.H., Christensen, O.B. (2007). A summary of the PRUDENCE model projections of changes in European climate by the end of this century. Clim Change 81 (Suppl 1),7–30 .

Fantini A., *et al*. (2016). Assessment of multiple daily precipitation statistics in ERA-Interim driven Med-CORDEX and EURO-CORDEX experiments against high resolution observations. Clim. Dyn. 51: 877. https://doi.org/10.1007/s00382-016-3453-4

Giorgi, F., Torma, C., Coppola, E., Ban, N., Schär, C., Somot, S. (2016). Enhanced summer convective rainfall at Alpine high elevations in response to climate warming. Nat. Geosc. 9, 584-589.

Gutiérrez C., Somot S., Nabat P., Mallet M., Gaertner M.A., Perpiñán O. (2018) Impact of aerosols on the spatiotemporal variability of photovoltaic energy production in the Euro-Mediterranean area. Solar Energy. 174 : 1142-1152, https://doi.org/10.1016/j.solener.2018.09.085

Haylock, M. R., Hofstra, N., Klein Tank, A. M. G., Klok, E. J., Jones, P. D., New, M. (2008). A European daily high-resolution gridded data set of surface temperature and precipitation for 1950-2006. J. Geophys. Res. Atmos. 113(20). https://doi.org/10.1029/2008JD010201

Kanamitsu, M., DeHaan, L. (2001). The Added Value Index: A new metric to quantify the added value of regional models. J. Geophys. Res. 116 (D11106): 1-10.

Kjellström, E, Bärring, L., Nikulin, G., Nilsson, C., Persson, G., Strandberg, G. (2016). Production and use of regional climate model projections - A Swedish perspective on building climate services. Clim. Serv. 2, 15–29

Kotlarski, S. *et al*. (2014). Regional climate modeling on European scales: A joint standard evaluation of the EURO-CORDEX RCM ensemble. Geosc. Mod. Develop. 7(4), 1297–1333. https://doi.org/10.5194/gmd-7-1297-2014

Laprise, R., de Elía, R., Caya, D. *et al*. Meteorol Atmos Phys (2008) **100**: 3. https://doi.org/10.1007/s00703-008-0292-9

Nabat, P., Somot, S., Mallet, M., Sanchez-Lorenzo, A., Wild, M. (2014). Contribution of anthropogenic sulfate aerosols to the changing Euro-Mediterranean climate since 1980. Geophys. Res. Let., 41(15), 5605-5611.

Osborn, T. J., Jones, P. (2014). The CRUTEM4 land-surface air temperature data set: construction, previous versions and dissemination via Google Earth. Earth. Syst. Science Data, 6(1), 61-68.

Rummukainen, M. (2016). Added value in regional climate modelling. Climatic Change. 7: 145-159.

Sanchez-Gomez, E., Somot, S. & Déqué, M. Clim Dyn (2009) **33**: 723. https://doi.org/10.1007/s00382-008-0502-7Müller, R., Pfeifroth, U., Träger-

Sørland, S. L., Schär, C., Lüthi, D., Kjellström, E. (2018). Bias patterns and climate change signals in GCM-RCM model chains. Environ. Res. Lett. 13:074017. https://doi.org/10.1088/1748-9326/aacc77

Tobin, I., Greuell W., Jerez S., Ludwig F., Vautard R., van Vliet M.T.H., and Bréon F.-M., 2018: Vulnerabilities and resilience of European power generation to 1.5°C, 2°C and 3°C warming, Environ. Res. Lett., 13 044024.

Torma C. *et al*. (2015). Added value of regional climate modelling over areas characterized by complex terrain – Precipitation over the Alps. J. Geophys. Res. Atmos. 3957-3972.

Copernicus Climate Change Service

ECMWF - Shinfield Park, Reading RG2 9AX, UK

Contact: info@copernicus-climate.eu

climate.copernicus.eu copernicus.eu ecmwf.int